

ADSORPTION OF POLLUTANTS ON CHARCOAL
CLOTH IN SIMULATED GUARD FILTERS

A Thesis submitted to the Board of the Faculty
of Engineering, University of Aston in Birmingham,
for the Degree of

DOCTOR OF PHILOSOPHY

by

SUBHASISH PODDER

Chemical Engineering Department
University of Aston in Birmingham

Far must thy researches go
Wouldst thou learn the world to know;
Thou must tempt the dark abyss
Wouldst thou prove what being is;
Naught but firmness gains the prize,
Naught but fullness makes us wise,
Buried deep truth ever lies.

Friedrich Von Schiller
(1759 - 1805)

TO
MY PARENTS

ACKNOWLEDGEMENTS

The author would like to express his thanks to the following people:

Professor G V Jeffreys. For allowing the use of the Chemical Engineering Department facilities.

The Ministry of Defence. For providing financial support for the research programme.

Dr R G Temple. For help and guidance provided during his supervision of the research programme.

Mr G A Hunt. For his help and suggestions from the Chemical Defence Establishment.

Mr N Roberts and the technical department for invaluable help during the construction of the experimental apparatus.

Mr John Holloway for producing such excellent photographs.

CONTENTS

	<u>Page No.</u>
SUMMARY	1
1. INTRODUCTION	3
2. LITERATURE SURVEY	6
2.1 Brief History	6
2.2 Manufacture of Activated Carbon	7
2.3 Manufacture of Charcoal Cloth	7
2.4 Advantages of Charcoal Cloth over Granular Charcoal	11
2.5 Properties of Charcoal Cloth	13
2.6 Application of Charcoal Cloth	13
3. ADSORPTION THEORY	17
3.1 Adsorption Isotherm	18
3.1.1 Introduction	18
3.1.1.1 Single Component Adsorption	19
3.1.1.1.1 Langmuir Adsorption Isotherm	19
3.1.1.1.2 Freundlich Adsorption Isotherm	20
3.1.1.1.3 BET Adsorption Isotherm	21
3.1.1.2 Multi Component Adsorption	24
3.1.1.2.1 Two Component Adsorption	25
3.2 General Thermodynamic Relations	27
3.2.1 Single Component	27
3.2.2 Two Component	29
3.3 Factors Affecting Adsorption	30
3.3.1 Porous Structure of Adsorbent	30
3.3.1.1 Macropores	31
3.3.1.2 Transitional Pores	31
3.3.1.3 Micropores	32

	<u>Page No.</u>	
3.3.2	Physical and Chemical Factors	33
3.3.2.1	Temperature	33
3.3.2.2	Moisture in the Air	34
3.3.2.3	Influence of pH Values	35
3.3.2.4	Functional groups	37
3.3.2.5	Surface Complexes on Carbons	38
3.3.2.6	Nature of the Adsorbate	43
3.3.2.7	Surface Area	48
3.3.2.8	Surface Tension Effects	50
3.3.2.9	Chemical Reactions on Surfaces	52
3.3.2.9.1	Mechanism of Surface Reactions	54
3.4	Physical Adsorption of Vapours in Micropores	55
3.4.1	Thermodynamic Analysis	58
3.5	Adsorption Mechanism	60
3.6	Mass Transfer	63
3.7	Potential Theory of Adsorption	67
3.7.1	Dubinin-Polanyi Equation	68
3.7.2	Limitations of Dubinin-Polanyi Equation	73
3.7.3	The Modified Dubinin-Polanyi Equation	78
3.8	Adsorption Kinetics	79
3.8.1	Adsorption Rate Constant	80
3.8.2	Adsorption Rate Limit	83
3.8.3	Alternative Method to Calculate Adsorption Rate Constant	84
3.9	Regeneration	85
3.9.1	Regeneration Techniques	86
3.9.1.1	Thermal Swing Desorption	86
3.9.1.1.1	Thermal Swing Desorption: Thermodynamic Calculations	87

		<u>Page No.</u>
3.9.1.2	Pressure Swing Desorption	89
3.9.1.3	Purge Gas Stripping	89
3.9.1.4	Displacement Desorption	90
3.9.1.5	Combination Desorption	90
4.	ADSORPTION STUDIES - PROCEDURE AND TREATMENT OF RESULTS	92
4.1	Experimental Objectives	92
4.2	Description of the rig	94
4.2.1	Solvent-Air Mixing Section	96
4.3	Experimental Procedure	96
4.4	Mass Spectrometer	97
4.4.1	Operating Procedure	99
4.4.1.1	Starting Up	99
4.4.1.2	Mass Tuning	99
4.4.1.3	Shutting Down	100
4.4.1.4	Sampling Technique (Respiratory Mode)	100
4.4.2	Fault Diagnosis	100
4.5	Treatment of Experimental Results	102
4.6	Effect of Number of Regenerations on the Activity of Charcoal Cloth	125
5.	DESIGN OF FILTER CANISTER	127
5.1	Introduction	127
5.1.1	Choice of Adsorbent	127
5.1.2	Flow Rate	128
5.1.3	Column Length	129
5.2	Design of the Proposed Filter	130
5.2.1	Canister Designs	132

	<u>Page No.</u>	
5.2.1.1	Design One	132
5.2.1.2	Design Two	134
5.2.1.3	Design Three	134
5.2.1.4	Design Four	134
5.3	Calculation of Reynold's Number	140
5.3.1	Design One (Between Two Layers of Cloth)	140
5.3.2	Design Four (Along the Cloth Surface)	140
6.	THEORETICAL DEVELOPMENT AND MATHEMATICAL MODELLING	144
6.1	Adsorption Isotherms	144
6.2	Rate of Mass Transfer	153
6.2.1	LUB and Equilibrium Concept	154
6.2.2	Present Work: Calculation of the Length of Unused Charcoal Cloth	159
6.3	Rate Controlled Breakthrough	160
6.3.1	Method of Calculation	161
6.4	Relation of Breakthrough time with Inlet Concentration and Number of Layers of Charcoal Cloth	162
7.	DISCUSSION	165
7.1	Low Temperature Oxidation	165
7.2	Heat of Adsorption	169
7.3	Discussion of Experimental Results	172
8.	CONCLUSIONS AND RECOMMENDATIONS	177
	Nomenclature	183
	References	189

LIST OF APPENDICESPage No.

I	Sample Calculations	202
II	Tables of the Experimental Conditions and the Results of Adsorption	207
III	Data used to Test the Application of the Langmuir and Freundlich Isotherms	216
IV	Summary of Data used in Evaluating the Length of Unused Adsorbent Bed at an Outlet Vapour Concentration of 10 p.p.m	221
V	Data used to Calculate the Theoretical Adsorbate-Adsorbent Ratio using Dubinin-Polanyi Equation	226
VI	Data used to Calculate Adsorbate-Adsorbent Ratio at Breakthrough	229
VII	Summary of Data used to Calculate Adsorption Rate Constant	234
VIII	Calculated Theoretical Breakthrough Time using Equation 6.10	239
IX	Summary of Results showing Oxidation during Adsorption of Solvent Vapours on Charcoal Cloth	241
X	List of Computer Programs	243

LIST OF FIGURES

<u>Number</u>	<u>Title</u>	<u>Page No.</u>
2.1	A Process for the Production of Granular and Powdered Charcoals	8
2.2	Process for the Manufacture of Activated Charcoal Cloth	9
2.3	Typical Solvent Recovery Plant	14
3.1	Adsorption Isotherms for the Uptake of Ammonia on Charcoal	22
3.2	Langmuir and BET Adsorption Isotherms	22
3.3	The Structure of the Adsorbed Phase According to Polanyi Potential Theory	69
3.4	Three Pore Model	69
4.1	Hot Glass Finger System	95
4.2	Solvent-Air Mixer	95
4.3	Mass Spectrometer Trace	101
4.4	Outlet Vapour Concentration of Heptane Against Time at Different Inlet Concentration (25 Layers of Charcoal Cloth)	105
4.5	Outlet Vapour Concentration of Heptane Against Time at Different Inlet Concentration (35 Layers of Charcoal Cloth)	106
4.6	Outlet Vapour Concentration of Heptane Against Time at Different Inlet Concentration (45 Layers of Charcoal Cloth)	107
4.7	Regeneration of Charcoal Cloth (Heptane Adsorption)	108
4.8	Outlet Vapour Concentration of Tetrachloroethylene Against Time at Different Inlet Concentration (25 Layers of Charcoal Cloth)	109
4.9	Outlet Vapour Concentration of Tetrachloroethylene Against Time at Different Inlet Concentration (35 Layers of Charcoal Cloth)	110
4.10	Outlet Vapour Concentration of Tetrachloroethylene Against Time at Different Inlet Concentration (45 Layers of Charcoal Cloth)	111

	<u>Page No.</u>
4.11 Regeneration of Charcoal Cloth (Tetrachloroethylene adsorption)	112
4.12 Outlet Vapour Concentration of Toluene Against Time at Different Inlet Concentration (25 Layers of Charcoal Cloth)	113
4.13 Outlet Vapour Concentration of Toluene Against Time at Different Inlet Concentration (35 Layers of Charcoal Cloth)	114
4.14 Outlet Vapour Concentration of Toluene Against Time at Different Inlet Concentration (45 Layers of Charcoal Cloth)	115
4.15 Regeneration of Charcoal Cloth (Toluene Adsorption)	116
4.16 Outlet Vapour Concentration of O-Xylene Against Time at Different Inlet Concentration (25 Layers of Charcoal Cloth)	117
4.17 Outlet Vapour Concentration of O-Xylene Against Time at Different Inlet Concentration (35 Layers of Charcoal Cloth)	118
4.18 Outlet Vapour Concentration of O-Xylene Against Time at Different Inlet Concentration (45 Layers of Charcoal Cloth)	119
4.19 Regeneration of Charcoal Cloth (O-Xylene Adsorption)	120
4.20 Time Required for Outlet Concentration to Reach 10% of Inlet Concentration Against Weight of Charcoal Cloth (Heptane)	121
4.21 Time Required for Outlet Concentration to Reach 10% of Inlet Concentration Against Weight of Charcoal Cloth (Tetrachloroethylene)	122
4.22 Time Required for Outlet Concentration to Reach 10% of Inlet Concentration Against Weight of Charcoal Cloth (Toluene)	123
4.23 Time Required for Outlet Concentration to Reach 10% of Inlet Concentration Against Weight of Charcoal Cloth (O-Xylene)	124
5.1 Canister Designs	133
6.1 Plot of $\frac{1}{\sqrt{V}}$ Against $\frac{1}{P}$ (Heptane)	145
6.2 Plot of $\frac{1}{\sqrt{V}}$ Against $\frac{1}{P}$ (Tetrachloroethylene)	146

	<u>Page No.</u>
6.3 Plot of $\frac{1}{V}$ Against $\frac{1}{p}$ (Toluene)	147
6.4 Plot of $\frac{1}{V}$ Against $\frac{1}{p}$ (O-Xylene)	148
6.5 Plot of $\ln V$ Against $\ln p$ (Heptane)	149
6.6 Plot of $\ln V$ Against $\ln p$ (Tetrachloroethylene)	150
6.7 Plot of $\ln V$ Against $\ln p$ (Toluene)	151
6.8 Plot of $\ln V$ Against $\ln p$ (O-Xylene)	152
6.9 Transfer Fronts Moving Through Adsorber	155

LIST OF TABLES

<u>Number</u>	<u>Title</u>	<u>Page No.</u>
2.1	Average Percentage Weight Uptakes and Adsorption Rates for the Dynamic Adsorption of Particular Solvents on Charcoal Cloth and Granular Charcoal under Dry Conditions and at 80% Relative Humidity	12
2.2	Properties of Charcoal Cloth	13
3.1	Properties of Aromatic Acids and Equilibrium Data for their Adsorption on Activated Carbon	36
3.2	Adsorption Parameters Derived from Regression Analysis Equation using Granular Carbon as Adsorbent	82
4.1	Summary of Results of the Effect of Number of Regenerations on the Activity of Charcoal Cloth	125
5.1	Summary of Results of Adsorption of Toluene on Charcoal Cloth Using Different Canister Designs of 0.1524m (6") Diameter	137
5.2	Summary of Results of Adsorption of Toluene on Charcoal Cloth Using Canister of 0.2286m (9") Diameter	138
5.3	Summary of Results of Adsorption of Toluene on Charcoal Cloth Using two different Canisters	139
6.1	Values of the Constants for Different Solvents at Different Inlet Concentrations	163

LIST OF PLATES

<u>Number</u>	<u>Title</u>	<u>Page No.</u>
4.1	General View of the Experimental Rig	93
4.2	Regeneration Oven	98
5.1	Parallel Flow Canister	135

ADSORPTION OF POLLUTANTS ON CHARCOAL CLOTH
IN SIMULATED GUARD FILTERS

submitted by SUBHASISH PODDER for the Degree of DOCTOR OF PHILOSOPHY in CHEMICAL ENGINEERING - 1984

SUMMARY

The removal of toluene, tetrachloroethylene, heptane and o-xylene from air by adsorption on activated charcoal cloth and the subsequent regeneration of the cloth in a stream of hot air was investigated. The above four solvents were chosen as typical organics, due to their less hazardous properties. They are all in reasonably common use and relevant detailed information is readily available about them.

The potential of charcoal cloth for use as a filter was studied. The experimental results could be represented by the Langmuir isotherm for the macropore region of the cloth. The micropore region is highly dependent on the manufacturing process due to variations in the quality of the cloth. This variation obstructs close correlation. The adsorbate-adsorbent mass ratio was obtained at breakthrough. The theoretical adsorbate-adsorbent mass ratio was calculated and gave a good approximation to experimental values.

Equations were developed to calculate the theoretical time required to reach an effluent concentration 10% of the inlet solvent vapour concentration. Experiments at various values showed reasonable correlation. The residual activity of the charcoal cloth remained fairly constant even after repeated regeneration.

The apparatus constructed for this study consisted of a solvent vaporiser, an air-solvent mixing section, a filter canister holding the cloth and a ventilated oven for regeneration. Four different designs of canister were tried and it has been found that perpendicular flow shows higher adsorption capacity than parallel flow, even though the former shows higher pressure drop.

A 0.2286 m (9") diameter canister was used to conform to typical fume cupboard dimensions. The results were compared with the 0.1524 m (6") diameter canister, and it was concluded that the smaller canister would be advantageous provided that the physical parameters, especially the volumetric flow rate were similar to the conditions used in the present research.

Keywords

Charcoal Cloth, Vapour Phase Adsorption, Regeneration, Kinetics, Carbon.

CHAPTER 1

INTRODUCTION

1. Introduction

Charcoal cloth is an advanced form of activated carbon, though the powdered and granular types are well known. In addition to its efficiency as an adsorbent, charcoal cloth can be handled more easily than the other activated carbons. Charcoal cloth has many applications. One such area is the ability of charcoal cloth to adsorb toxic vapours and thus helping to combat air pollution.

There is plenty of literature available on granular and powdered carbon, but the knowledge of charcoal cloth and its behaviour towards different adsorbates is limited. This thesis describes research carried out to extend that knowledge.

The difference between the properties of granular carbons and charcoal cloth are mentioned and includes results of experiments undertaken at CDE Porton Down which investigated the dynamic uptake of solvent vapours by these two different forms of activated carbon. A general survey of adsorption theory is thus presented followed by a discussion of various factors affecting adsorption. Kinetics of adsorption has been discussed in detail and different theories to calculate adsorption rate constant are included. The different techniques available for regeneration are outlined.

The performance of charcoal cloth in adsorbing toluene, tetrachloroethylene, o-xylene and heptane vapours from air mixtures under dynamic conditions has been studied. Details of the rig and experimental procedures are described.

Charcoal cloth is regenerated in an oven, using hot air, a mass spectrometer being used to measure the exit solvent vapour concentration. The effect of the number of regenerations upon the activity of charcoal cloth is also reported.

An important objective of this work is to design a suitable filter canister to be used in the exit duct of a fume cupboard. Four different types of canisters have been used in this research and their efficiencies in the adsorption process have been experimentally determined. The different factors important for the design are discussed along with some other workers' contribution in this field.

Mathematical models have been developed to express the equilibrium data and to calculate the adsorption capacity and adsorption rate constants. Number of layers of charcoal cloth has been related to the breakthrough time when effluent concentration reaches 10% of inlet solvent vapour concentration. An equation has been developed to calculate the minimum length of charcoal cloth necessary to have a particular effluent concentration.

Finally, a detailed discussion is included to explain some of the deviations from ideal values in relation to the experimental results. Suggestions for future work in this direction make up the concluding chapter of this thesis.

CHAPTER 2

LITERATURE SURVEY

2 Literature Survey

2.1 Brief History

Carbon has been known throughout history as an adsorbent, its usage dating back centuries before Christ (1). The ancient Hindus filtered their water with charcoal. In the thirteenth century sugar solutions were purified using carbon materials. Scheele (2) discovered that gases were adsorbed onto carbon and the decolourizing properties of activated charcoal were noted by Lowitz (3) some twelve years later. Early in the nineteenth century, powdered bone char was used as a purifying agent in the sugar industry. Bone char was initially discarded when it became saturated, but later regenerated when it became scarce. Late in the nineteenth century coconut char was found to have gas adsorbing powers (2) and it was about the same time Stenhouse (4) produced a decolourizing carbon by heating a mixture of tar, flour and magnesium carbonate. The development of more modern commercial activated carbons started at the beginning of the twentieth century. It involved selective oxidation of carbonaceous materials using carbon dioxide at elevated temperature, and in another process such materials were treated with metallic chlorides.

More recently, since 1970, Maggs (5) and the Ministry of Defence have developed a manufacturing process which produces a highly adsorptive charcoal in the form of charcoal cloth.

2.2 Manufacture of Activated Carbon

Activated charcoal has been manufactured from many cellulosic materials (2), the most popular present day starting materials are lignite, animal bones, coconut shells and wood. Activated charcoal cannot be described as a single chemical entity and must only be used as a general term. A typical variation is between manufacture of charcoal from coconut shells which produces a charcoal for gas adsorption, while bone char is more suitable for decolourization.

The manufacturing process of activated charcoal can take one of two forms, carbonisation of the base material, followed by oxidation or chemical dehydration of the carbonised intermediate. In the first instance, the base material is carbonised, in the absence of air, at about 200°C to 600°C. The resultant char is then oxidised at between 800°C and 950°C using steam or carbon dioxide. Alternatively, the carbonaceous base material is chemically dehydrated and charred at between 200°C to 650°C using dehydrating agents such as zinc chloride, sulphuric and phosphoric acid. Both of these methods yield highly porous charcoal and are currently used extensively in industry. A current list of activated charcoals is presented by Hassler (132).

2.3 Manufacture of Charcoal Cloth

Bailey and Maggs (5) have used a combination of both the oxidation and chemical dehydration methods to produce a reasonably strong, flexible charcoal cloth from viscose rayon. The rayon cloth is first soaked with a mixture of Lewis acids which are halides of zinc,

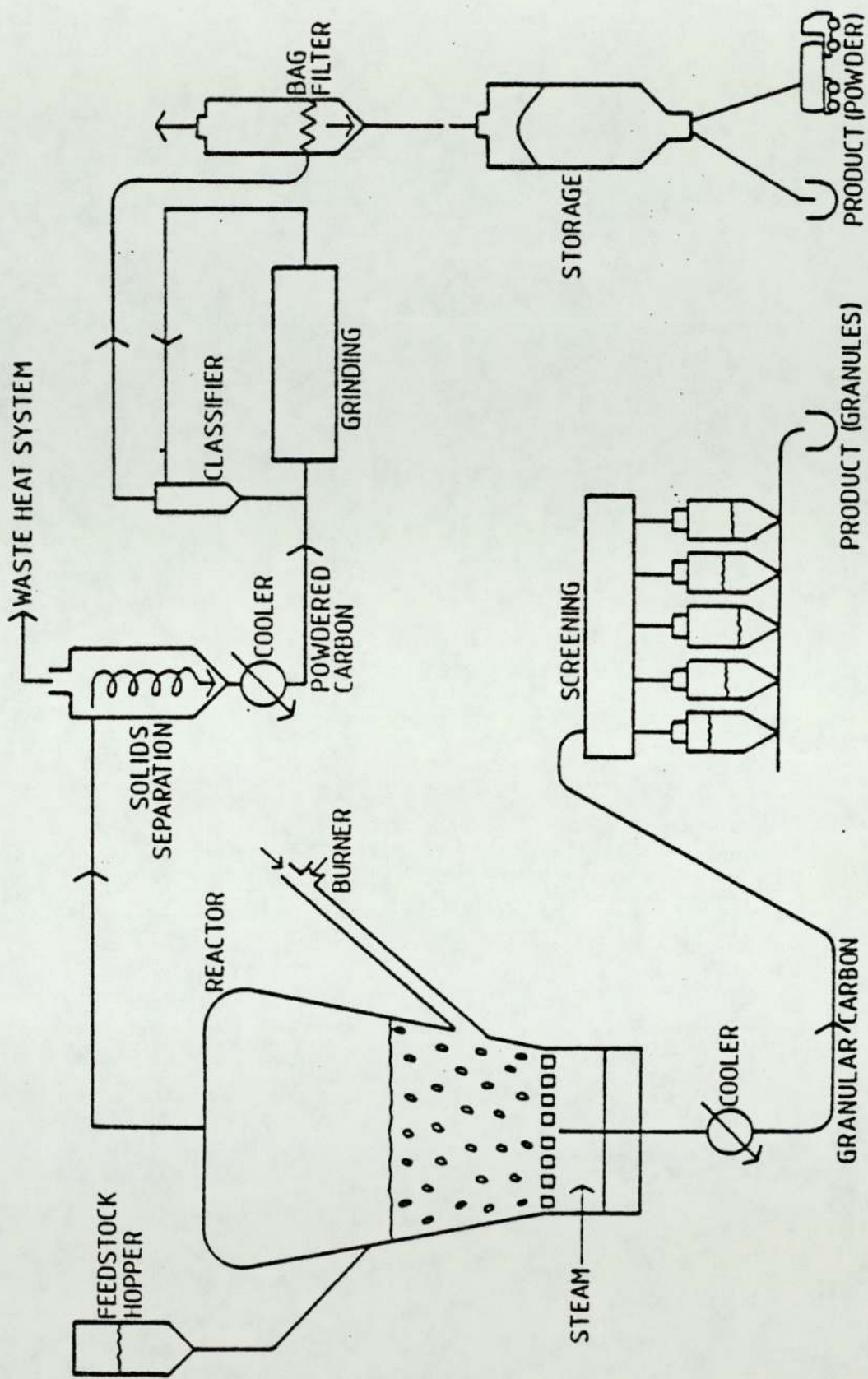


FIGURE 2.1 A PROCESS FOR THE PRODUCTION OF GRANULAR AND POWDERED CHARCOALS (13)

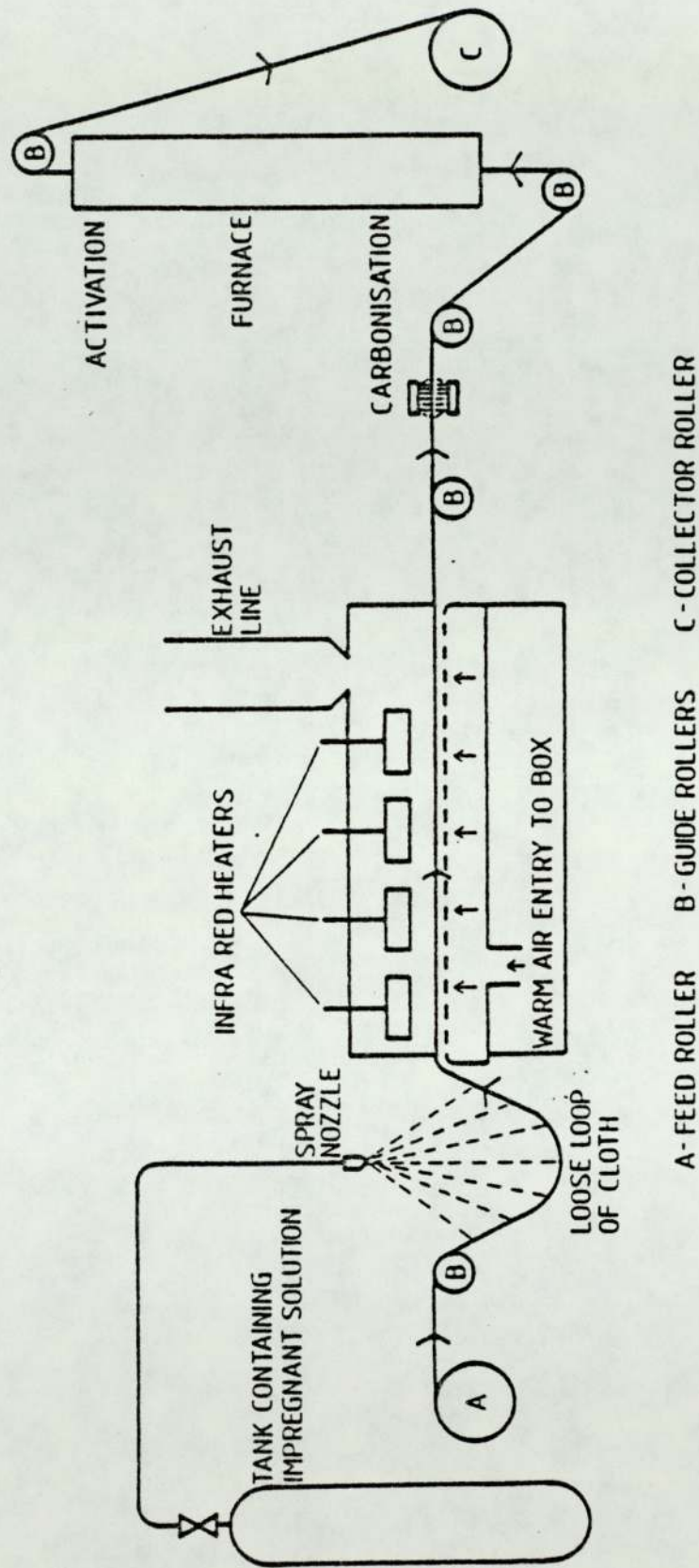


FIGURE 2.2 PROCESS FOR THE MANUFACTURE OF ACTIVATED CHARCOAL CLOTH (13)

magnesium, calcium, aluminium or iron. The Lewis acid solution should normally have a concentration of between 1 and 30% by weight of the Lewis acid. The temperature and concentration of the Lewis acid solution are both kept as low as consistent with a useful level of incorporation for a reasonable contact time. For some coated fibrous carbohydrates, such as viscose rayon cloths coated with ureaformaldehyde resin to give crease resistance, it may be necessary to use concentrations at the upper end of the range and temperatures of up to about 100°C. Considerable care is taken to optimise the extent of contact of the fibres with Lewis acid.

When a fibrous carbohydrate is dried after contact with the Lewis acid solution, it is generally found that adjacent fibres are weakly attached to one another possibly due to formation of a 'gel' type of structure on the fibre surface during contact with the Lewis acid solution. The resulting stiffness in the treated carbohydrate must be removed by flexing the dried material if good flexibility is to be obtained in the activated fibrous carbon finally produced. Flexing may be adequately achieved by manual working to restore suppleness or by a variety of mechanical treatments. A useful way is to pass the fibrous material around a smooth surfaced edge so that its direction changes fairly sharply and flexibility is restored.

Carbonisation is carried out at 250°C by heating in an inert atmosphere. The properties of the fibrous carbon may be influenced by the rate of heating. Slow heating

rates over wide temperature ranges have generally been advocated although the authors (6) indicated that slow heating rates between 280° and 320° are beneficial. Finally, oxidation in an activation furnace at 900°C in the stream of activating gas, usually steam or carbon dioxide, provides activated charcoal cloth.

2.4 Advantages of Charcoal Cloth over Granular Charcoal

Work carried out by Smith and Davies at C.D.E.

Porton Down indicates that charcoal cloth adsorbs more solvent vapour per unit weight than granular charcoal (7-11). Charcoal cloth has a marked advantage over the granular charcoal when humid conditions are examined (12). Smith and Davies (7-11) reported that the adsorptive capacity is reduced under humid conditions but the deterioration is much more exhibited in granular charcoal.

Charcoal cloth can be more easily handled and has less deterioration during handling than granular charcoal. The mass transfer zone is smaller for adsorption onto charcoal cloth as opposed to granular carbon. Dorman and Maggs (14) reported that a high rate of interaction by the small mass transfer zone is due to the very small 'granule size' of the cloth filaments - approximately 14 μm in diameter - comprising the threads.

Solvent	Condi- tions	Charcoal Type	Average % Weight Uptake (%)	Average Adsorption Rate (kmol s^{-1})
Chlorobenzene ($\text{C}_6\text{H}_5\text{Cl}$)	Dry	Charcoal Cloth	58.2	9.14×10^{-8}
		Granular Charcoal	34.8	9.14×10^{-8}
	80% RH	Charcoal Cloth	44.7	8.73×10^{-8}
		Granular Charcoal	16.0	11.79×10^{-8}
Chloroform (CHCl_3)	Dry	Charcoal Cloth	46.7	8.11×10^{-8}
		Granular Charcoal	27.9	8.13×10^{-8}
	80% RH	Charcoal Cloth	8.5	9.29×10^{-8}
		Granular Charcoal	2.4	8.62×10^{-8}
Trichloroethylene (C_2HCl_3)	Dry	Charcoal Cloth	52.1	6.10×10^{-8}
		Granular Charcoal	30.5	7.00×10^{-8}
	80% RH	Charcoal Cloth	18.6	6.27×10^{-8}
		Granular Charcoal	4.7	5.98×10^{-8}
Carbon Tetrachloride (CCl_4)	Dry	Charcoal Cloth	61.0	4.60×10^{-8}
		Granular Charcoal	29.5	5.32×10^{-8}
	80% RH	Charcoal Cloth	15.6	4.73×10^{-8}
		Granular Charcoal	1.7	4.43×10^{-8}
Penthrane ($\text{CHCl}_2 \cdot \text{CF}_2 \cdot \text{OCH}_3$)	Dry	Charcoal Cloth	56.1	11.07×10^{-8}
		Granular Charcoal	33.3	10.58×10^{-8}
	80% RH	Charcoal Cloth	32.5	10.28×10^{-8}
		Granular Charcoal	7.2	10.64×10^{-8}

Table 2.1 Average percentage weight uptakes and adsorption rates for the dynamic adsorption of particular solvents on charcoal cloth and granular charcoal under dry conditions and at 80% relative humidity (13)

2.5 Properties of Charcoal Cloth

The properties of charcoal cloth have been determined and extensively studied at C.D.E. Porton Down. The cloth properties will depend on the sub-microscopic pore structure which in turn may vary with the carbonising treatment as well as the time of subsequent activation and the temperature at which it is carried out. Since the raw material is a viscose rayon fabric, the thread and filament diameters may vary. Consequently, the cloth strength, flexibility and surface density will alter. The properties of charcoal cloth are summarized in Table 2.2 .

Surface Density	0.10 - 0.14 kg m ⁻²
Bulk Density	250 - 300 kg m ⁻³
Cloth Weight	> 0.11 kg m ⁻²
Specific Surface Area	> 1.3 x 10 ⁶ m ² kg ⁻¹
Air-flow Resistance	14m H ₂ O m ⁻¹ s ⁻¹ layer ⁻¹
Thermal Conductivity	0.08 watts m ⁻¹ K ⁻¹
Electrical Conductivity	20 - 50 ohm.square ⁻¹
Heat of Wetting	0.063 J kg ⁻¹ (benzene)
" " "	0.025 J kg ⁻¹ (silicone)

Table 2.2 Properties of charcoal cloth (13)

2.6 Applications of Charcoal Cloth

The main non-military demand for charcoal cloth is a limited use by the health service where cloth pads are used for dressing wounds. Typical uses include the application to ulcerated legs, faecal fistulae and athlete's foot. The patient's odour bandage can be re-used

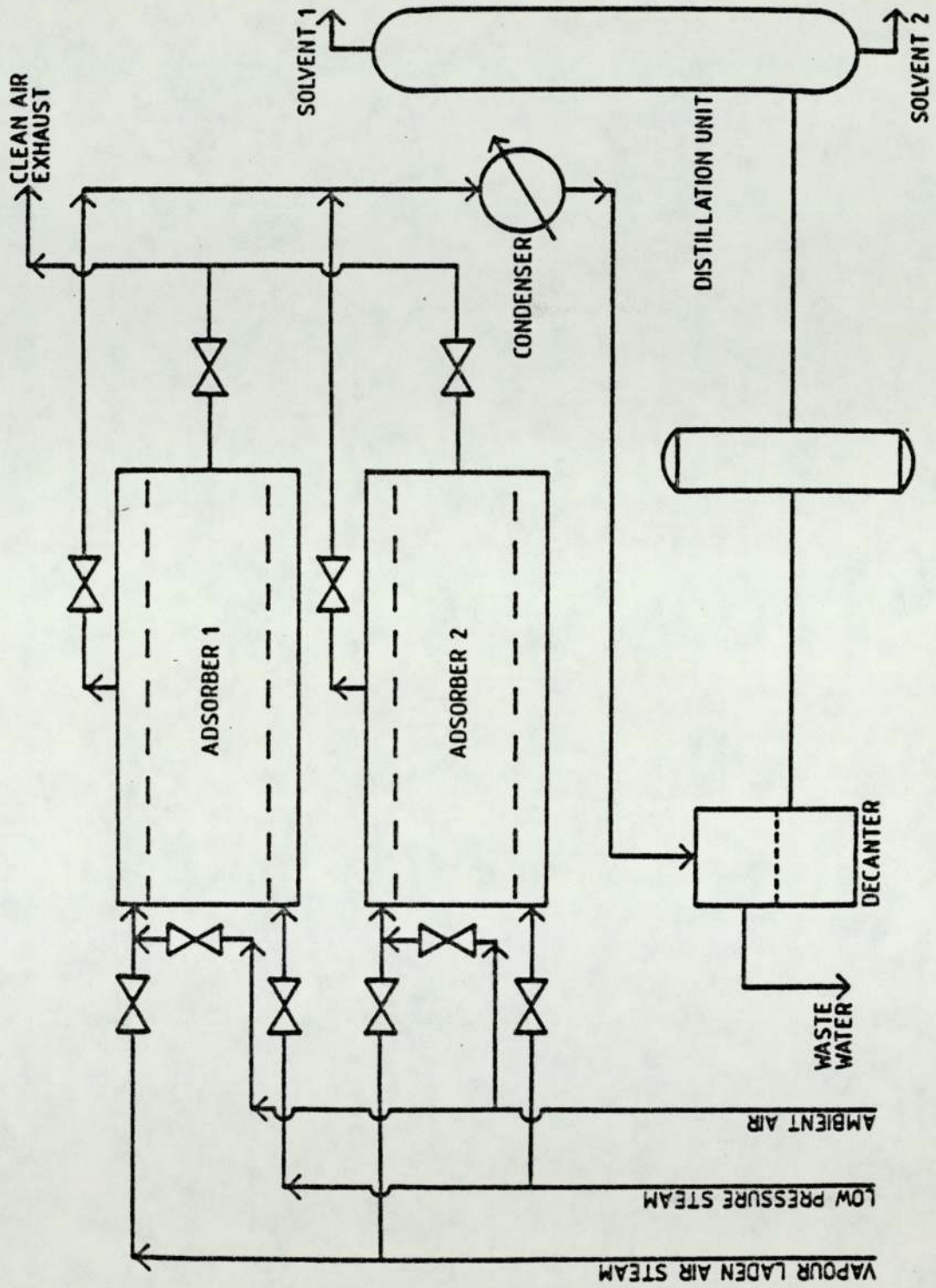


FIGURE 2.3 TYPICAL SOLVENT RECOVERY PLANT (13)

provided that soiling has not occurred.

Surgical masks containing charcoal cloth are comfortable, have a low breathing resistance and adsorb odour and vapours. Halothane protection is afforded to operating department staff; medical staff can inspect and dress wounds and mortuary staff can benefit from the odour adsorbing properties (15).

Charcoal cloth is used in air filtration devices. It can reduce SO_2 gas released into the atmosphere from combustion processes. Sulphur dioxide is a harmful vapour, especially when it reacts with atmospheric moisture to produce sulphuric acid and causes acid rainfall. Using charcoal cloth, sulphur might be recovered as a by-product and used again.

The same is true for solvents. The cost of solvents has steadily increased and great savings can be made in using efficient solvent recovery equipment. Emission of organic vapours from industrial and commercial sources is a contributor to photochemical smog and nuisance odours. Charcoal cloth can be used to trap those vapours and to purify the atmospheric air. The adsorption rate of various pollutant vapours in fume cupboard exit gases, their adsorption kinetics and the adsorption capacity of charcoal cloth for different vapours are the main technical objectives of this research programme. Particular attention is to be paid to the configuration of the charcoal cloth as a filter element for fume cupboards.

CHAPTER 3

ADSORPTION THEORY

3 Adsorption Theory

Adsorption is a process whereby vapour and liquid molecules adhere to a solid surface as a result of intermolecular or chemical forces. It is a spontaneous, exothermic process and is accompanied by a reduction in the free energy of the system as well as a decrease in entropy. The degree of adsorption depends on the nature and character of the adsorbate (the component fluid which is removed from the carrier stream) - adsorbent (solid surface) system (106)

The adsorbent is made up of numerous fine pores, which vary greatly between adsorbents which generally have a high surface area per unit weight. For example, active carbons have surface areas between 1.00×10^5 and $1.20 \times 10^6 \text{ m}^2/\text{kg}$ in commercial adsorption processes.

Equilibrium and kinetic data are needed to design adsorption units and data for the life of the adsorbent is also required if the adsorptive system is a regenerative one. If equilibrium data is not available, it can be determined from theoretical isotherms which have been postulated (106), and the better known isotherms are described in this chapter. The equilibrium distribution of adsorbate molecules between the adsorbent surface and vapour phase depends on a number of factors and their influence upon the effectiveness and efficiency of adsorption are discussed below. Adsorption mechanism and its thermodynamic analysis is included. The theory of rate constant and its calculation are outlined, and finally, the general theory related to regeneration and different methods of adsorbent regeneration are discussed.

3.1 Adsorption Isotherm

3.1.1 Introduction

Adsorption in a solid-liquid or solid-gas system results in the removal of solutes from liquid or gaseous medium and their concentration at the surface of the solid, until such time as the concentration of the solute left behind is in a dynamic equilibrium with that at the surface. At this position of equilibrium, there is a defined distribution of solute between the bulk of the solute and the solid adsorbent. The distribution ratio is a measure of the position of equilibrium in the adsorption process. It may be a function of the concentration of the solute, the concentration and nature of competing solutes or the temperature etc. of the solution.

The preferred form for depicting this distribution is to express the quantity of solute adsorbed per unit weight of solid adsorbent as a function of solute concentration at fixed temperature. An expression of this type is termed as adsorption isotherm. The adsorption isotherm is a functional expression for the variation of adsorption with concentration of adsorbate in bulk at constant temperature (16).

There are several theories and equations describing the quantitative relationship between adsorbates and adsorbents. The bulk of published experimental data pertaining to adsorption represents equilibrium measurements. Numerous empirical and theoretical approaches

have been proposed to characterize both pure component and multicomponent equilibria. However, no theory has yet been devised which on its own satisfactorily explains all the observations on a theoretically rigorous basis.

3.1.1.1 Single Component Adsorption

For a given gas and a unit weight of a given adsorbent, the amount of gas adsorbed at equilibrium can be expressed as a function of final pressure and temperature:

$$W = f(p, T) \quad 3.1$$

where W = Amount of gas adsorbed in liquid volume per unit weight of adsorbent

p = Equilibrium partial vapour pressure of the adsorbate

T = Absolute temperature

3.1.1.1.1. Langmuir Adsorption Isotherm

The Langmuir equation is the most important single equation in the field of adsorption. Although there are other isotherm equations that fit experimental data which do not obey the Langmuir equation, and others that fit the data over a wider range, in most cases the starting point in their derivations is the Langmuir equation (132).

According to Langmuir, adsorption is a physical process and the adsorbed layer is unimolecular. Forces acting in adsorption are concentrated at points of residual valency on the surface of a crystal. The force between the atoms of the adsorbent surface and the atoms of the adsorbed species decreases rapidly with the distance between the atoms. The adsorption equation can be

written as:

$$\frac{V}{V_m} = \frac{K_3 P}{1 + K_3 P}$$

3.2

where

V = Volume of vapour adsorbed per unit mass of adsorbent

V_m = Volume of vapour adsorbed per unit mass of adsorbent with a layer one molecule thick

K_3 = constant

Langmuir isotherm is based on a detailed molecular model which makes it possible to obtain particular expressions or even numerical values of the various parameters of adsorption equilibrium. It is clearly evident that even in the most favourable situations, this type of adsorption theory is applicable only to idealised, usually very simple models of the adsorbent and of the nature of adsorption interaction. Although the modern theory of physical adsorption is based on simple idealized models, Bering et al. believed that attempts at applying such theories even to a semiquantitative description of adsorption phenomena on real microporous adsorbents would not be suitable at all (17).

3.1.1.1.2 Freundlich Adsorption Isotherm

In the adsorption process gas molecules attach themselves to the solid surface through weak Van der Waals attraction resulting from unbalanced forces between adsorbate and adsorbent. Adsorption continues until an equilibrium is established between them. The Freundlich

isotherm is usually used to quantify this equilibrium relationship between the amount adsorbed and the amount in equilibrium. Mathematically it can be expressed as

$$V = K_1 p^{1/n} \quad 3.3$$

$$\text{or } \ln V = \ln K_1 + \frac{1}{n} \ln p \quad 3.4$$

where K_1, n are constants.

The above relationship may be linearized graphically by plotting the logarithm of the volume of the gas adsorbed and its equilibrium partial pressure. The actual plots show a slight curvature, especially at low temperatures, and the above equation, although very simple and convenient, can be regarded as approximately applicable for a small range of pressure only (18). In view of its empirical nature, its main use is as an interpolation formula.

3.1.1.1.3 BET Adsorption Isotherm

A multimolecular theory of adsorption was advanced by Brunauer, Emmett and Teller (19). The assumption in this case is that the same forces which are effective in condensation are also largely responsible for the binding energy of multimolecular adsorption. The generalization of the ideal localized monolayer treatment is effected by assuming that each first layer adsorbed molecule serves as a site for the adsorption of a molecule into the second layer and so on. The concept of localization prevails through all the layers and the forces of mutual interaction are neglected. The extent of the surface area rather than the nature of the adsorbent is an important factor.

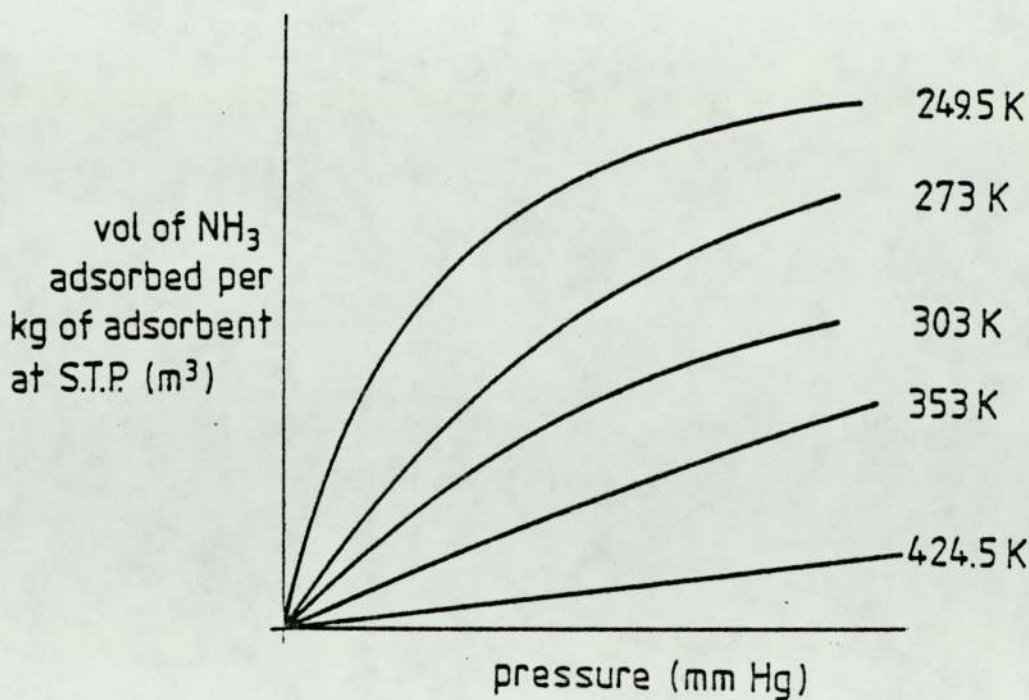


FIGURE 3.1 ADSORPTION ISOTHERMS FOR THE UPTAKE OF AMMONIA ON CHARCOAL (13)

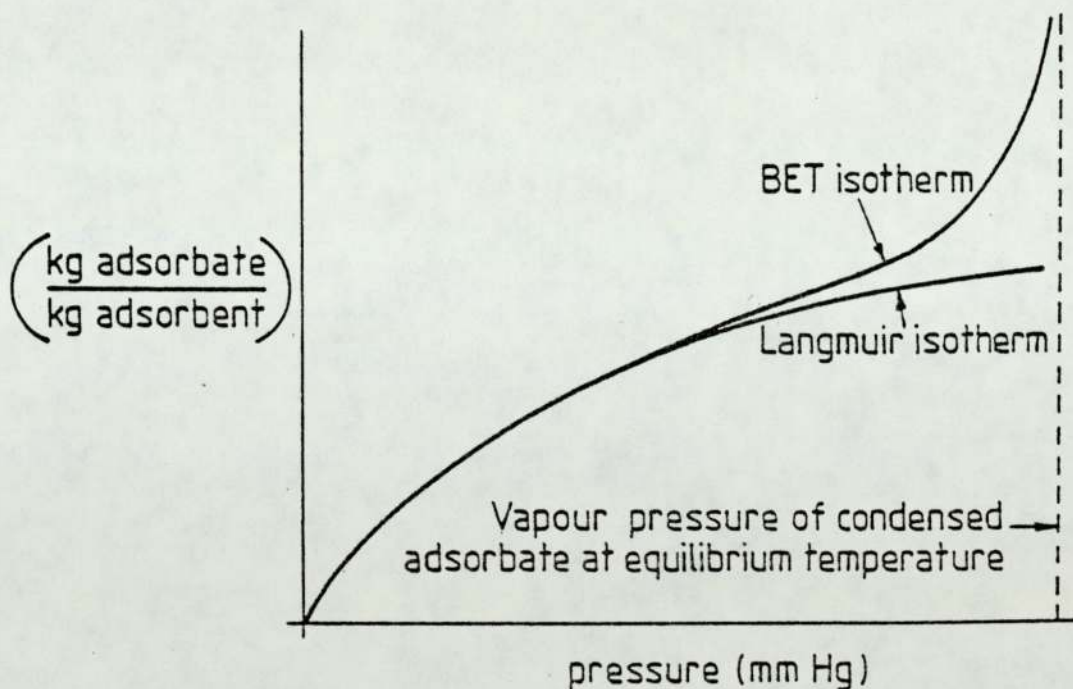


FIGURE 3.2 LANGMUIR AND BET ADSORPTION ISOTHERMS (19, 137)

The BET equation can be written as

$$\frac{V}{V_m} = \frac{K_2 \lambda_1}{(1-\lambda_1)[1-(1-K_2)\lambda_1]} \quad 3.5$$

where $K_2 = \text{constant}$

$$\begin{aligned} \lambda_1 &= \frac{P}{P_0} \\ &= \frac{\text{Adsorbed Vapour pressure}}{\text{Saturated vapour pressure}} \end{aligned} \quad 3.6$$

The BET equation has its limitations, such as the assumption that the heat of adsorption is constant over the entire surface coverage of the monolayer and that the monolayer is completed before the formation of secondary layers with a heat of adsorption equal to the heat of condensation. However, the consequent good agreement between the calculated and observed isotherms is accepted with the reservation that it may be due to the added flexibility conferred on the equation by the new parameters (20).

The perfect adsorption theory which takes all factors into account would lead to an isotherm equation of such complexity that it could not fail to describe any isotherm shape. Such an equation would also be quite useless because none of its constraints could be evaluated unequivocally. As Gorter and Frederikse (21) have noted, the kinetical BET theory gives a simple and valuable first picture of the phenomenon of adsorption but it seems difficult to correct its obvious shortcomings without destroying the simplicity which perhaps constitutes its main attraction.

3.1.1.2 Multi Component Adsorption

The study of mixed adsorption is of tremendous practical importance. Most of the technical applications of adsorption processes involve gas mixtures rather than one gas alone. The phenomenon of mixed adsorption is encountered in the recovery of acetone, ethyl and butyl alcohol from the gases produced in fermentation processes; in the recovery of benzene and light oil from illuminating gas and in the refining of helium. These are examples of mixed physical adsorption; mixed chemisorption forms the basis of many important industrial catalytic reactions. The compounds may mutually enhance adsorption, may act relatively independently, or may interfere with one another. Mutual inhibition of adsorption can be predicted to occur provided adsorption is confined to a single or a few molecular layers, the adsorption affinities are very similar, and there is not a specific interaction between solutes enhancing adsorption. Adsorption of one substance will tend to reduce the number of open sites and hence the concentration of adsorbent available as a driving force to produce adsorption of the other substances will be reduced. Therefore mutually depressing effects on adsorption rates may be predicted. The degree of mutual inhibition of competing adsorbates should be related to the relative sizes of the molecules being adsorbed, to the relative adsorption affinities, and to the relative concentrations of the solutes. Weber reported an earlier breakthrough for a mixture than for a single solute adsorbate (22).

3.1.1.2.1 Two Component Adsorption

In any mixed gas adsorption, a competitive adsorption model for equilibrium becomes an essential part of the mass transfer model used to predict the performance of adsorption beds. From a practical viewpoint, it is of course impossible to predict the breakthrough behaviour of every trace of adsorbate leaving the adsorption system. Nevertheless, having identified some of the key constituents, knowledge of their competitive adsorption behaviour can be used to determine the bed life of the adsorbent.

The ideal adsorption model should use the equilibrium data for each single component of the mixture. This condition must be met without great mathematical difficulties. Otherwise, the complexity of data collection or the mathematics will outweigh the model's usefulness as a practical aid in adsorber bed design.

So far, research with binary mixtures by Jain and Snoeyink (23) among others, has indicated the inadequacy of the Langmuir model as proposed originally by Butler and Ockrent (24). Radke and Prausnitz (25) put forward a model based upon fundamental thermodynamic principles which could be extended to any number of competing exponents. Good agreement between predicted and experimental results has been reported for several binary systems (26). Arnold (27) proposed that Raolt's law should be obeyed but only for adsorption sites having the same heat of adsorption. Using two additional assumptions, Arnold proposed a method for calculating mixture data from pure component adsorption isotherms. The disadvantages of this model are it is

thermodynamically inconsistent and separate numerical integrations are required for each vapour composition. Dubinin proposed an equation for a binary mixture of vapours (28):

$$\log W_{12} = \log W_0 - \frac{K_S}{\beta_{12}^2} \times 2.3 \left[RT \log \frac{P_0}{P_{12}} \right]^2 \quad 3.7$$

where $W_{12} = W_1 + W_2 \quad 3.8$

$$\beta_{12} = \beta_1 + \beta_2 \quad 3.9$$

$$P_{12} = P_1 + P_2 \quad 3.10$$

W_1 = Adsorbed amount in liquid volume per unit weight of adsorbent for component 1

W_2 = Adsorbed amount in liquid volume per unit weight of adsorbent for component 2

W_0 = Apparent limiting amount of adsorption for each adsorbent

K_S = A parameter for each system of adsorbent and standard adsorbate

β_1 = Affinity coefficient of component 1 for adsorption on activated carbon.

β_2 = Affinity coefficient of component 2 for adsorption on activated carbon

P_0 = Saturated vapour pressure

P_1 = Adsorbed vapour pressure for component 1

P_2 = Adsorbed vapour pressure for component 2

R = Gas constant

T = Absolute temperature

N_1 = Mole fraction of component 1 in the adsorbed phase

N_2 = Mole fraction of component 2 in the adsorbed phase

Three different mixtures were used and the difference between the theoretical and experimental values were small. But there is yet no evidence that the equation 3.7 is valid in a wide range of temperature and pressure for a variety of binary systems (29).

3.2 General Thermodynamic Relations

3.2.1 Single Component

In describing adsorption equilibria it is essential to consider thermodynamic functions - enthalpy, entropy, Gibbs free energy etc. which characterize these equilibria. To compute the significance of these functions in adsorption, it is necessary to agree on the choice of the standard states. In adsorption of vapours it is expedient to consider the standard state of an adsorbate in the form of a bulk liquid in equilibrium with its saturated vapour and an adsorbent at the same temperature in equilibrium with the adsorbate at a pressure P (fugacity f). This choice of the standard state leads us to differential thermodynamic functions. To obtain integral functions one should consider a pure adsorbent. If the system is at a temperature higher than the critical temperature of the adsorbate, the choice of the standard state requires special consideration.

As is well known, Gibbs differential molar free energy of adsorption ΔG is equal

$$\Delta G = RT \ln(P/P_0) \quad 3.11$$

For the differential molar entropy of adsorption ΔS , Bering et al. (30) reported that

$$\begin{aligned}\Delta S &= - \left(\frac{\partial \Delta G}{\partial T} \right)_a \\ &= - \left[\left(\frac{\partial \Delta G}{\partial T} \right)_{\theta_1} + \alpha_1 \left(\frac{\partial \Delta G}{\partial \ln a} \right)_T \right]\end{aligned}\quad 3.12$$

In the above equation, a is the adsorption value at an equilibrium pressure P

$$\begin{aligned}\theta_1 &= \text{degree of volume filling} \\ &= \frac{a}{a_0}\end{aligned}\quad 3.13$$

where a_0 is the adsorption value at $P = P_0$

$$\begin{aligned}\alpha_1 &= \text{thermal coefficient of limiting adsorption} \\ &= - \frac{d \ln a_0}{dT}\end{aligned}\quad 3.14$$

For the differential molar enthalpy of adsorption ΔH , Dubinin reported (31) that

$$\begin{aligned}\Delta H &= - (\text{Heat of adsorption}) \\ &= - q \\ &= \Delta G + T \Delta S \\ &= \Delta G - T \left[\left(\frac{\partial \Delta G}{\partial T} \right)_{\theta_1} + \alpha_1 \left(\frac{\partial \Delta G}{\partial \ln a} \right)_T \right]\end{aligned}\quad 3.15$$

ΔG can be calculated from equation 3.11 for any adsorption value, provided the adsorption isotherm is known.

Dubinin (32) assumed the conception of temperature invariance as a rational approximation for the numerous adsorption systems he himself studied. He concluded that for a given adsorbent-adsorbate system, the dependence of differential molar free energy on the degree of filling θ_1 is temperature invariant.

$$\therefore \left(\frac{\partial \Delta G}{\partial T} \right)_{\theta_1} = 0 \quad 3.16$$

Equation 3.12 becomes

$$\Delta S = -\alpha_1 \left(\frac{\partial \Delta G}{\partial \ln a} \right)_T \quad 3.17$$

The coefficient α_1 is always positive. The derivative $\left(\frac{\partial \Delta G}{\partial \ln a} \right)_T$ is also always positive, since at a constant temperature, adsorption increases with equilibrium pressure. That leads to a negative value of the differential entropy of adsorption. But this is not so when the degree of filling is small, as that makes the adsorption entropy positive and more work is required in this field.

3.2.2 Two Component

Myers and Prausnitz (33) applied the concept of activity coefficient. They based their thermodynamic equations for the adsorbed phase upon three assumptions:

1) The adsorbent is assumed to be thermodynamically inert, i.e. the change in a thermodynamic property of the adsorbent, such as internal energy is assumed to be negligible compared with the change in the same property for the adsorbing gas.

2) The adsorbent possesses a temperature invariant area which is the same for all adsorbates.

3) The Gibbs definition of adsorption corresponds to the usual volumetric technique of obtaining experimental adsorption isotherms.

Substituting pressure P and volume V with spreading pressure π and area A_1 , Myers and Prausnitz (33) have

rewritten the internal energy and Gibbs free energy equations:

$$dU = TdS - \pi dA_1 + \sum \mu_i dn_i \quad 3.18$$

$$dG = -SdT + A_1 d\pi + \sum \mu_i dn_i \quad 3.19$$

For the adsorbed phase, the mechanical work PdV is substituted by πdA . In physical adsorption π is positive, and therefore the system does work on the surroundings during the conceptual process of increasing the adsorbent area. It was emphasized that spreading pressure is as much a fundamental thermodynamic variable as entropy or internal energy (33).

3.3 Factors Affecting Adsorption

3.3.1 Porous Structure of Adsorbent

Adsorbent pores are voids or cavities in solids which usually communicate with each other. Their shapes and sizes differ widely and depend on the nature of the adsorbent and the method by which it is obtained. The linear sizes of pores of any cross-sectional shape are characterized by the ratio of the area of the normal cross section of the pore to its perimeter. This ratio has the dimension of length and is termed hydraulic mean diameter. The conception of adsorbent pore varieties is based on the differences in the mechanisms of adsorption and capillary condensation occurring in them (31).

With regard to adsorption in porous adsorbents, Dubinin divided all the pores into three basic varieties depending on the pore size (17, 28, 31).

3.3.1.1 Macropores

The largest variety of active carbon pores are macropores. Smooth surfaces may be regarded as a limiting case of such a porous structure. The upper limit of the curvature radius is large and the lower limit may be taken between 1000 to 2000A°. This choice of the lower limit means that the volume filling of macropores by the mechanism of capillary condensation of vapour can take place only at relative pressures very close to unity. Therefore, in conventional adsorption apparatus this phenomenon is practically indistinguishable from normal bulk condensation corresponding to a plane meniscus. Thermodynamically, it is convenient to characterize such a porous structure by the value of surface area with no allowance for its curvature.

3.3.1.2 Transitional pores

Smaller pores, for which besides the surface area, the curvature should also be considered. For such pores as for macropores, the linear dimensions characterizing them may be considered to exceed by far those of the adsorbate molecules. On the surface of these pores, monolayer and multilayer adsorption takes place. Besides this, in a certain easily realised range of relative pressures volume filling of these pores by the capillary condensation mechanism takes place. It may be assumed that the curvature radius of the surface of such pores are within the range $500 - 1000\text{A}^\circ > r > 15 \text{A}^\circ$. These pores are known as transitional pores.

3.3.1.3 Micropores

The smallest variety of pores are known as micropores. Their effective radii are usually smaller, i.e. 10 to 15 Å and they are commensurate with the molecules adsorbed. In some cases, micropores are inaccessible to molecules of certain adsorbates for sterical reasons. The entire volume of micropores represents a space where an adsorption field exists. At any point of this space, adsorption potentials set up by the opposite walls of the pores are superimposed on each other. Since there is an adsorption-force field in the entire volume of micropores, adsorption of vapours in micropores leads to their volume filling and the concept of layer-by-layer filling lose their physical significance.

Dubinin reported (31) that such a systematic classification of the pores of adsorbents by no means implies that it is simultaneously the classification of the adsorbents themselves. On the contrary, as a rule one and the same adsorbent may contain pores of all the three types. Therefore a comprehensive description of adsorption on a particular real adsorbent should include the peculiarity of phenomena of all pore varieties. It is very usual to find adsorbents where only one of the pore varieties is very well developed compared to others. Besides, the volume filling of micropores and transitional pores occur in different intervals of equilibrium pressures. The above classification of pores which is of a general nature is particularly convenient when applied to

activated carbons with a polymode volume distribution of pores according to their radii (34).

3.3.2 Physical and Chemical Factors

3.3.2.1 Temperature

Adsorption reactions are normally exothermic and the extent of adsorption generally increases with decreasing temperature. Enthalpy change in adsorption is usually of a similar order to that of condensation. Thus small variations in temperature do not change the extent of adsorption to a significant extent (35). Dedrick and Beckmann (36) conducted three experiments at three different temperatures ranging from 30° to 60°C. They found that the rate increases rapidly with increasing temperature but the equilibrium amount adsorbed decreases very little.

Early developments relating adsorption of micropores were based on Polanyi's potential theory of adsorption. With time it became more and more obvious that the initial principles of the potential theory have no physical meaning for adsorption in micropores. However, the basic principle of the theory concerning the temperature invariance of adsorption due to temperature independent dispersion interaction is true precisely for microporous adsorbents. Dubinin (28) found that using the Dubinin-Polanyi equation, the experimental points at different temperatures make a good fit on straight lines, indicating the constancy of the limiting volume of the adsorption space of each carbon. Those

experiments also point to the constancy of relative differential molar work of adsorption and their independence of the microporous structure.

3.3.2.2 Moisture in the Air

Water vapour is generally present in the atmosphere and an adsorbent filter will very probably contain adsorbed water when in use. Charcoal cloth filters will still be effective in the protection against other vapours and the reason for this lies in the ability of many vapours to displace the adsorbed water. Maggs (37) found that the efficiency of filters in general is reduced but more strongly adsorbed vapours are less affected than those which are weakly adsorbed. The extent of the effects of moisture is not readily predicted because it will vary with the adsorbate and its concentration, as well as with bed depth, flow rate and the microporous structure of charcoal cloth.

For some vapours such as phosgene and hydrogen-chloride, efficiency increases with increasing humidity. In these cases hydrogen bonds are formed between adsorbate and the water molecules.

The popularity of charcoal cloth as a protective adsorbent system stems from the fact that water molecules are held far less strongly on carbon surfaces than on those of other adsorbents such as silica gel or alumina; and also that most common vapours are much more strongly adsorbed on carbon than water. Therefore, the displacement of adsorbed water by vapours takes place readily on a

charcoal cloth surface. Atkinson et al.(120) also confirm the above fact.

3.3.2.3 Influence of pH Values

James S. Mattson et al. (38) reported that adsorption of weak acids differs with change in pH. Increasing pH decreases the solubility and lowers the adsorption capacity. Such uniform behaviour indicates an increase of molecular species and decrease of ionic species simultaneously. Similar correlations have been observed by Rovinskaya and Koganovskii (121) for salicylic acids on charcoal and by Schwartz (39) for 2-4-dichlorophenoxyacetic acid on charcoal. There is a marked decrease in the adsorption capacity on going from pH 3.0 to pH 7.0 and a smaller decrease from pH 7.0 to pH 11.0. The increase in adsorption capacity with a lowering of pH is attributed to the increase in hydrogen ion concentration. The protons increasingly bind to the available sites on the carbon and in turn enhance the removal of the acid anions. This augmentation of the total adsorption must decrease at some point as the pH is lowered because the percent of ions decreases rapidly (40).

A list of some of the aromatic acids which have been adsorbed on activated carbon at different pH is shown in Table 3.1.

No.	Acid	pK _A	pH of Solution	Adsorbate Adsorbent (moles kg ⁻¹ x10 ³)
1.	Benzoic	4.20	3	489
			7	113
			11	67
2.	-2,4-dichloro	2.76	3	651
			7	147
			11	69
3.	-3-amino-2,5-dichloro	3.40	3	510
			7	127
			11	51
4.	-3-nitro-2,5-dichloro	3.23	3	491
			7	120
			11	72
5.	-2-methoxy-3,3-dichloro	1.94	3	313
			7	149
			11	59
6.	Phenoxyacetic	3.03	3	436
			7	86
			11	43
7.	-4-chloro	2.36	3	560
			7	180
			11	133
8.	-2,4-dichloro	3.31	3	607
			7	205
			11	135
9.	-2,4,6-trichloro	3.35	3	666
			7	216
			11	127
10.	2,4-dichloro-phenylacetic	3.92	3	630
			7	218
			11	54

Table 3.1 Properties of aromatic acids and equilibrium data for their adsorption on activated carbon (40)

3.3.2.4 Functional Groups

In the adsorption of substituted aromatics it has been shown that the substituent present in the aromatic ring is not directly involved in the solute adsorption. The interaction of the surface ring as a whole with the surface of carbon is the major factor. The interaction takes place through the pi-electron system of the ring. There is considerable evidence in the literature of the formation of donor-acceptor complexes between phenol and several kinds of electron donors (41). Two factors will influence the stability of such complexes; (a) the availability of electron density in the donor, and b) the electron affinity of the acceptor.

It is well known that the electron density of an aromatic ring is strongly influenced by the nature of the substituent groups. A nitro group acts as a strong electron drawing group in reducing the overall electron density in the pi-system of the ring. Thus nitro-substituted aromatic compounds act as acceptors in such complexes and form stronger donor-acceptor complexes with a given donor than phenol, because the phenol has no low-lying acceptor orbitals and forms complexes with very strong donors. The isotherms for m-nitrophenol and p-nitrophenol are essentially identical, indicating that the net energy of interaction at the surface is comparable for both of them (38).

Drago et al. (42) have shown that phenol forms strong donor-acceptor complexes with oxygen groups

and the oxygen group dipole moment is the determining factor in the strength of the donor-acceptor complex formed. Carbonyl oxygen has a larger dipole moment than carboxylic acid oxygen and thus would be accepted as a stronger donor. These aromatic compounds adsorb on active carbon by a donor-acceptor complex mechanism involving carbonyl oxygens of the carbon surface acting as the electron donor and the aromatic ring of the adsorbate ring as an acceptor.

3.3.2.5 Surface Complexes on Carbons

Many studies of chemisorption of gases and vapours have been made on carbons of diverse forms, ranging from well defined crystalline materials, such as diamond and graphite, to amorphous or microcrystalline structures, such as activated carbons and cokes. In carbons, the fraction which exists in the disordered form is more susceptible, while the fraction which shows some degree of well-ordered parallel stacking, is less susceptible to chemisorption of gases and vapours. The disordered fraction is higher in microcrystalline carbons than in crystalline carbons. At the same time there are many exposed defects, dislocations and discontinuities in the layer planes of the microcrystalline carbons, apart from the edges of carbon layers. Such sites, called the 'active sites' are associated with high concentrations of unpaired electron spin centres and are expected to play a significant role in chemisorption. The surface carbon atoms located at the active sites show a strong

tendency to chemisorb other elements, like oxygen, hydrogen, nitrogen and sulphur and give rise to nonstoichiometric stable surface compounds, called "surface complexes".

Oxygen is adsorbed more readily than many other elements and carbon-oxygen complexes are by far the most important in influencing surface reactions, surface behaviour and electrical and catalytic properties of carbon. Smith (43) suggested that when oxygen is adsorbed on a carbon surface, it undergoes a chemical change. He found that adsorption of oxygen on charcoal did not cease even after a month; and that while nitrogen and other gases adsorbed on charcoal could be easily desorbed as such, oxygen could be removed only on strong heating and then as carbon dioxide. Rhead and Wheeler (44) concluded that oxygen combines with surface carbon directly to form a physicochemical complex, C_xO_y , of variable composition which decomposes over a wide range of temperature, giving a mixture of carbon monoxide and carbon dioxide. The methods of formation of carbon-oxygen surface complex may be classified into two categories: methods involving reactions with oxidizing gases and methods involving reactions with oxidizing solutions. The most common gases are oxygen, water vapour, carbon dioxide and oxides of nitrogen. Some of the oxidizing solutions used are acidified potassium permanganate, nitric acid, mixtures of nitric and sulphuric acids, chlorine water, sodium hypochlorite and ammonium persulphate.

It is common practice to classify the surface oxides as basic or acidic. Acidic surface oxides are formed when the carbon is exposed to oxygen at temperatures between 200 and 500°C or by the action of aqueous oxidizing solutions. Basic surface oxides, on the other hand, are formed when a carbon surface is first freed from all surface oxides by heating in a vacuum or in an inert atmosphere and then brought in contact with oxygen only after cooling to low temperatures. Carbons outgassed at high temperatures and exposed to oxygen between 200° and 700°C have been shown (45) to adsorb appreciable amounts of strong bases but little of strong acids. The optimum temperature for the development of maximum capacity to adsorb bases has been shown to lie close to 400°C. This fact led some workers (46) to think that the base adsorption capacity of carbon is closely related to its oxygen content. On the other hand, if outgassed carbons are exposed to oxygen either below 200°C or above 700°C, they adsorb strong acids but very little strong bases. There is no definite temperature range within which exposure to oxygen results in exclusive development of acid character and outside of which it results in exclusive development of basic character. Actually, there is a certain overlap of temperature where one type of character starts declining and other type starts rising. Base adsorption capacity of carbon, when it is acidic in nature, is far in excess of its acid adsorption capacity, when it is basic in character (47).

Interaction of carbon with the halogens other than fluorine, has also been investigated by several workers. The maximum temperature for chemisorption has been found to be 400°C for chlorine (48), 500°C for bromine (49) and 300°C for iodine. The reaction also involves appreciable dehydrogenation of the carbon resulting in formation of hydrogen halide. The chemisorption has been found (50) to involve addition at the unsaturated sites and substitution of hydrogen associated with the edge carbon atoms. Since unsaturated sites are rather few in carbon blacks, the major portion of the halogen is fixed by substitution process. In charcoals and activated carbons, the hydrogen content is low, but unsaturated sites are high, hence the bulk of the fixation takes place by the addition process. The relative amounts of fixation of the halogens under respective optimum conditions decrease in the order $\text{Cl}_2 > \text{Br}_2 > \text{I}_2$. The stability of the surface complexes also decreases in the same order (51).

Study of simultaneous chemisorption of oxygen and chlorine at 400°C shows that while both the gases compete against each other for fixation at the unsaturated sites, there are other separate sites where fixation of oxygen and chlorine can take place independently of each other (52). These sites, for the fixation of oxygen are provided by certain active centres where formation of acidic carbon-oxygen complexes and quinonic or phenolic groups is possible. They also help the fixation of chlorine by edge carbon atoms associated with hydrogen. Oxygen has been found to be more rapidly chemisorbed at the unsaturated sites than chlorine under similar conditions.

Chemisorption of sulphur by carbons on suitable treatment has also been investigated by different workers. Treatment of carbon blacks with aqueous hydrogen sulphide at room temperature has been shown to result in appreciable fixation of sulphur almost exclusively at the unsaturated sites (53). The amount of sulphur fixed is seen to be almost equivalent to surface unsaturation present initially in the carbon black. If there is no surface unsaturation in a carbon black, there is no fixation of sulphur.

The carbon-sulphur complexes have been found to be stable (53). The desorption of the combined sulphur commences on evacuating at temperatures $>600^{\circ}\text{C}$, largely as hydrogen sulphide and carbon disulphide and is completed only at 1000°C . This establishes a close analogy between carbon-sulphur and carbon-oxygen surface complexes since the combined oxygen is known to come off as water vapour and oxides of carbon under similar conditions (47).

The effect of chemisorbed oxygen on surface properties such as acidity, polarity, hydrophilicity and selectivity in adsorption from binary solutions has been covered in literature by Puri (47). He concluded that it is the presence of the acidic carbon-oxygen complex and not the total combined oxygen as such which imparts acidic, polar and hydrophilic character to the surface. The rest of the combined oxygen has little or no effect on these properties (54).

3.3.2.6 Nature of the Adsorbate

Adsorption of a solute on a particular adsorbent is related to its various physical parameters namely solubility, polarity, length of the chain, molecular weight etc. Adsorption from solution is closely related to the solubility of the solute in the solvent. An inverse relationship can be defined between the extent of adsorption of a solute and its solubility according to Lundelius' rule (109). Adsorption of an aliphatic series of organic acids on carbon from aqueous solution increases in the order of formic-acetic-propionic-butyric, whereas the order is reversed for adsorption from toluene (108). In both cases adsorption increases with decreasing solubility of the solute in the solvent. For adsorption of iodine from various solvent systems on carbon, observed ratios for uptake from CCl_4 , CHCl_3 , and CS_2 are 1:2:4.5 respectively (109). These ratios are close to the inverse ratios for the solubility of iodine in these solvents. Hansen and Craig (110) found that adsorption isotherms for an homologous series of fatty acids are nearly superimposable when plotted as amount adsorbed versus equilibrium concentration of solute reduced through division by the solubility of the solute, rather than against the equilibrium concentration of solute in the solution phase. The effects noted relative to solubility-adsorption relationships can be interpreted by postulating the necessity of breaking some form of solute-solvent bond before adsorption can occur. The greater the solubility, the stronger the solute-solvent

bond and the smaller is the extent of adsorption.

The solubility of organic compounds in water decreases with increasing chain length because the compound becomes more hydrocarbonlike as the number of carbon atoms become greater. This forms the basis regarding the relationship between adsorption and the nature of the solute - Traube's rule. Adsorption from aqueous solution increases as an homologous series is ascended, largely because the expulsion of increasingly large hydrophobic molecules from water permits an increasing number of water-water bonds to reform.

Molecular size is of significance also as it relates to rate of uptake of organic solutes by porous active carbon if the rate is controlled by intraparticle transport, in which case the reaction generally will proceed more rapidly with smaller adsorbate molecule, within a given class of compound. Weber (55) found that rates of adsorption of a series of sulphonated alkylbenzenes of different molecular size clearly demonstrate a decrease in molar rate of uptake with increasing molecular weight in rapidly-stirred, batch reactors where intraparticle transport is rate-limiting; on a weight uptake basis, the rate is essentially constant. It must be borne in mind that the rate-independence on molecular size can be generalized only with a particular series of molecules and is expected in rapidly-agitated batch reactors.

Variations in geometry of molecules seem to have much smaller effects on equilibrium conditions than increases in chain length. Studies on the adsorption of three sulphonated alkylbenzenes substituted at the 2,3 and 6 positions on the hydrocarbon chain respectively, showed virtually no variations in constants for the Langmuir equation (111). The position of substitution in hydroxy- and amino benzoic acids has been reported as having a marked effect on adsorption on carbon, the sequence of decreasing strength of adsorption being ortho, para, and meta.

Many adsorbents have the potential of existing as ionic species. Acids such as sulphonated alkylbenzenes, fatty acids, phenolic species, amines are a few of the numerous compounds having the property of ionizing under appropriate conditions of pH. Activated carbon carries a net negative surface charge which is believed to be of significance for adsorption. Also many of the physical and chemical properties of certain compounds undergo drastic changes upon ionization. The bulk of the observations related to ionization effects on adsorption seem to point to the generalization that as long as the compounds are structurally simple, adsorption is at a minimum for the charged species and at a maximum for the neutral species. As compounds become more complex, the effect of ionization becomes of decreasing importance. Weber (56) reported decreasing adsorption for many different organic acids. He found that adsorption of

propionic acid on carbon decreases markedly with increasing pH to a minimum in the range pH 3.5 to 5.5 and succinic acid has been observed to decrease to a minimum between pH 4.0 and 7.0.

There are also amphoteric compounds which have the capacity to act both as an acid and a base. Studies on this type of compound indicate an adsorption maximum at the isoelectric point (111). This again accords with the observation that adsorption is at a maximum for neutral species.

Molecules that have dipoles, such as organic halides, ethers, ketones etc., will be attracted by the electrostatic field emanating from the surface of an ionic crystal. As the electrostatic field is not very strong and decreases with increasing distance, a significant high contribution to the adsorption energy can be expected only if a dipole of sufficiently high dipole moment is situated at such a place in the polar molecule that it can approach to within a very short distance of the surface. Hydrogen bearing compounds like water, ammonia, phenols, alcohols, possess dipoles between the hydrogen atoms of the functional groups and the atoms to which these hydrogen atoms are bound. All these dipoles are situated near the periphery of the molecules. These peripheral dipoles all point with their positive end towards the outside of the functional group. As the ion arrangement of most ionic surfaces is such that the negative ions form the outside layer,

these peripheral dipoles show a strong tendency to take up an oriented position perpendicular to the surface and the hydrogen atom of each dipole tends to make a close contact with one of the negative surface ions (57).

A dipole that is not situated near the periphery of the adsorbed molecule, makes a far smaller contribution towards the adsorption energy than do peripheral dipoles. Such nonperipheral dipoles may cause enough difference in adsorption energy to effect a preferential adsorption between molecules that otherwise would show equal adsorption energies. They may also lead to a fixed and an oriented position of the adsorbed molecule instead of an adsorption of more or less freely-moving and rotating molecules (57).

A general rule for prediction of the effect of solute polarity on adsorption is that a polar solute will prefer the phase which is more polar. A polar solute will be strongly adsorbed from a nonpolar solvent by a polar adsorbent, but will much prefer a polar solvent to a nonpolar adsorbent. Polarity of organic compounds is a function of charge separation within the molecule. Most of the assymmetric compounds are more or less polar, but several types of functional groups tend to produce higher polarities than the others. Hydroxyl, carboxyl, nitro, nitrile, carbonyl, amine are some of the examples. Ethanol is polar because it has an incremental negative charge on the hydroxyl and positive charge on the ethyl group. Solvation by water involves formation of a

hydrogen bond from one of the positively charged hydrogens of the water to a group bearing more or less of a negative charge along with some bonding in the reverse direction to the water oxygen. Water solubility is then expected to increase with increasing polarity. Adsorption then decreases as polarity increases (61).

3.3.2.7 Surface Area

Adsorption is a surface phenomena. The amount of adsorption is proportional to specific surface area. It can be defined as the portion of the total surface area available for adsorption. Adsorption capacity increases with increasing surface area. Adsorption rate thus should exhibit a monotonic increase with some function of the inverse of the diameter of the adsorbent particles. This inverse relationship holds also for porous adsorbents when the transport rate to internal surface areas is controlled by an external resistance. But in cases where intraparticle diffusion controls the adsorption rate, the variation should be with the reciprocal of some higher power for the diameter (122).

Alteration in the adsorbent surface can be caused by external factors such as heat, impurities etc., or by the adsorption process itself. The alteration can take place in both the positive and negative sense. The process of increasing the surface is called activation. The process of decreasing the surface by heat is called sintering. All adsorbents sinter when heated to very

high temperatures. Pure iron catalyst used for ammonia synthesis begins to sinter at 350°C whereas charcoal sinters only above 1000°C (58). The mechanism of sintering differs from one another. The most common cause is the growth in particle size. High temperature causes the small particles composing the adsorbent to fuse together into larger ones, resulting in a decrease of the surface. The structure of the surface also changes as a consequence of high temperature heating. One type of developed crystal face is replaced by another with a resulting change in the heat of adsorption. Such effects are much more marked in chemisorption than in physical adsorption. Brunauer and Emmett (59) concluded that sintering does not merely reduce the area but also changes the body-centred cubic lattice into a face-centred cubic lattice structure. Heating may also change the chemical nature of the surface, which in turn may cause a change in the heat of adsorption. McGarack and Patrick (60) noted that the decrease in adsorption was not due to a decrease in the surface caused by particle growth, but rather to a decrease in the heat of adsorption produced by changing the chemical composition of the surface.

Activation is the opposite of sintering. It is the increase of the adsorptive power of a substance. Activation may also be produced by heating. Chemical agents are used along with heat. Thus charcoal can be activated to some extent by heat and vacuum alone but

to get the most active product air, steam or some other activating agent is to be used. One of the most common methods of activating metallic catalysts is the alternate oxidation and reduction. Another activating mechanism consists in removing a part of the adsorbent to create a large internal surface, or in removing certain adsorbed impurities that block the entrance to an already existing internal surface. The removal of the water of crystallization from a hydrate usually creates a large internal surface. Activation is always accompanied by a change in composition of the surface of the adsorbent. Charcoal cloth is activated by soaking rayon cloth in Lewis acids, dried and then carbonising in an inert atmosphere as has been mentioned in section 2.3.

3.3.2.8 Surface Tension Effects

Adsorption is a process in which solute is extracted from one phase and concentrated at the surface of another. Surface reactions of this type occur as a result of the forces active within the phase boundaries. These forces result in characteristic boundary energies. Classical chemistry defines the properties of a system by the properties of its mass, for surface phenomena the significant properties are those of the surface or boundary.

A very usual feature of surface energy occurs when a drop of water is placed on a plate. The water drop will resist spreading and attempt to retain a

nearly spherical shape. The water tries to minimize its surface area and hence the surface energy. This phenomenon - the development of a tension at the surface which tends to keep the drop from spreading into a thin flat layer results from attractive forces between molecules of water within the drop. Because molecules of water are attracted to one another by cohesion forces more strongly than they are by adhesion forces to molecules of the solid plate or molecules of air at the liquid-solid and liquid-gas interfaces respectively, the water molecules at the surface will be pulled mainly towards the interior of the drop. The liquid drop thus tends to decrease its exposed surface as a result of the surface tension developed by molecular cohesion forces within the drop.

A pure liquid always tends to reduce its free surface energy through surface tension, which is quantitatively equal to the amount of work necessary to compensate the natural reduction in free surface energy. From a molecular point of view, enlarging a surface requires the breaking of bonds between molecules making up the liquid phase and the formation of bonds between molecules of different phases. To increase the liquid surface an input of work is required in excess of that necessary to compensate the tension at the surface.

Large numbers of soluble materials can effectively alter the surface tension of the liquid. They are known as wetting or surface-active agents. If a material which

tends to be active at the surface is present in the liquid system, a decrease in the surface tension will occur upon movement of the solute to the surface. Migration of the substance to the surface results in a net reduction of the work required to enlarge the surface area, the reduction being proportional to the concentration of the adsorbate at the surface. Hence the energy balance of the system favours the adsorptive concentration of such surface-active substances at the phase interfaces. A solute that decreases the surface tension must be concentrated at the surface because the solvent molecules have a smaller attractive force for the molecules of solute than for each other. Any lowering of surface tension of the adsorbate help the adsorption system (66).

3.3.2.9 Chemical Reactions on Surfaces

The rates of many reactions are influenced by solid surfaces. This fact is frequently a serious complication to the study of homogeneous gas reactions, in that an appreciable amount of reaction may occur on the surface of the reaction vessel and must be allowed if the homogeneous reaction is the one of special interest. It has been found that many processes can be made to occur much more rapidly by the introduction of a suitable surface upon which the reaction proceeds. The solid material is then said to catalyze the reaction. In particular, a number of processes that do not occur homogeneously at an appreciable rate can be made to do so on surfaces (62).

It is generally accepted that chemisorption plays an important role in surface catalysis and at least one of the reactants or activated complexes should be chemisorbed on the catalyst surface (63). Zelinski (64) finds that oxygen chemisorbed on carbon imparts either oxidizing or reducing power to the surface, depending upon the adsorption temperature and oxygen pressure. Exposure of carbons to oxygen or carbon dioxide at different temperatures and pressures drastically changes the acid and base adsorbing power of the surface. The major conclusion to be drawn from numerous findings is that there is more than one type of carbon-oxygen complex which can form on a carbon surface.

In chemisorption, it is known that the surface atoms must have free valence electrons in order to form strong chemical bonds with gas molecules or atoms. Using electron paramagnetic resonance absorption techniques, Ingram and Austen (65) confirmed the presence of unpaired electrons in various types of carbons. Observing the marked effect of exposure of carbon to oxygen on the resonance absorption, the authors (65) concluded that these unpaired electrons are located primarily at, or close to, the carbon surface. Number of unpaired electrons is a complex function of carbon heat-treatment temperature and they are affected primarily by the number and nature of imperfections in the carbon structure.

Chemisorption experiments have shown the carbon surface to be heterogeneous. In addition to the normal sources of heterogeneity, carbon is a multicrystalline

material which means that its surface, in most instances, are composed of different crystallographic planes. The degree of heterogeneity in carbon surfaces varies depending upon the percentage of different crystallographic planes composing the surface and their sizes.

3.3.2.9.1 Mechanism of Surface Reactions

A reaction occurring on a surface may usually be regarded as involving five consecutive steps as follows:

- a) Diffusion of the reacting molecules to the surface
- b) Adsorption of the gases on the surface
- c) Reaction on the surface
- d) Desorption of the products
- e) Diffusion of the desorbed products into the main body of the gas.

At one time it was generally believed that one of the diffusion processes, a) or e) was the slowest process and hence determined the overall rate. More detailed investigations of surface reactions showed that this could not be the case except in certain technical processes involving porous catalysts. This is evident from the fact that heterogeneous processes nearly always involve appreciable activation energies, whereas diffusion in the gaseous state involves no activation energy. The diffusion process is thus much more rapid than the overall process and cannot be the slowest process.

The processes of adsorption or desorption are much more likely to be slow steps in heterogeneous reactions as both may involve appreciable activation energies.

The activation energies for desorption are particularly high, and it is likely that in very many reactions the desorption of the products is the rate-determining step. In practice, it is not always convenient to separate the reaction stage from the desorption of the products. It is usual, therefore, to regard the reaction on the surface, giving the gaseous products, as a single step. This concept is in fact the basis of the usual modern treatment reactions, due to Langmuir (67) and Hinshelwood (68). This treatment involves obtaining an expression for the concentrations of reactant molecules on the surface, and then expressing the rate of formation of gaseous products in terms of these surface concentrations. The rate is then expressed in terms of the concentrations of the gaseous reactants. If there is a single reactant, the surface process is a simple unimolecular change; if there are two reactants, reaction may take place between two molecules adsorbed on neighbouring surface sites and the probability of this happening is proportional to the individual concentrations of two reactants in the adsorbed state.

3.4 Physical Adsorption of Vapours in Micropores

The radical differences between adsorption phenomena taking place in micropores and on the surface of transitional pores or macropores require different theoretical approaches to achieve their sensible description and interpretation. All the existing theories of physical adsorption, despite their apparent differ-

ences, proceed from the same physical image in describing adsorption both on non-porous and porous adsorbents. This physical image is based on the concept of the geometric surface of the interface on which adsorption occurs with the formation of one or more successive adsorption layers.

The theory of physical adsorption of vapours in micropores, which excludes the concept of the surface coverage and formation of successive adsorption layers in such pores, will be referred to as the theory of volume filling of micropores. The concept of micropores as space volumes in a solid body which are commensurate with the molecules adsorbed permits us to assert that whatever the nature of adsorption interactions which determine physical adsorption, the whole micropore space has an adsorption field set up by the solid body. The micropore adsorption space may contain discrete adsorption centres which increase the electrostatic components of adsorption interactions. They however lead only to a greater energy non-uniformity of the micropore adsorption space and do not change the essence of the idea of the existence of an adsorption field in the total volume of micropores. Due to the limited adsorption space of the micropores the molecules successively adsorbed in the micropores do not form adsorption layers. Adsorption in micropores is characterized by the volume filling of the adsorption space. Therefore it turns out that the basic geometrical parameter characterizing a microporous adsorbent is the volume of micropores rather than their surface.

Most adsorbents in modern technology are microporous adsorbents. In spite of the fact that in the general case they may contain some larger pore varieties, it is the micropores that play the decisive part in gas and vapour adsorption. Equilibrium states in adsorption of a gas or vapour are expressed by the thermal equation of adsorption, which establishes the relationship between the adsorption value as equilibrium pressure P , and temperature T . Any one of these values can be regarded as a function of the other two. For vapours, the adsorption function A is expressed by

$$A = RT \ln (P_0/P) \quad 3.20$$

and is interpreted thermodynamically as a decrease in the free adsorption energy if the adopted standard state is the state of a normal liquid, which is, at temperature T , in equilibrium with its saturated vapour at pressure P_0 . The value of A is equal to the difference between the chemical potential of a substance in the state of a normal liquid and in the adsorbed state at the same temperature.

The second function is the filled volume of the adsorption space W_3 :

$$W_3 = av^* \quad 3.21$$

where v^* is the molar volume of the substance adsorbed.

In contrast to adsorption on nonporous and relatively large pore adsorbents, a specific feature of adsorption in micropores is the temperature invariance of the differential molar work of adsorption A at constant degree

of volume filling θ_1 of the micropore adsorption space. The temperature invariance of A, analytically is expressed by Dubinin (31) as

$$(\partial A / \partial T)_{\theta_1} = 0 \quad 3.22$$

and is confirmed by him for a number of adsorption systems. This assumption is satisfactory for temperatures below the boiling point of a normal liquid at atmospheric pressure. For higher temperatures and in particular in the subcritical region, the compressibility coefficient of the normal liquid rises abruptly, and the assumption that the molar volume of the substance in the adsorbed state is the same as in the bulk liquid phase, is no longer physically substantiated (17).

3.4.1 Thermodynamic Analysis

It is generally accepted that the term adsorption refers to numerous phenomena greatly differing both in the nature of intermolecular interactions and in mechanisms which require the consideration of various models and the application of different mathematical language.

It is asserted that the entire range of physical adsorption is enclosed, at least from the thermodynamic point of view between two limiting cases: adsorption on nonporous smooth surfaces, and adsorption in micropores. All real cases of adsorption represent a more or less complex superposition of these two types of adsorption phenomena (30).

In adsorption on nonporous surfaces, for which the

curvature of the surface has practically no effect on the adsorption process in the absence of capillary condensation, a pictorial model of adsorption is the coverage of the adsorbent surface with the formation of successive adsorption layers. The most important parameter characterizing adsorption equilibrium in this case is the adsorbent surface area.

In adsorption on microporous adsorbents, the concept of surface area loses its meaning. The notion of a geometrical surface is a macroscopic concept, and micropores are assumed to be voids in a solid which have linear dimensions commensurate with the sizes of the molecules adsorbed.

Bering et al. (30) considered it analogous between transition from large pore adsorbents to microporous ones and transition from coarse suspension to true molecular solutions of low molecular weight substances. Considering a coarse suspension to be a two phase system, the interface area is a very important thermodynamic parameter characterizing the behaviour of a system. The system properties vary with increasing degree of porosity. When the degree of dispersity exceeds the range of colloid systems, the concept of interface loses its meaning because the system becomes a true molecular solution and behaves as a single phase system.

Transition from large pore adsorbents to microporous ones involves some quantitative differences in the beginning which invariably lead to qualitative differences.

The interface disappears and the adsorbent-adsorbate system becomes a single phase system. A pictorial molecular model of adsorption in micropores is not layer-by-layer coverage of the surface but volume filling of the micropores whose size does not allow us to regard the adsorbate in them as a separate phase.

3.5 Adsorption Mechanism

Adsorption is a physical process where a dispersed material in a continuous phase is removed from that phase onto a highly porous solid material. The fundamental nature of the forces which cause adsorption to occur have been the subject of considerable discussion in the literature, but it is probably safe to say that no completely satisfactory mechanism has yet been described. In general, however, adsorption appears to take place as a result of unsatisfied forces in a surface creating a force field in the immediate environment which attracts and holds for a finite time the molecules of a contracting species. The residence time of the molecules on the surface is a direct function of the energy with which the molecules are held. In practical terms, the adsorption energy determines the strength with which the molecule is adsorbed relative to other molecules in the force field and the efficiency with which the molecules can be separated.

The overall kinetics of the adsorption system used are affected by the gas-solid contacting method and the transport processes of the adsorbate from the bulk gas

to the internal adsorbate surfaces. There are essentially three consecutive steps in the adsorption of materials from the bulk gas stream by the porous adsorbents. The first of these is the transport of the adsorbate through a surface film to the exterior of the adsorbent. Many theories have been postulated to explain the mass transfer in this region. However, the fluid mechanics of this region is not well understood (69). Boundary layer theory accounts for a velocity distribution and is more realistic than film theory, which assumes a laminar film surrounding the particle. The second step is the transfer of adsorbate from the external surface to the internal surface of the porous adsorbent by some diffusive mechanism. The final step is the adsorption of the adsorbate on the interior surfaces bounding the pore and capillary spaces of the adsorbent.

Consideration of rates at which interfacial tensions are lowered by chemical compounds represent the nature of the adsorbate. It indicates that the adsorption process itself is probably not rate-determining and that a much slower process must control the overall rate of uptake by the porous adsorbent. Under laminar conditions, the transport of the adsorbate through the boundary layer to the adsorbent is the rate limiting step; if sufficient turbulence is provided, transport of the adsorbate within the porous carbon controls the rate of uptake. One of the most significant parameters to be considered is the nature of the step which controls the speed at which the reaction proceeds.

Certain properties of the adsorbate are useful in

determining the nature of the rate controlling step. For example, if intraparticle transport determines the rate of reaction, the size and structure of an individual adsorbate will affect the rate to the extent that it affects molecular mobility. The rate controlling step can also be characterized in part by the observed activation energy in the process.

For a process in which the overall rate is controlled by a strictly adsorptive reaction, the variation of rate should be proportional to the concentration of the solute and for very simple diffusion the rate is expected to be proportional to the first power of the concentration. But for intraparticle diffusion the mathematical expression is of complex nature. Since concentration affects a number of parameters of these equations, it is not possible to predict an exact concentration-rate relation for this reaction.

For processes where the rate-limiting reaction is adsorption on the exterior surfaces of the adsorbent, the rate is expected to vary as the reciprocal of the diameter of the adsorbent particles. Variation of the rate with particle size is then another method which is useful for the characterization of rate-limiting for a particular system.

The transfer method giving the maximum resistance and hence controlling the overall rate is dependent upon the method by which the adsorbate is in contact with adsorbent. In a batch reactor which provides a

high degree of agitation of mixing, pore diffusion is often rate limiting. In a continuous flow system such as beds of charcoal cloth through which the vapour is passed, pore diffusion is the most likely to be the rate limiting factor for normal flow rates.

3.6 Mass Transfer

With regard to adsorption Weber (70) considered molecular diffusion to be the most representative of the overall transport process, because other physicochemical phenomena mentioned in the earlier pages tend to interfere with the gradient-oriented movement of migrating species. The diffusion process is subject to more quantitative analytic description than any of the other processes because the driving force for diffusion, the concentration gradient, can be characterized more readily.

The flux of adsorbate across the external gas film surrounding the adsorbent particle can be expressed in terms of a mass transfer coefficient. Thus the flux through the particle surface can be equated to that across the gas film by the relation

$$K_c(Y - Y_p) = -D_e \left(\frac{\partial Y_p}{\partial r} \right) \quad 3.23$$

where Y and Y_p represent the bulk gas phase and pore gas concentrations respectively, r is the radial parameter. D_e is the effective diffusivity within the particle and K_c is the external mass transfer coefficient. The mass transfer coefficient can be computed from correlations such as that of De Acetis and Thodos (71) for fixed beds.

The following step is intraparticle diffusion whereby organic solvent molecules are transferred from the external surface of the adsorbent to its internal surface by some diffusive mechanism. The rate of diffusion within a porous material can be expressed by means of Fick's law. Assuming the adsorbent particles to be spherical,

$$\frac{\partial Y}{\partial \theta} = \frac{1}{r^2} \frac{\partial}{\partial r} \left(D_e r^2 \frac{\partial Y_p}{\partial r} \right) \quad 3.24$$

The type of diffusion taking place within the pores depends on the relative size of the pore diameter and the mean free path of the vapour under the conditions which exist in the pores. At low pressures, or in small diameter pores, Knusden (72) showed the diffusion coefficient to be given by

$$D_K = 1.33 r_p \left(\frac{2RT}{\pi M} \right)^{0.5} = 0.66 r_p \bar{U} \quad 3.25$$

where D_K is the Knusden diffusion coefficient, r_p the pore radius, and \bar{U} the mean molecular velocity.

In larger pores, or at high pressures, most collisions are between molecules and the diffusive mechanism is the same as in the bulk gas. Values of such diffusion coefficients can be obtained from the literature (73, 74).

Finally, in physical adsorption such as in the adsorption of organic vapours on charcoal cloth, the actual adsorption rate is extremely rapid and is regarded as not to influence the overall kinetics. The relative effects of interparticle and intraparticle mass transfer can be evaluated from the Nusselt Number (69). The

ratio of the resistance to mass transfer to that in the external gas film is defined by the Nusselt Number and generally shows that most of the resistance is in the solid. Vermeulen (75) has shown that under isothermal conditions the diffusional resistances may be combined to give one overall resistance to mass transfer.

Since the rate limiting step controls the rate at which the adsorption proceeds, adsorption can be analogous to a chemical reaction e.g. $A \rightarrow B$. However, the actual mechanism of transport and adsorption is not yet well understood. Because of the complexity of the internal pore structure, kinetics have generally been modelled with a single effective diffusion parameter active throughout the particle even though it is accepted that charcoal cloth like other activated carbons shows heterogeneous surface properties and a wide range of pore sizes.

In the phenolic adsorption studies with granular charcoal by Snoeyink (123) and Zogorski et al. (124), among others, a rapid initial uptake phase followed by a slow approach to equilibrium was noted. Such behaviour is not consistent with the single effective diffusion parameter model. In addition, several authors (125,126) have demonstrated that the effective diffusion parameter in small pores is strongly dependent on the pore diameter to solute diameter ratio, and that diffusion rates decrease with decreasing pore size. Since charcoal cloth shows wider range of pore sizes depending on the

carbonising treatment as well as the time of subsequent activation and the temperature at which it is carried out, a corresponding range of diffusion rates should be expected. Rapid saturation of the fast diffusing pores would result in a net decrease in effective diffusion rate as adsorption proceeds.

As an approximation to the microscopic description of the diffusional process, a model has been developed which divides the whole adsorption mechanism into two regions of different diffusion rates:-

- a) Diffusion of the organic vapour from the air through the gas film to the external surface of the adsorbent cloth. This region is called the macropore region.
- b) Diffusion of the solvent vapour molecules into the pores of the charcoal cloth. This region is called the micropore region.

Relatively rapid diffusion and adsorption occurs in the macropores, and the remaining slow approach to equilibrium occurs in the micropores.

The micropores are assumed to be homogeneously distributed throughout the particle and to branch off the larger macropore network which is responsible for radial transport. However, it is not possible to define the dimensions of the microporous sub-units when dealing with activated carbons. Thus, a lumped parameter approach is used to describe diffusion in the micropores. A surface diffusion mechanism is assumed to be responsible for transport in the macropores.

Measured surface diffusion coefficients within the macropore network are comparable to previously reported coefficients obtained using a single parameter approach. This agreement is due to the large amount of adsorption into the macropores which is observed in a typical, relatively brief kinetic experiment. Adsorption into the micropores is so slow that the macropore region is essentially saturated before significant micropore capacity is utilized.

The capacity in the micropore region constitutes about 30% of the total adsorptive capacity. This slowly utilized capacity is neglected by the standard single interparticle rate model; it constitutes the differences between adsorptive capacity realized in a short batch kinetic experiment and the capacity measured over an extended period in an isotherm evaluation.

Comparison of the calculated adsorption capacities within the micropore region at different equilibrium liquid-phase concentrations indicates that the micropore capacities are essentially constant, independent of liquid-phase concentration. Such behaviour is indicative of very strong adsorbate-adsorbent interaction and suggests that adsorption within this region may be of a different type to that in the larger pores (76).

3.7 Potential Theory of Adsorption

The potential theory of adsorption originates with De Saussure (77) as far back as 1814. According to him,

the adsorbent exerts a strong attractive force upon the gas in its vicinity, this attraction giving rise to adsorption. The forces of attraction reaching out from the surface are so great that many adsorbed layers can form on the surface. These layers are under compression, partly because of the attractive force of the surface, partly because each layer is compressed by all the layers adsorbed on top of it. The compression is the greatest on the first adsorbed layer, less on the second, and so on until the density decreases to that of the surrounding gas. Thus the structure of the adsorbed phase is analogous to that of the atmosphere surrounding the earth.

3.7.1 Dubinin-Polanyi Equation

Eucken (78) was the first to conceive of the force of adsorption as an intermolecular potential gradient, but the correct quantitative formulation of the theory is due to Polanyi (79). According to him, the determining role is played by dispersion forces. The views developed are applicable to the physical adsorption of gases and vapours on carbonaceous adsorbents that consist of a nonpolar substance - carbon. They are also equally applied for other adsorbate-adsorbent systems in which dispersion forces are the dominant component of adsorption interaction (80).

Active carbons are adsorbents with energetically non-uniform surfaces, which is a consequence of the disordered arrangement of the elementary crystallites of

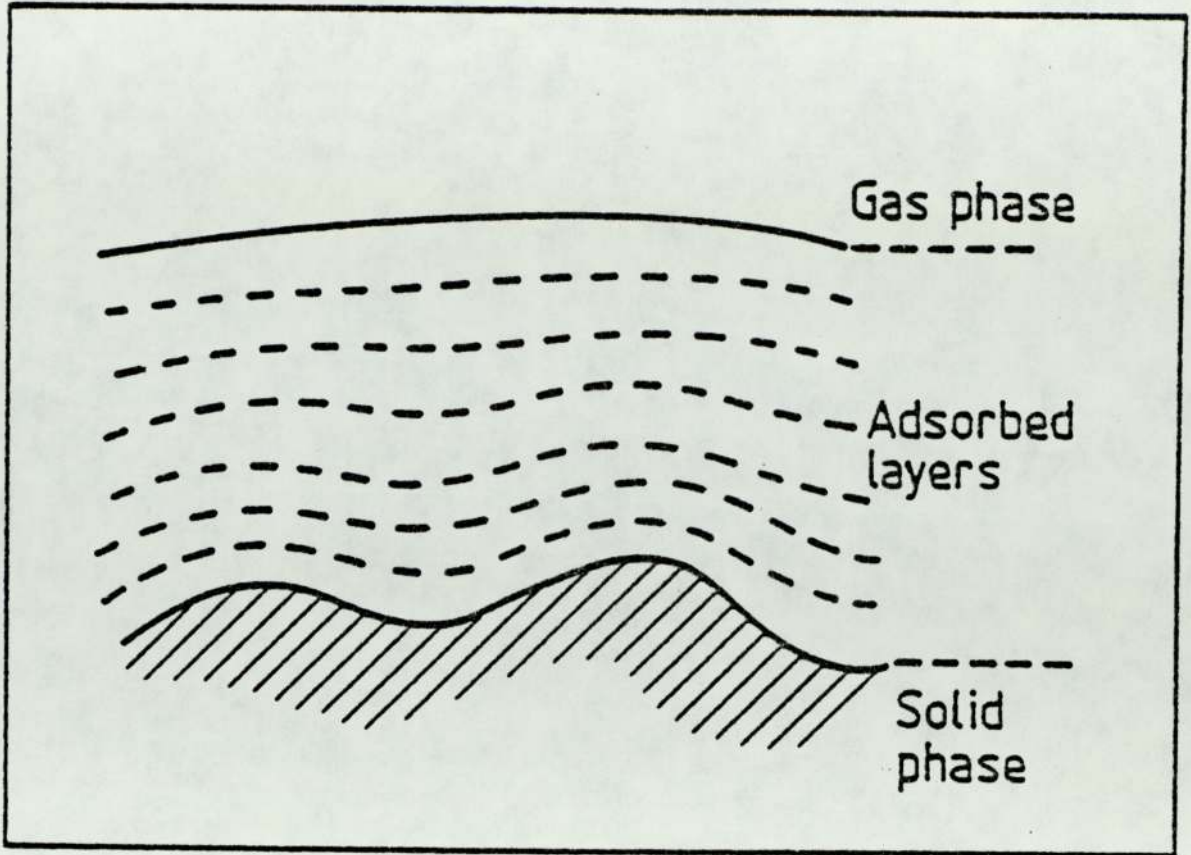


FIGURE 3.3 THE STRUCTURE OF THE ADSORBED PHASE ACCORDING TO THE POLANYI POTENTIAL THEORY (128)

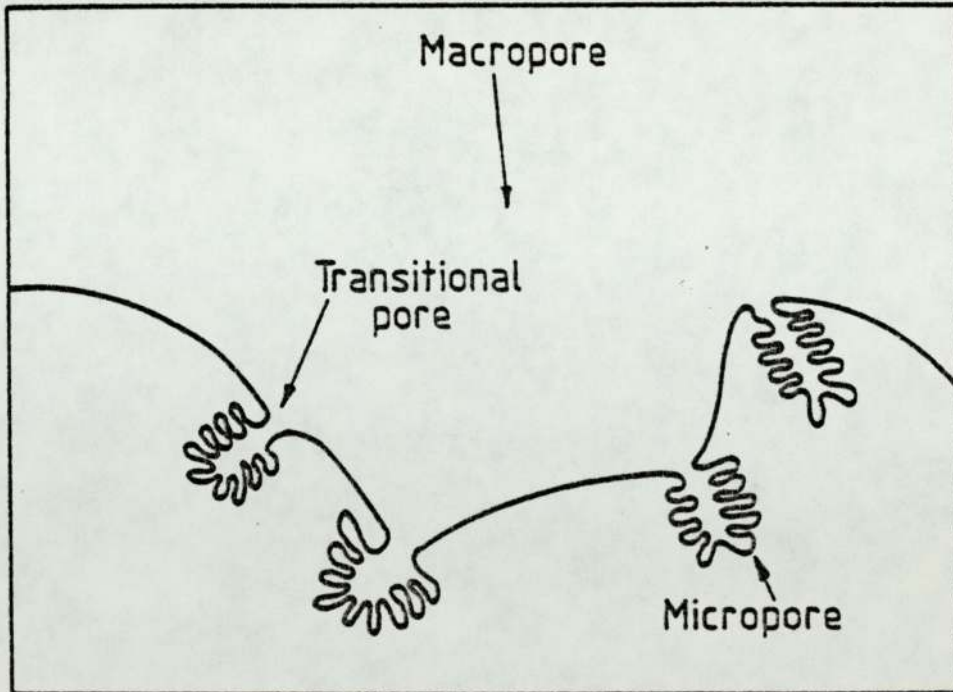


FIGURE 3.4 THREE PORE MODEL (86)

carbon at the surface of the adsorbent, giving the surface a mosaic-like structure. This results in an enhanced adsorption energy in the micropores of the carbon due to the superposition of the fields of the opposite walls of the pores. The vapour adsorbed on the surface mainly of the smallest pores of active carbon is converted into a liquid, due to compression. From the conditions of equilibrium it follows that the surface of the condensed adsorption layer is equipotential. As a reasonably good approximation, the volume of liquid expresses the volume of filled adsorption space.

Although there are many theories concerning adsorption of vapour on activated carbon, the Dubinin-Polanyi equation is a simple and practically useful equation of estimation of adsorption capacity for the organic vapour on activated carbon. Dubinin (28) reported that the adsorbed amount in liquid volume per unit weight of microporous adsorbent, W , could be shown by the following equation from Polanyi's adsorption potential theory:

$$\ln (W/W_0) = -KA^2 \quad 3.26$$

Here W_0 is an apparent limiting amount of adsorption for each adsorbent, K is a parameter for each system of adsorbent and adsorbate, A is differential molar work of adsorption, R is the gas constant, and T is the absolute temperature of adsorption. P_0 and P are saturated vapour pressure and adsorbed vapour pressure, respectively.

For a standard adsorbate eq 3.26 was replaced by eq. 3.27:

$$\ln (W/W_o) = -K_s A_s^2 \quad 3.27$$

K_s and A_s stand for K and A for a standard adsorbate

A and A_s are related by the eq. 3.28:

$$\frac{A}{A_s} = \beta \quad 3.28$$

Substituting the value of A_s from eq. 3.28 and the value of A from eq. 3.20 to eq. 3.27, we have

$$\begin{aligned} \ln (W/W_o) &= -(K_s/\beta^2) A^2 \\ \ln W &= \ln W_o - \frac{K_s A^2}{\beta^2} \\ &= \ln W_o - \frac{K_s [RT \ln(P_o/P)]^2}{\beta^2} \\ \log W &= \log W_o - \frac{2.3 K_s [RT \log(P_o/P)]^2}{\beta^2} \quad 3.29 \end{aligned}$$

β is the affinity coefficient for adsorption on activated carbon and it could be approximated by the ratio of molar volumes or parachors of an adsorbate to the standard adsorbate.

The adsorbed vapour pressure P can be calculated from the ideal gas law.

$$P = 0.062 (273 + t) \frac{C}{M}$$

t = Adsorption temperature

C = Concentration of adsorbate

M = Molecular weight of adsorbate

The saturated vapour pressure P_o is given approximately

by the Antoine equation:

$$\log P_o = a_1 - \frac{b_1}{c_1+t} \quad 3.31$$

where a_1 , b_1 and c_1 are parameters of the adsorbate

$$\begin{aligned} Q &= \text{Adsorption capacity} \\ &= \text{Mass of adsorbate per unit mass of adsorbent} \\ &= Wd_t \\ &= W(d_o - \alpha t) \end{aligned} \quad 3.32$$

where,

d_t = Density of the liquid adsorbate at $t^\circ\text{C}$

d_o = Density of the liquid adsorbate at 0°C

α = Thermal coefficient of expansion of liquid

Taking the logarithm of eq. 3.32 we have

$$\log Q = \log W + \log (d_o - \alpha t) \quad 3.33$$

Substituting the value of $\log W$ from eq. 3.29 in the above equation we have

$$\begin{aligned} \log Q = \log W_o - \frac{2.3 K_s [RT \log(P_o/P)]^2}{\beta^2} \\ + \log (d_o - \alpha t) \end{aligned} \quad 3.34$$

Urano et al.(81) assumed that

$$2.3 K_s R^2 = 4.6 \times 10^{-7} \quad 3.35$$

$$\text{and } W_o = v_{3.2} + 0.000055 \quad 3.36$$

Equation 3.34 then becomes

$$\begin{aligned} \log Q = \log [(v_{3.2} + 0.000055)(d_o - \alpha t)] \\ - (4.6 \times 10^{-7}) \left(\frac{273+t}{\beta}\right)^2 (\log P_o - \log P)^2 \end{aligned} \quad 3.37$$

where, $v_{3.2}$ = Volume of the micropores smaller than
 3.2×10^{-9} m in diameter
 $= 0.56 \times 10^{-3} \text{ m}^3 \text{ kg}^{-1}$ (82)

β can be related to surface tension, molecular weight and density of the adsorbate (94):

$$\beta = \frac{\gamma^{1/4} M/d_{15}}{[\frac{1}{\gamma} M/d_{15}]_{\text{Benzene}}} \quad 3.38$$

where

γ = Surface tension at 15°C

d_{15} = Density of the adsorbate at 15°C

The values of a_1 , b_1 , c_1 , d_0 , α , γ and d_{15} for all the four solvents used in the present work can be obtained from literature (83-85) and is listed in appendix V. From these values the adsorption capacity for each of the four solvents can be calculated using equation 3.37.

3.7.2 Limitations of the Dubinin-Polanyi equation

The Dubinin-Polanyi equation 3.29 can be expressed in the linear form

$$\log W = \log W_0 - D_1 \log^2 (P_0/P) \quad 3.39$$

where $D_1 = \frac{2.3K_S R^2 T^2}{\beta^2} \quad 3.40$

Dubinin (34, 86) presented experimental data to show that equation 3.39 adequately describes, over a wide pressure range, the adsorption data of many adsorbates onto a wide variety of microporous carbons, both activated and unactivated. Also it has been shown (29,87,88)

that many cases of adsorption of vapours on nonporous solids can be linearized in the submonolayer region by equation 3.29. Therefore, it would appear that the Dubinin-Polanyi equation has surprisingly wide applicability. But deviations from linearity can be observed at low values of $\log^2 (P_0/P)$ due to capillary condensation in transitional pores or multilayer formation on the walls of macropores (28) When the plot deviates upwards with increased slope.

The Dubinin-Polanyi equation is empirical in origin and predicts that there is a distribution of free energies with adsorption volume of the form,

$$f(\Delta G) = \frac{-2K\Delta G}{\beta} \exp\left(-\frac{K\Delta G^2}{\beta^2}\right) \quad 3.41$$

The above equation is known as the Rayleigh distribution. Marsh and Rand (89) reported that the distribution is skewed towards high values of $-\Delta G$. It has been suggested by Marsh and Siemieniowska (90) that linear plots result because the distribution of adsorption free energy with adsorption volume follows the Rayleigh distribution. But Gregg and Sing (91) consider that the wide applicability of the equation 3.29 arises because the plot of $\log W$ vs $\log^2 (P_0/P)$ is inherently insensitive and the distribution of adsorption free energy with adsorption volume need not be of the Rayleigh type.

In accordance with the basic equation 3.27 of the theory, K_s and W_0 depend on the nature of the adsorbent.

In the present research K_s has been taken as $2.8 \times 10^{-9} \frac{\text{mol}^2}{\text{J}^2}$ as reported in (81).

It has been mentioned in the literature that values of K_s do vary depending on the adsorbent (28,31, 92,93). Dubinin found (28) that the values of K_s for benzene would usually range from 1.1×10^{-9} to $2.7 \times 10^{-9} \frac{\text{mol}^2}{\text{J}^2}$ and they were influenced by the pore size distribution pattern of micropores. Urano et al. (81) suggested $K_s = 2.8 \times 10^{-9} \frac{\text{mol}^2}{\text{J}^2}$ as a good approximation without complicated correction. They also suggested that W_o , the apparent limiting amount of adsorption is equal to $0.000055 \text{ m}^3 \text{ kg}^{-1}$ ($0.055 \text{ cm}^3 \text{ g}^{-1}$), plus the micropore volume of the adsorbent. Jayson et al. (82) found that the micropore volume of charcoal cloth is $0.56 \times 10^{-3} \text{ m}^3 \text{ kg}^{-1}$. But upon heat treatment this value is bound to be changed and the original equation 3.29 does not make any allowance for this.

The adsorbed substance stays in the adsorption force field in a highly compressed state. And since upon approaching the critical temperature the compressibility of the liquid increases rapidly, the conception that the volume does not change ceases to be justified.

Dubinin (80) related the temperature dependence of density by a linear relationship in the range of boiling temperature to critical temperature. Adsorption capacity does not change below the critical temperature region. The invariance of temperature has been reported in various

literature (28,31,80). Above critical temperature $\log^2\left(\frac{P_0}{P}\right)$ in equation 3.29 is to be substituted by $\log^2\left(\frac{P_{cr}T_1}{P}\right)$ where $T_1 = \frac{t}{t_{cr}}$ and P_{cr} is the critical pressure and t_{cr} is the critical temperature.

Dubin (28) reported that the affinity coefficient β for adsorption on activated carbon could be approximated by the ratio of parachors of an adsorbate to the standard adsorbate, regardless of the activated carbon. Benzene was used as a standard adsorbate. Reucroft et al. (94) reported that β could be approximated by the ratio of polarities for polar organic adsorbates better than parachors. When the adsorbate molecules are polar in nature, electrostatic interactions may play a greater role in determining the total adsorptive interaction which determines the adsorption isotherm. In the case of a non-polar adsorbent there will be contributions from dipole-induced forces (95). If the adsorbent possesses some polar nature due to the presence of ionic impurities, there will be an additional contribution from ion-dipole forces. Reucroft et al. (94) concluded that electronic polarization P_e gives better results in case of polar adsorbates.

$$\beta = \frac{P_e}{P_{e_{ref}}} \quad 3.42$$

$$\text{where } P_e = \frac{N^2-1}{N^2+2} \frac{M}{d_t} \quad 3.43$$

- N = Refractive index of liquid adsorbate
 measured at sodium D wavelength
- M = Molecular weight of the adsorbate
- d_t = Density of the adsorbate at $t^\circ\text{C}$

Reucroft et al. suggested (94) that the reference substance should be chosen according to the nature of the adsorbate. They divided all the adsorbates into three categories and assigned three compounds as the reference compounds:- carbon tetrachloride for non-polar adsorbates, chloroform for weakly polar adsorbates, and acetone for polar adsorbates as reference substances. It was found that the ratio of parachors gives good agreement between the theoretical and experimental values of affinity coefficients of non-polar compounds whereas for weakly polar and strongly polar compounds, ratio of polarization gives better agreement. In the present work, β is calculated using equation 3.38.

The general equation representing the theory of volume filling of micropores is expressed (92) by the following equation:

$$\ln \left(\frac{W}{W_0} \right) = -K A^n \quad 3.44$$

The above equation is identical to equation 3.26 if $n = 2$ and then the eq. 3.44 is known as the Dubinin-Polanyi equation. It has been suggested (96) that non-integral ^{ex} values of n can provide a better fit of experimental results to equation 3.39 in particular for carbons with high degrees of activation. Stoeckli

et al. (92) suggest a range of n between 1.2 and 2.0. Rand (96) found n to be equal to 3 for some adsorption experiments. It is agreed that n decreases with increasing activation but no clear correlation could be found between them (92).

3.7.3 The Modified Dubinin-Polanyi Equation

Assuming Dubinin-Polanyi equation to be applicable to a homogeneous system of micropores, some authors (92, 97) suggested that for a heterogeneous collection of micropores, the overall adsorption isotherm is a sum of contributions.

$$W = \sum W_{oj} \exp [-B_j (T/\beta)^2 \log^2 (P_o/P)] \quad 3.45$$

The quantities W_{oj} and B_j correspond to a given class of micropores.

$$\text{From equation 3.29, } B = K_s (2.3 R)^2 \quad 3.46$$

Accepting the possibility of a continuous distribution of the microporosity, the equation is replaced by an integral:

$$W = \int_0^{\infty} f(B) \exp[-B y] dB \quad 3.47$$

$$\text{where } y = (T/\beta)^2 \log^2 (P_o/P) \quad 3.48$$

Huber et al. (97) suggested a Gaussian-based general equation:

$$W = W_o \exp(-B_o y) \exp(y^2 \Delta^2 / 2) (1 - \text{erf}(x)) / 2 \quad 3.49$$

$$\text{where } x = (y - B_o / \Delta^2) \Delta / (2)^{0.5} \quad 3.50$$

B_o = average value of B

Δ = distribution width

Dubinin (98) suggested a linear relationship between n and Δ :

$$n = 2.00 - 1.90 \times 10^6 \Delta \quad 3.51$$

The value of $10^6 \Delta$ varies between 0.14 and 0.35.

It is now well established that for microporous materials many isotherms obtained by Dubinin (80) do fit the Dubinin-Polanyi equation. There can be no doubt that this particular equation does describe the overall adsorption process. The non-agreement of isothermal data is the result of an inability to establish positions of thermodynamic equilibrium because of slow rate of adsorption. Deviation is most pronounced at lowest relative pressures. Heterogeneity in strongly-activated carbons manifests itself through the variable Δ and the structural constant B of the original equation, but more detailed information is needed as to the relation between B and exact pore dimensions.

3.8 Adsorption Kinetics

Hiester and Vermeulen (99) and Masamune and Smith (100) have considered physical gas adsorption to be kinetically second order, involving the interaction between an active site and a free gas molecule. Jonas and Svirbely (101) have shown that the sigmoid curve, resulting from a plot of gas concentration exiting from a packed bed of activated carbon granules against time, displays second order kinetics only in the linear or mid-portion of the curve where the exit concentration rises rapidly with time. The first portion of the sigmoid

curve showing trace gas penetration of the bed and characterized by its convexity with the time axis, represents the condition of an excess of active sites over free gas molecules, and displays pseudo first order kinetics with respect to gas molecules. Analogously, the final portion of the curve, where the number of vacant active sites is rapidly being depleted, and which shows a concavity toward the time axis, represents an excess of free gas molecules over active sites, and displays pseudo first order kinetics with respect to active sites.

3.8.1. Adsorption Rate Constant

The kinetic equation, applicable to the study of vapour adsorption on activated carbon at various flow rates was originally derived by Wheeler and Robell (102) from a continuity equation of mass balance between the gas entering an adsorbent bed and the sum of the gas adsorbed plus that penetrating through the bed. Four basic differential equations were derived which described concurrent gas adsorption phenomena in a bed and which required simultaneous solution. By means of various simplifying assumptions the four equations were reduced to one differential equation:

$$\frac{-dF_1}{d\lambda} = (K_V/V_L)F_1\psi(F_1) \quad 3.52$$

Combining the above equation with the mass balance equation,

$$C_0 V_L \theta_b = \int_0^\lambda W(x) dx + V_L \int_0^\theta C(\lambda) d\theta \quad 3.53$$

a relation between the breakthrough time θ_b and rate constant K_v was established (103, 105).

$$\theta_b = \frac{W_e}{C_o \cdot F} \left[W_4 - \frac{\rho_B F \ln (C_o / C_x)}{K_v} \right] \quad 3.54$$

where

λ = Bed thickness

V_L = Superficial velocity

C_x = Outlet gas concentration at a point x in the bed

C_o = Inlet concentration

$$F_1 = \frac{C_x}{C_o}$$

$\psi(F)$ = A function of W_4/W_e

W_4 = Adsorbent weight

W_e = Kinetic adsorption capacity

K_v = Pseudo first order adsorption rate constant

$C(\lambda)$ = Concentration at a point λ in the bed

$W(x)$ = Adsorbed amount in liquid volume per unit weight of adsorbent at a point x in the bed

θ_b = Breakthrough time

F = Volumetric flow rate

ρ_B = Bulk density of the bed

Values of θ_b plotted as a function of W_4 yield a straight line from whose slope and intercept W_e and K_v can be calculated provided the inlet vapour concentration, volumetric flow rate, temperature, adsorbent type are kept constant.

Vapour	Kinetic Adsorption Capacity W_e ($kg\ kg^{-1}$)	Adsorption Rate Constant K_v (sec^{-1})
Carbon tetrachlo- ride	0.741	12.3
Chloroform	0.728	13.0
Benzene	0.404	18.2
p-Dioxane	0.476	18.1
sec-Butylamine	0.331	15.5
1,2-Dichloroethane	0.616	17.5
Pyridine	0.661	16.4

Table 3.2 Adsorption parameters derived from regression equation using granular carbon as adsorbent (103)

3.8.2 Adsorption rate limit

Although the basic process of physical gas adsorption is considered to be kinetically second order (99,100) from a molecular viewpoint, the presence of excess active sites over gas molecules makes the reaction pseudo first order (101) with respect to gas molecules. Under these conditions, the concept of a maximum or limiting value to this first order rate constant, originally developed by Wheeler (104) for catalytic reaction rates, can be applied to gas adsorption. The maximum value would be mass transfer limiting, and would require, when applied to gas adsorption, diffusion and surface adsorption to be so rapid that mass transfer of the gas to the external surface limits the adsorption rate. In addition, Wheeler (104) assumed no back evaporation or desorption of gas molecules after initial adsorption. Based upon the initial assumptions that all gases have the same viscosity and Schmidt number ($Sc = \frac{\mu}{\rho D}$),

where

μ = Viscosity

ρ = Density

D = Diffusivity

Wheeler (104) approximated the mass transfer limiting value as

$$K_{\infty} = 10 \left[\frac{V_L}{\bar{M} \cdot d_p^3 P_T} \right]^{0.5} \quad 3.55$$

where P_T = Total pressure

\bar{M} = Average molecular weight of air-vapour mixture

As the vapour concentration is low, \bar{M} can be taken as that of air and P_T as one atmosphere. This simplifies the equation 3.55 to

$$K_{\infty} = 1.86 V_L^{\frac{1}{2}} d_p^{-3/2} \quad (S^{-1}) \quad 3.56$$

3.8.3 Alternative Method to Calculate Adsorption Rate Constant

Jonas and Rehrmann (105) found the pseudo first order adsorption rate constant K_v to be a function of superficial linear velocity V_L of the gas air flow. They conducted some adsorption experiments with benzene on activated carbon granules. Despite the close agreement between the calculated and experimental values for the rate constant, equation 3.56 showed its weakness as a mathematical form. As $V_L \rightarrow 0$, $K_{\infty} \rightarrow 0$ despite the fact that a condition of zero flow velocity should still exhibit a diffusional component with a small but finite adsorption rate constant. As $V_L \rightarrow$ infinity, K_{∞} increases without limit.

Consistent with the concept of limiting values for the rate constants in gas adsorption by activated carbon, Jonas and Rehrmann have proposed a generalized mathematical model (105).

$$K_v = \frac{a_2 + b_2}{1 + \left(\frac{a_2}{b_2}\right) e^{-(a_2+b_2)c_2 V_L}} \quad 3.57$$

a_2 , b_2 and c_2 are constants which depend on the nature of the adsorbent. In the above equation 3.57,

$$\lim_{V_L \rightarrow 0} K_V \rightarrow \frac{a_2 + b_2}{1 + \left(\frac{a_2}{b_2}\right)} = b_2 \quad 3.58$$

$$\lim_{V_L \rightarrow \infty} K_V \rightarrow a_2 + b_2 = a_2 + b_2 \quad 3.59$$

Adsorption rate constants for activated carbon as a function of linear velocity were calculated using equations 3.56 and 3.57. The authors (105) reported that whereas equation 3.56 compares favourably with the experimental values only at the velocity extremes (at 0.02 and 0.5 m s⁻¹), equation 3.57 was consistent with all the intermediate velocities as well as the extreme ones. Since the model equation 3.57 contains only three constants, three sets of experimental values are used to calculate the constants using an iterative process for convergence of 0.001 between the observed and calculated values of the dependent variable.

3.9 Regeneration

The key to the effectiveness of activated carbon as an adsorbent is its ability to regenerate. Short adsorption cycles dictate that in-place non-destructive regeneration be used in order to avoid the carbon losses that are typical of thermal techniques. Systems using thermal regeneration are restricted to low inlet concentrations. During adsorption, the free energy of the system is decreased and so energy is to be provided to drive off the adsorbate from the adsorbent. A lower equilibrium-loading capacity is to be reached by

increasing temperature or decreasing the partial pressure. Desorption can also be achieved by introducing a more strongly adsorbed material to displace the previously adsorbed compounds. Vapour phase adsorption systems are usually regenerated using steam, hot gas or a combination of vacuum and hot gas. Solvent regeneration is usually limited to desorption of nonvolatile organics collected from aqueous phases (106).

The choice of regeneration method depends on the downstream use of the desorbed organics. The adsorption step itself serves only to concentrate the organics for subsequent destruction by other techniques. Although condensing them from the regenerating fluid is the customary approach, incinerating them in the regenerant can be a cost-effective alternative to direct incineration of dilute fumes - if the savings in capital and energy that result from using a smaller fume incinerator offset the expense of the adsorption system.

3.9.1 Regeneration Techniques

There are five basic techniques for desorbing a loaded bed of adsorbent (69,106). These will be discussed below.

3.9.1.1 Thermal Swing Desorption

Thermal swing desorption, the most commonly used regeneration method, involves driving off the adsorbate by raising the adsorbent bed temperature. The temperature

can be increased by circulating a hot desorbate vapour through the bed, heating with internal coils or a combination of both. The rate of heat transfer limits the desorption rate. Mass transfer rate is negligible and the adsorbate loading remains in equilibrium with the vapour over the bed during the desorption.

In the case of materials immiscible with water, steam or hot water provides the simplest and most rapid method of introducing the required heat. The drying of the charcoal after the removal of the adsorbed materials by steam seems to be unnecessary in many cases due to the non-selective adsorption of the steam and its easy displacement by preferentially adsorbed vapours. This possible omission of the drying step constitutes an economic advantage in certain adsorption cycles using charcoal as an adsorbent (107).

3.9.1.1.1 Thermal Swing Desorption: Thermodynamic Calculations

Thermal swing desorption removes an adsorbate almost completely from an adsorbent. This method is simple and equipment requirements are minimum. But its disadvantage lies in the long time required for a complete operation ranging from 8hr to 24 hr. The long generation time makes this method unattractive for use in bulk separation processes.

The application of heat with vacuum is an essential to remove the adsorbate component. Without vacuum,

there is a possibility of readsorption when the system cools. Desorption is limited by the rate of heat addition to the system which depends on the fluid flow rate. The fluid flow is controlled by the pressure drop. Therefore heat balances alone are insufficient to design a thermal regeneration system. Some indirect heating complicates the design criteria and also results in non uniform addition of heat.

The minimum amount of heat necessary to change the temperature of W_4 kgs of adsorbent from t_s to t_f is

$$\begin{aligned} Q_1 &= W_4 C_{ps} (t_s - t_f) \\ &= A_1 \lambda \rho_B C_{ps} (t_s - t_f) \end{aligned} \quad 3.60$$

The rate of heat input to the bed is

$$q_1 = G A_1 C_{pf} (t_s - t_f) \quad 3.61$$

At any time θ , the total amount of heat supplied to the bed is

$$Q_2 = G A_1 C_{pf} (t_s - t_f) \theta \quad 3.62$$

where

- Q_1 = Minimum heat requirement
- C_{ps} = Specific heat of adsorbent
- t_s = Initial temperature of adsorbent
- t_f = Inlet temperature of fluid
- A_1 = Cross-sectional area of adsorbent
- λ = Bed thickness
- ρ_B = Bulk density of adsorbent
- G = Feed rate of carrier fluid
- C_{pf} = Specific heat of fluid
- Q_2 = Total heat supplied
- θ = Time

Combining equations 3.60 and 3.62

$$\begin{aligned} \text{Efficiency} &= \frac{Q_1}{Q_2} \\ &= \frac{\lambda \rho_B C_{ps}}{G \theta C_{pf}} \end{aligned} \quad 3.63$$

The minimum regeneration temperature varies for each adsorbate-adsorbent combination and depends on the residual loading to be achieved. For water desorption from molecular sieves the regeneration temperature is 190°C (106). In large commercial adsorbers it is common practice to design for a ΔT of 10°C (50°F) between the heater outlet and the bed effluent.

3.9.1.2 Pressure Swing Desorption

Pressure swing desorption can be accomplished at constant temperature by carrying out desorption under pressure and regeneration at a lower total system pressure. Pressure swing cycle is relatively simple. It can be changed rapidly, heating and cooling steps are eliminated and a pure adsorbate is recovered since no separation of the desorbate and stripping agent is necessary. A fast adsorption-desorption cycle substantially reduces the adsorber dimensions.

3.9.1.3 Purge Gas Stripping

Purge gas stripping is achieved by passing an essentially non-adsorbed gas through the adsorbent bed. The purge gas removes the desorbate from the adsorbent

surfaces, thus keeping the partial pressure of the component over the bed below its equilibrium value. The amount of material desorbed is influenced by the temperature and total pressure of the operation. The lighter the desorbate equilibrium vapour pressure for a given bed loading, the more material is transferred from the adsorbed phase to the purge gas before equilibrium is approached. Higher operating temperatures aid the overall desorption rate since the equilibrium desorbate vapour pressure for a given bed loading increases with temperature. Lower total operating pressures result in a more efficient utilization of the stripping gas since a higher desorbate concentration in the effluent is obtained for a fixed desorbate vapour pressure.

3.9.1.4 Displacement Desorption

A displacement desorption cycle is one whereby a more strongly adsorbed adsorbate is used to displace the original adsorbate. This regeneration technique is often used to desorb a temperature sensitive material, but a further desorption cycle is required to desorb the displaced substance before commencing adsorption on the next cycle.

3.9.1.5 Combination Desorption

Thermal swing, purge gas stripping and displacement desorption techniques are all involved in this regeneration cycle. Removal of solvents from charcoal using steam is an example of this process.

CHAPTER 4

ADSORPTION STUDIES - PROCEDURE
AND TREATMENT OF RESULTS

4 Adsorption Studies - Procedure and Treatment of Results

This chapter describes the investigations into the adsorption capacities of charcoal cloth for four different organic solvents from an air stream. The experimental objectives are outlined, followed by a description of the rig. Experimental procedures and analytical methods are then discussed in the subsequent sections.

4.1 Experimental Objectives

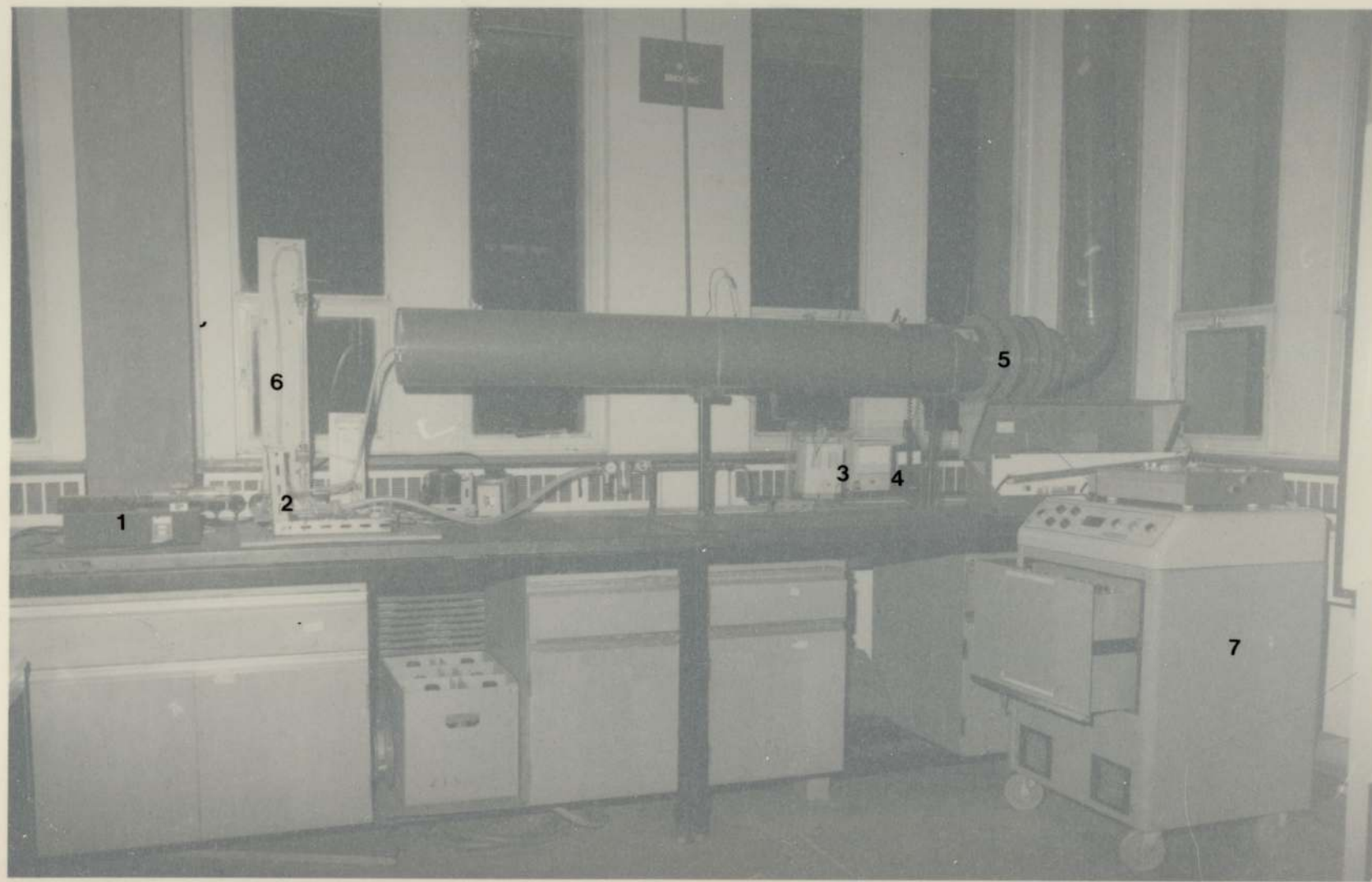
Adsorption of toluene, heptane, tetrachloroethylene and o-xylene on charcoal cloth is studied. Adsorption is continued until the cloth is saturated, that is, when the system has reached the equilibrium stage. Effluent concentration is plotted against time to find the saturation time. 25, 35 and 45 layers of charcoal cloth are used for each liquid solvent flow rate. Adsorbate-adsorbent ratios are calculated for the whole length of experiment and also at the first sign of saturation. For each solvent three different weights of charcoal cloth are used for each flow rate. Five different flowrates are used ranging from $.0025 \times 10^{-6} \text{ m}^3 \text{ s}^{-1}$ to $0.01 \times 10^{-6} \text{ m}^3 \text{ s}^{-1}$. For each run, breakthrough time required for the outlet concentration to reach 10% of the inlet concentration, is found from the graph of outlet vapour concentration against time. Three such times are plotted against weight of charcoal cloth used for the respective experiments. A regression analysis is performed with those three values and from the slope and intercept, the rate constant is calculated.

Charcoal cloth is regenerated using hot air in an oven

PLATE 4.1

GENERAL VIEW OF THE EXPERIMENTAL RIG

1. Syringe Pump
2. Hot Finger Vaporiser
3. Thermometer
4. Anemometer
5. Canister
6. Flow Meter Manometer
7. Mass Spectrometer



1

6

2

3

4

5

7



and the concentration of the vapour leaving the oven is measured and plotted against time.

4.2 Description of the Rig

Adsorption of solvent vapour on charcoal cloth takes place in a 0.1524 m (6") long canister which is a part of a 1.8 m long pipe. The diameter of the pipe is 0.1524 m (6"). The adsorbing region is at a distance of ten diameters from the entrance point of the vapour. This is to avoid stratification. The entrance section of the canister is covered by a PVC plate with a .0254 m (1") diameter hole in the centre. At the exit section, there is a similar PVC plate with a .0254m(1") diameter hole at the centre. This arrangement is to allow the vapour maximum residence time. Circular segments of charcoal cloth, cut approximately to about 0.1524m(6") diameter, are interleaved with a plastic mesh between each to support the cloth. To avoid leaking through the edges of the canister, the cloth pieces are cut so as to overlap the edges of the rigid plastic mesh.

The air-vapour mixture enters the rig through a .0254m (1") diameter hole at a point which is about 1.6 m from the entrance of the canister. The 1.8 m long pipe is connected to the fume cupboard and through the fan the exhaust vapour is released to the atmosphere.

Four thermocouples are placed at equidistant points alongside the long pipe to check the variation of temperature of the air-solvent vapour mixture as they proceed towards the canister, the adsorbing region. The thermo-

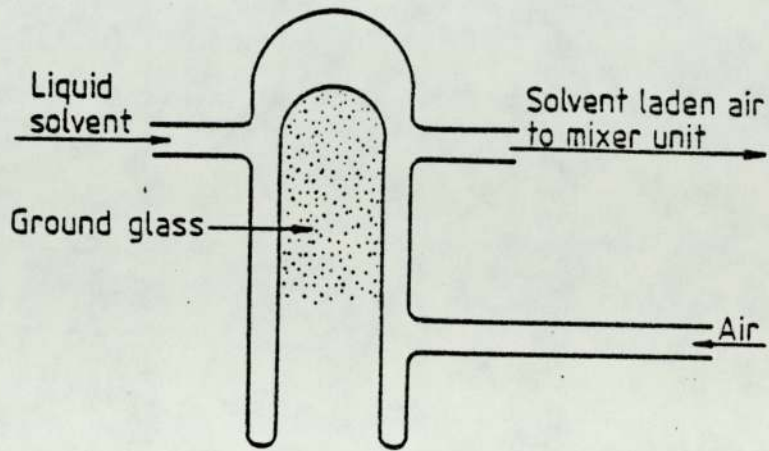


FIGURE 4.1 THE HOT GLASS FINGER SYSTEM

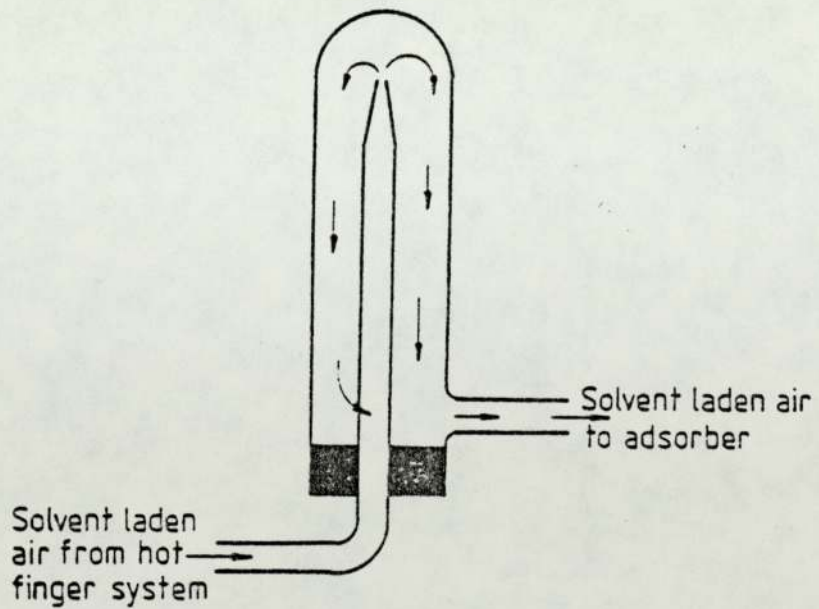


FIGURE 4.2 MIXER UNIT

couples are connected to a thermometer placed below the rig. A hot wire anemometer is used on the rig to monitor the velocity of the air-solvent vapour mixture.

4.2.1 Solvent-Air Mixing Section

Air, to carry the organic vapour, is available from a pipeline in the laboratory. Its volumetric flow is measured by a metric 7A rotameter and can be varied between rates of $1.66 \times 10^{-5} \text{ m}^3 \text{ s}^{-1}$ and $1.83 \times 10^{-4} \text{ m}^3 \text{ s}^{-1}$ by a plug valve immediately preceding the flow indicator. The relative humidity of the air is determined from a hygrometer enclosed in a perspex box through which the air flows.

A syringe pump, Model 351 ex Sage Instruments, which can deliver liquids at rates between $2.5 \times 10^{-9} \text{ m}^3 \text{ s}^{-1}$ and $1.0 \times 10^{-6} \text{ m}^3 \text{ s}^{-1}$ is used to deliver the liquid solvent onto the glass 'hot finger' element. The 'hot finger', used to vapourize the solvent, is heated by 1.95 m of heating wire which has a resistance of $150 \Omega \text{ m}^{-1}$. The heating wire is coiled inside the 'glass finger', and the ends of the wire are connected to the terminals of a 2A Torovolt with an output voltage ranging from 0 - 270v.

The set-up shown in Figure 4.2 is used to mix the air and solvent vapour before it is passed through a PVC tube to the base of the adsorber.

4.3 Experimental Procedure

The adsorption canister is fitted into the pipe in the appropriate section and the 'hot finger' switched

on to warm-up. The syringe pump is set to required flow rate. The mass spectrometer is to be switched on at least one hour before the experiment is to be started. The inlet and outlet sampling probes of the adsorbing section are installed. Compressed air is passed through the rotameter, the liquid is passed on the 'hot finger' and the air-vapour mixture thus created is diluted by the atmospheric air drawn by the fan of the fume cupboard which is attached to exit section of the adsorbing region. The temperature is measured at four equidistant points along the path of the adsorber and the anemometer fitted near the adsorbing zone indicates the velocity of the incoming air-solvent vapour mixture. The pressure drop across the canister is measured by a water manometer.

After the cloth is saturated with the vapour, the canister is separated from the pipe and layers of cloth are removed and placed in the oven at a pre-set temperature. The vent pipe of the oven leads to an extracting fan. A probe, fitted in this line, is connected to mass spectrometer to record the exit concentration of described vapour.

4.4 Mass Spectrometer

The inlet and outlet concentration of vapour passing through the adsorbing section are measured by mass spectrometer.

The following paragraphs describe the operating procedure of mass spectrometer. A description of the

PLATE 4.2
REGENERATION OVEN



fault diagnosis is outlined at the end.

4.4.1 Operating Procedure

4.4.1.1 Starting Up

The mass spectrometer is to be connected to a suitable mains supply. The off indicator will be illuminated once the standby is depressed. The inlet rotary pump and the ventilation pumps will start running.

After about 45 seconds the inlet rotary pump will start and if no gross leak is detected by the capsule switch, the diffusion pump heater will itself start together with the left hand timer on the vacuum control unit. If a high pressure is detected by the capsule switch, the off button indicator will be extinguished.

4.4.1.2 Mass Tuning

In order to set the mass tuning correctly a mixture containing the required gases must be sampled by the inlet. One of the inlets has to be connected and selected by the rear inlet valve. The electronics unit is to be pulled out to expose the control panel. All automatic sensitivity control switches will be switched off and channel gains are to be reduced to minimum. Mass position of the digital panel meter function switch is selected according to the vapour to be tested. A detailed list of mass number and their relative peaks for many compounds are included in the literature (129). The mass tuning meter is to be watched for a deflection

indicating the ion current being collected. If no deflection is obtained, the sensitivity will have to be increased until a deflection of approximately half scale is obtained.

The operate button is then depressed and if all the warning indicators are extinguished, the mass spectrometer is then ready to use.

4.4.1.3 Shutting Down

The mass spectrometer must be kept on standby condition when it is not used. To shut down, the inlet selector valve should be moved to off position before moving to standby. About five minutes should be allowed for the ion source to cool when the off button can be depressed.

4.4.1.4 Sampling Technique (Respiratory Mode)

The inlet capillary assembly is a nylon luer fitting with the fine bore capillary extending half inch from the tip. The orifice of the fine bore capillary must be immersed directly in sample flow to avoid protracted response times due to any dead volumes surrounding the tip.

4.4.2 Fault Diagnosis

The four warning indicators on the top panel should be extinguished when the instrument is functioning correctly. However, there are occasions when one or more of the warning lights may be illuminated. The inlet light shows when the inlet tube is blocked. A high

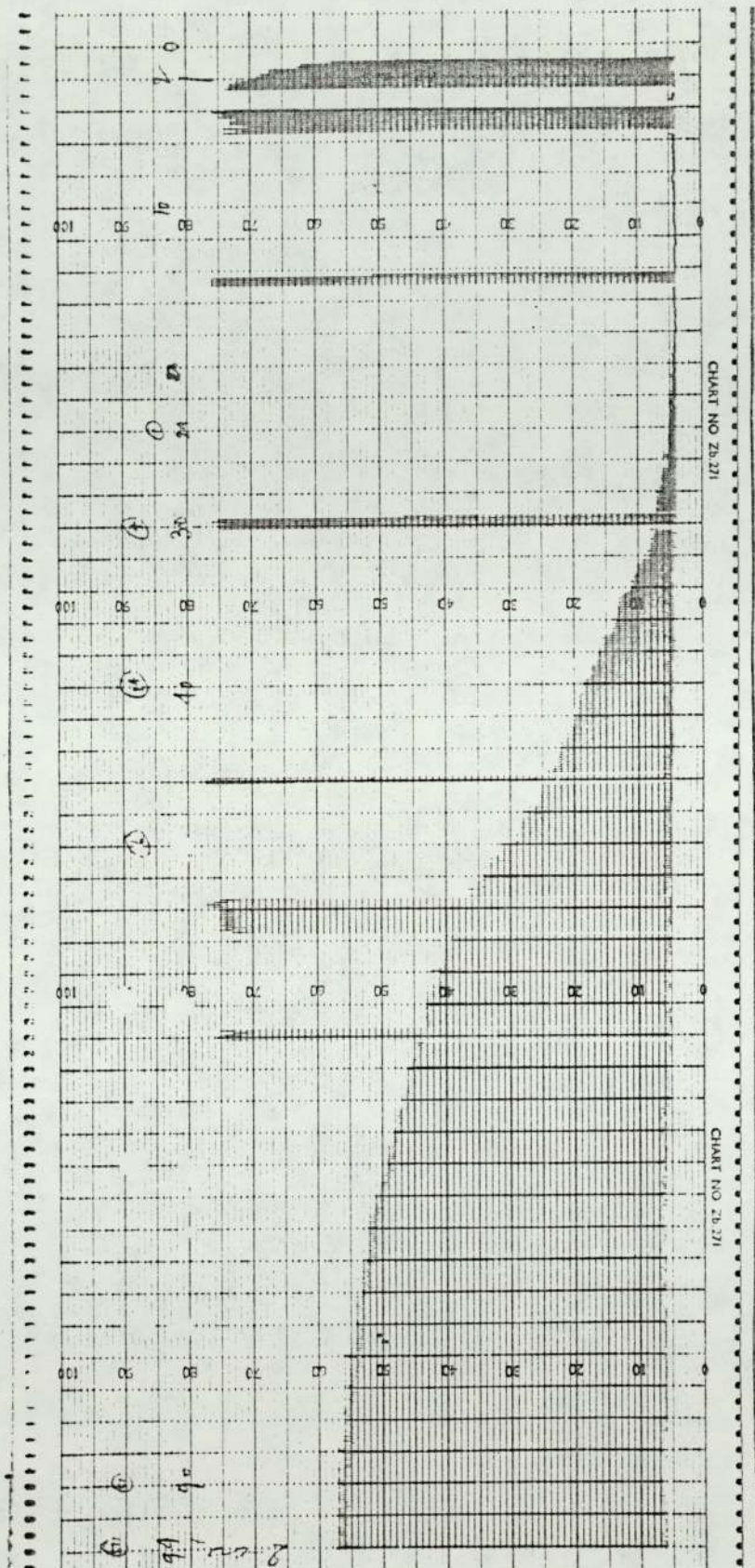


FIGURE 4.3 MASS SPECTROMETER TRACE

pressure in the vacuum system causes the HiVac indicator on. In case of a burnt filament, it should be replaced by a new one. And if the ion current available is insufficient sensitivity alarm will show up. In this case amplifier gain control is to be increased. On every occasion of incorrect functioning, the machine is to be put to standby before any alteration is carried out.

4.5 Treatment of Experimental Results

For each solvent, five different flowrates were used ranging from $0.25 \times 10^{-8} \text{ m}^3 \text{ s}^{-1}$ to $1.0 \times 10^{-8} \text{ m}^3 \text{ s}^{-1}$. For each flowrate three different weights of charcoal cloth were used. The outlet vapour concentrations were calculated from the peak heights on the mass spectrometer trace. The inlet vapour concentration was calculated beforehand from the experimental known flowrates. A sample of calculation of inlet and outlet concentration is outlined in Appendix I.

Three graphs are plotted for each of the four solvents showing the variation of outlet vapour concentration against time. As expected, the breakthrough occurs more swiftly with the highest inlet solvent concentration and vice versa. Almost all of the experiments were continued a significant time after saturation to make sure that all stages of adsorption could be observed. Breakthrough time has been shown separately in Appendix VI. Appendix II shows the total time of the experiment where the adsorbate-adsorbent

ratio has been calculated based on the total mass of the inlet solvent. It also tabulates the experimental condition of each run. The area under the curve of outlet vapour concentration against time is calculated with the help of a computer program. From the area the mass of the solvent vapour leaving the adsorbent is calculated. The weights of charcoal cloth before and after the experiment gives the amount of solvent vapour adsorbed. By a material balance over the adsorbent bed, it has been found that a part of the inlet solvent vapour cannot be traced. One possible explanation is that the solvent vapour, mixed with large amount of air, reacts on the surface of charcoal cloth, the latter behaving as a catalyst in this case.

It has been mentioned before that the first sign of saturation occurs before the experiments are finished. From the outlet vapour concentration vs time graph, the saturation time has been deduced and the adsorbate-adsorbent ratio has been calculated at this time. This ratio is less than the same value calculated based on the total time of the experiment.

The time required for the outlet vapour concentration to reach 10% of the inlet vapour concentration has been recorded. Three values were obtained for each flow rate and they were plotted against the different weights of charcoal cloth used. Regression analysis was performed using three of these values and from the slope and intercept of the best straight line drawn

through these three points, the adsorption rate constant was calculated using equation 3.54. An example of the calculation of the adsorption rate constant has been included in Appendix I. Five rate constant values were obtained for five of the inlet solvent flowrates.

The Dubinin-Polanyi equation has been used to calculate the theoretical value of the adsorbate-adsorbent ratio using the physical characteristics of the solvent and the experimental conditions. A computer program for the calculation has been listed in Appendix X.

It has been assumed that the loss of the solvent vapour due to some chemical reaction on the cloth surface happens after the charcoal cloth becomes saturated. Reaction occurs near the saturation point due to the excess of solvent vapour over the active free sites of the adsorbent. To verify the above assumption two runs were carried out for each of the solvents with the highest and lowest inlet liquid solvent flowrates. With the lowest flowrate ($0.25 \times 10^{-8} \text{ m}^3 \text{ s}^{-1}$), the run was for 5400 seconds (90 minutes) and with the highest flowrate ($1.00 \times 10^{-8} \text{ m}^3 \text{ s}^{-1}$) the run was for 1800 seconds (30 minutes). But the rate of loss did not differ very much from the loss observed after saturation has been reached. This shows that the chemical reaction goes on simultaneously with the adsorption process. The results are tabulated in Appendix IX.

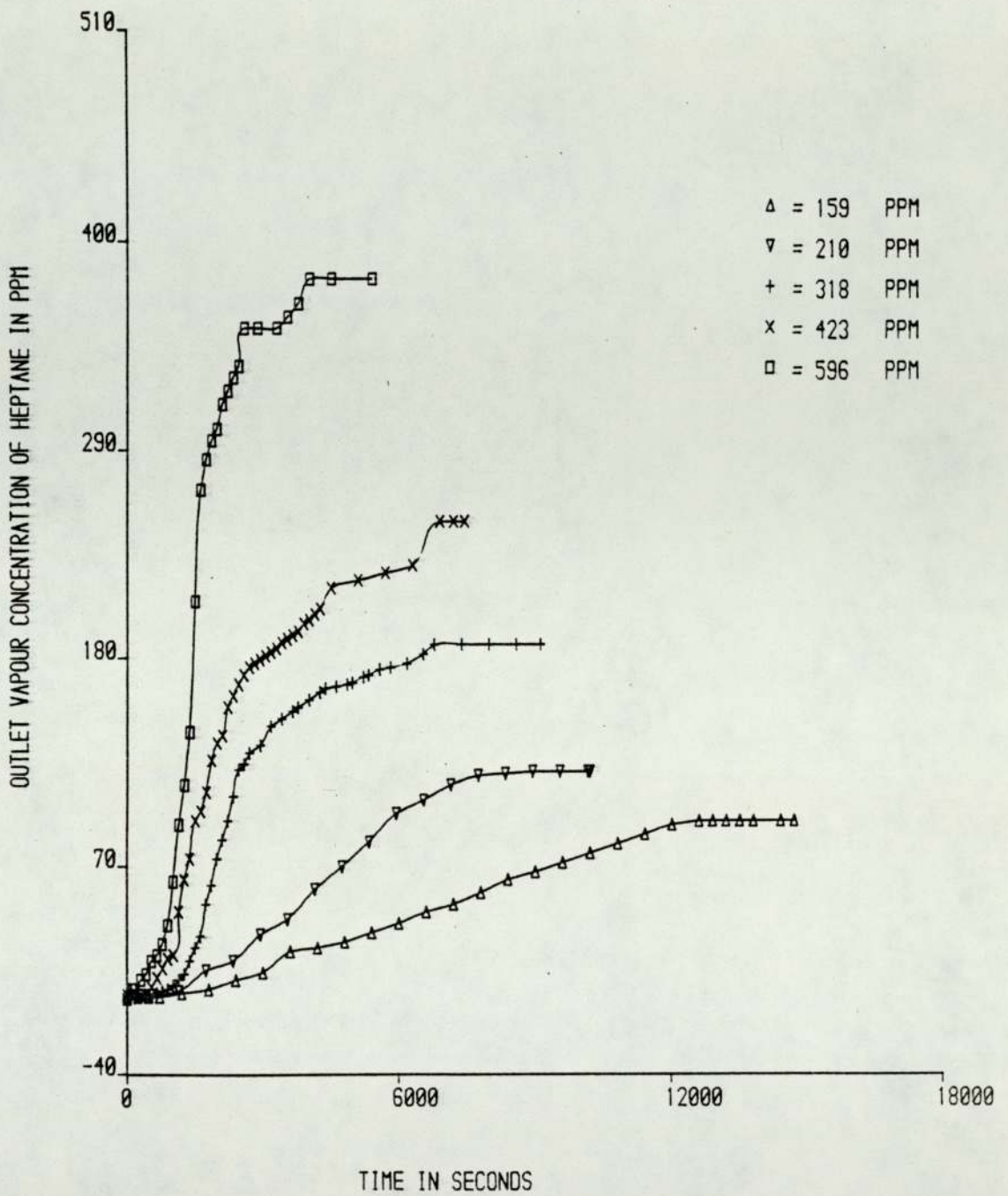


FIGURE 4.4 OUTLET VAPOUR CONCENTRATION VS TIME AT DIFFERENT INLET CONCENTRATION
(25 LAYERS OF CHARCOAL CLOTH)

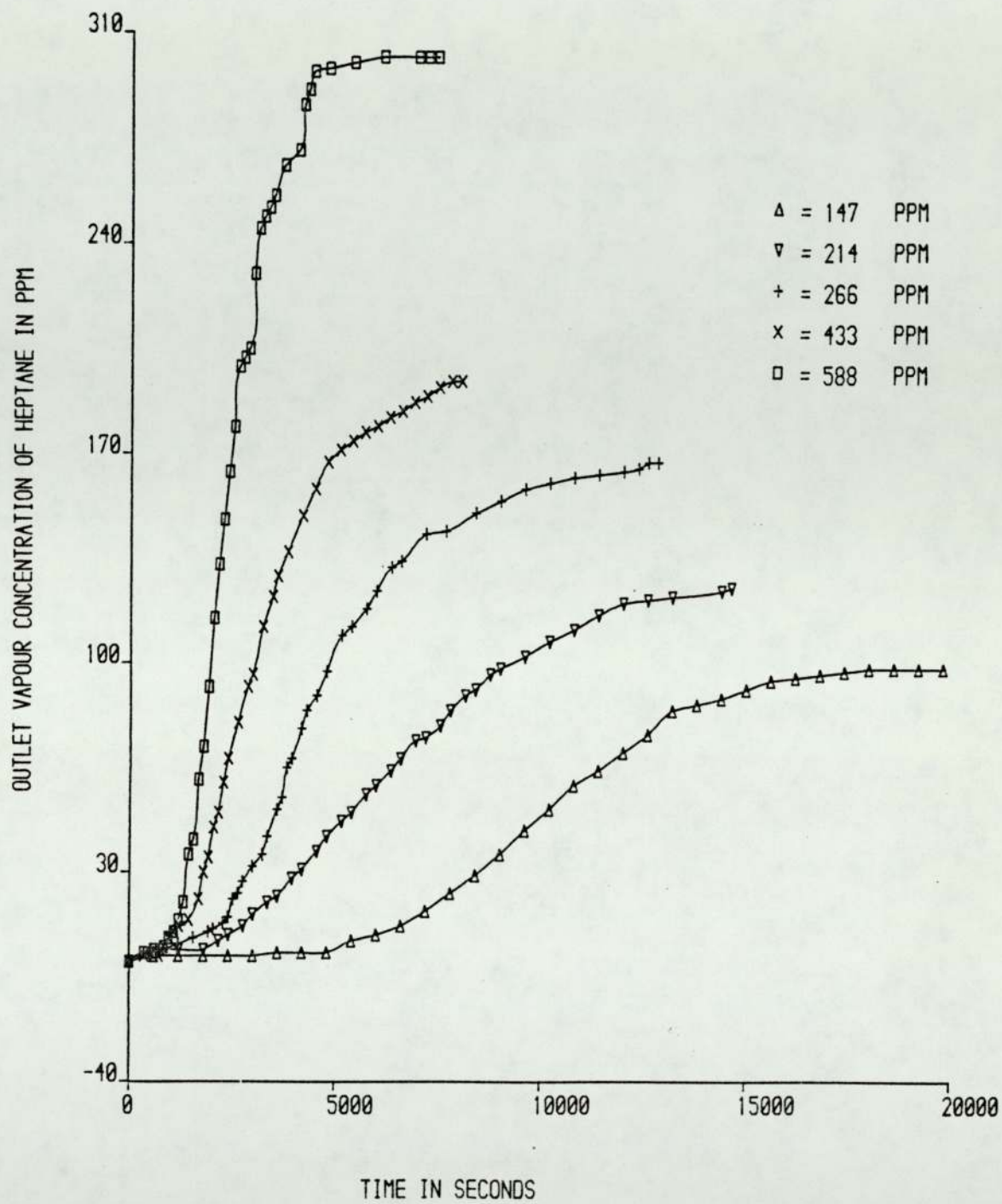


FIGURE 4.5 OUTLET VAPOUR CONCENTRATION VS TIME AT DIFFERENT INLET CONCENTRATION
(35 LAYERS OF CHARCOAL CLOTH)

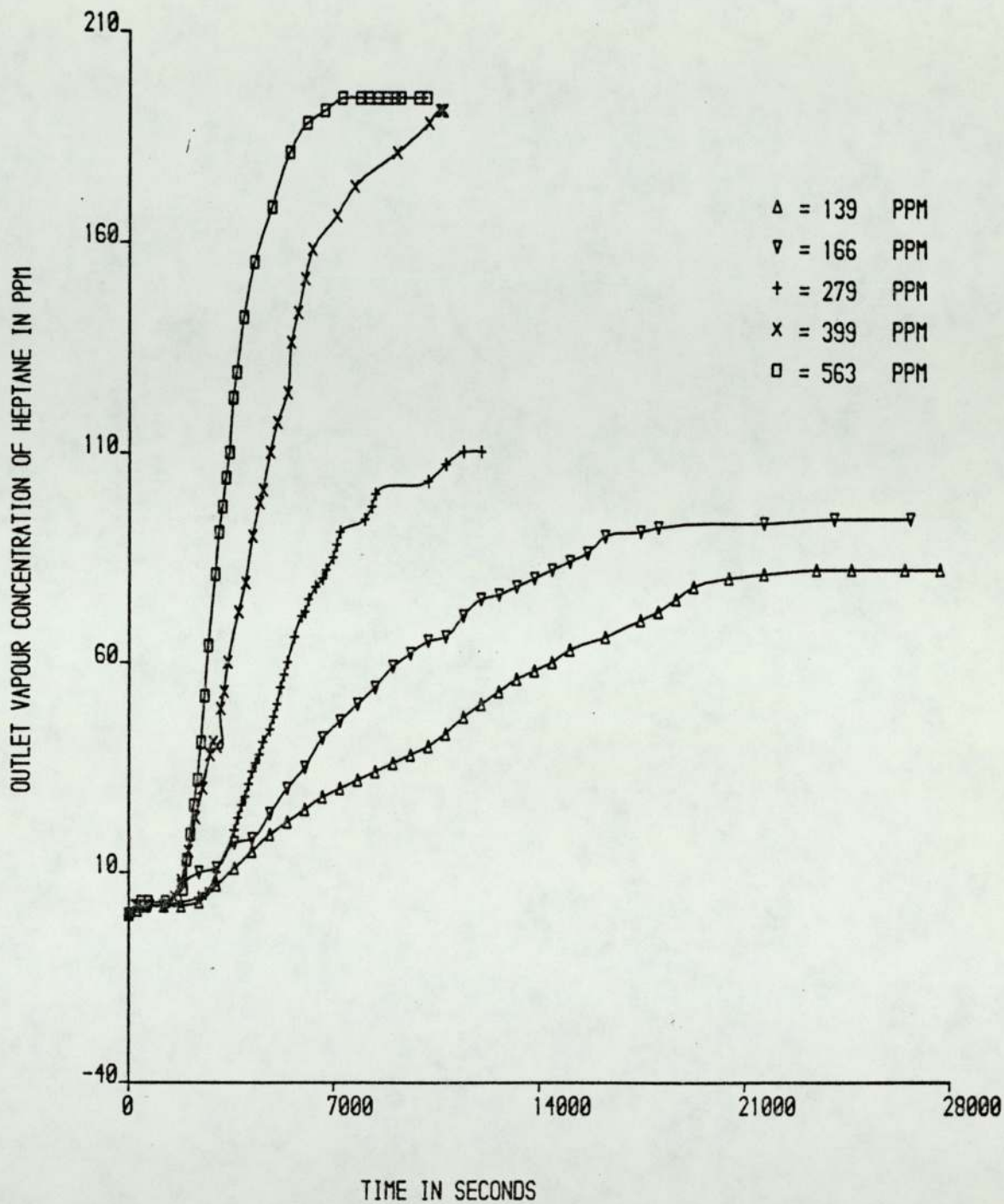


FIGURE 4.6 OUTLET VAPOUR CONCENTRATION VS TIME AT DIFFERENT INLET CONCENTRATION
(45 LAYERS OF CHARCOAL CLOTH)

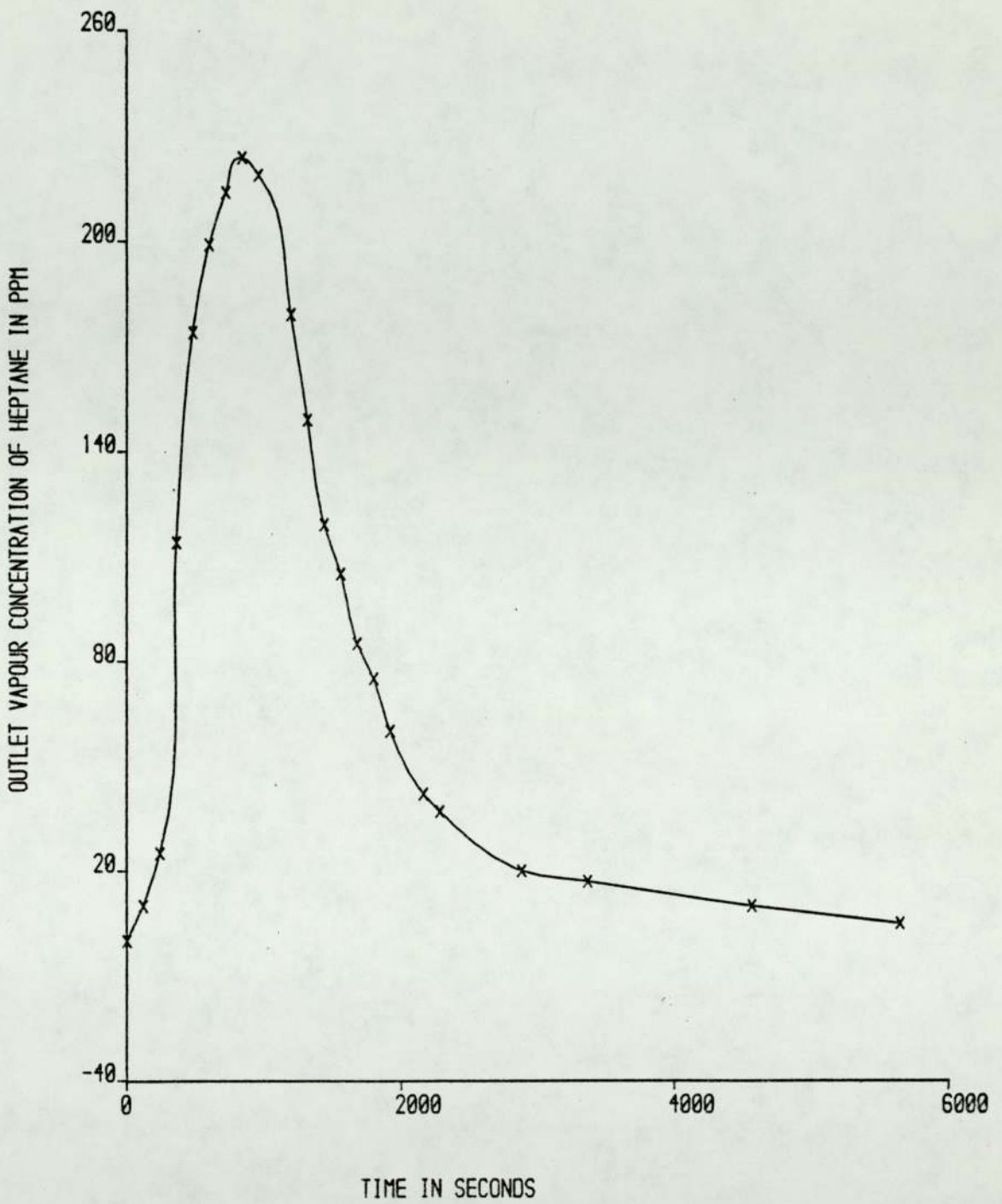


FIGURE 4.7 REGENERATION OF CHARCOAL CLOTH (HEPTANE ADSORPTION)

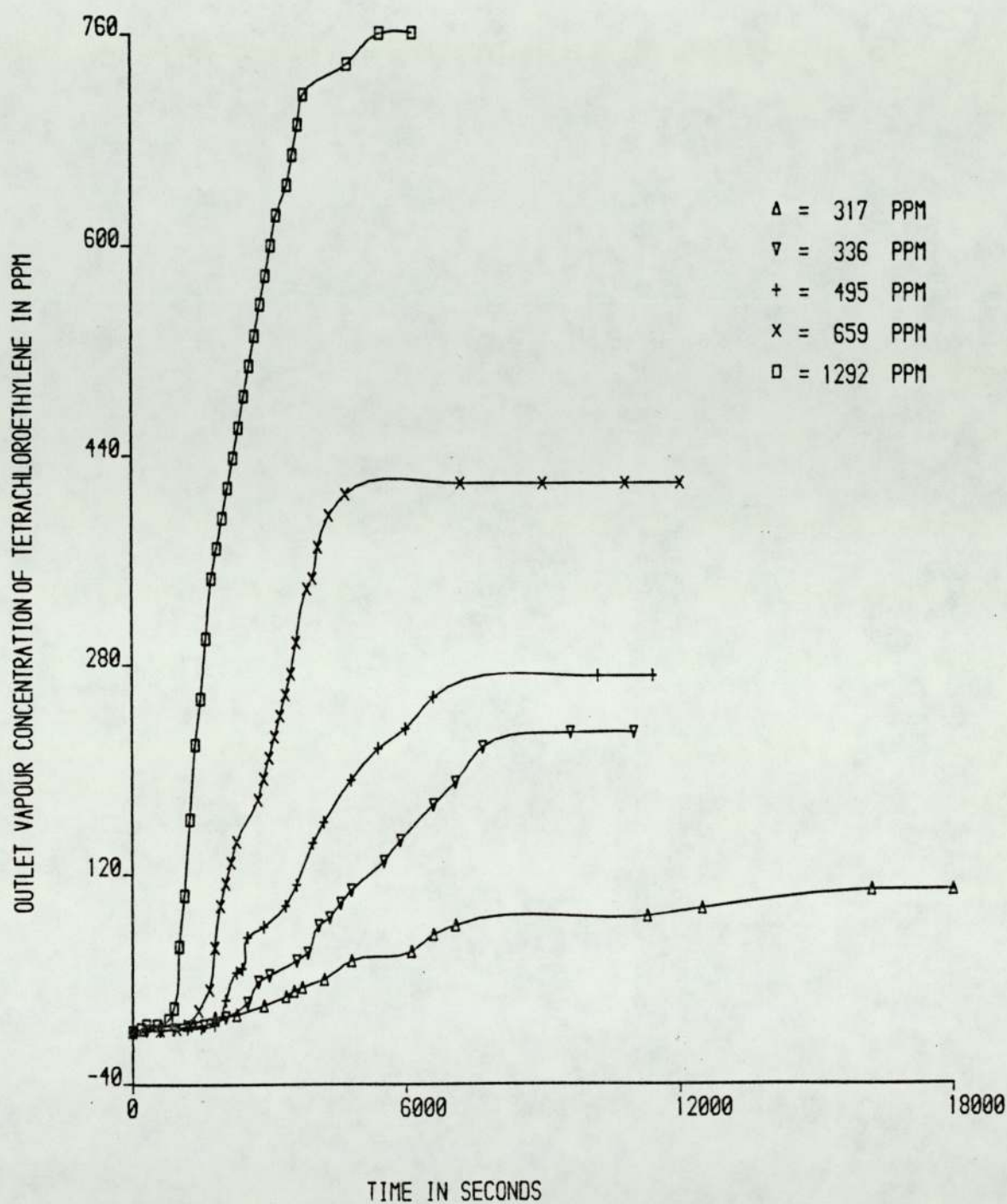


FIGURE 4.8 OUTLET VAPOUR CONCENTRATION VS TIME AT DIFFERENT INLET CONCENTRATION
(25 LAYERS OF CHARCOAL CLOTH)

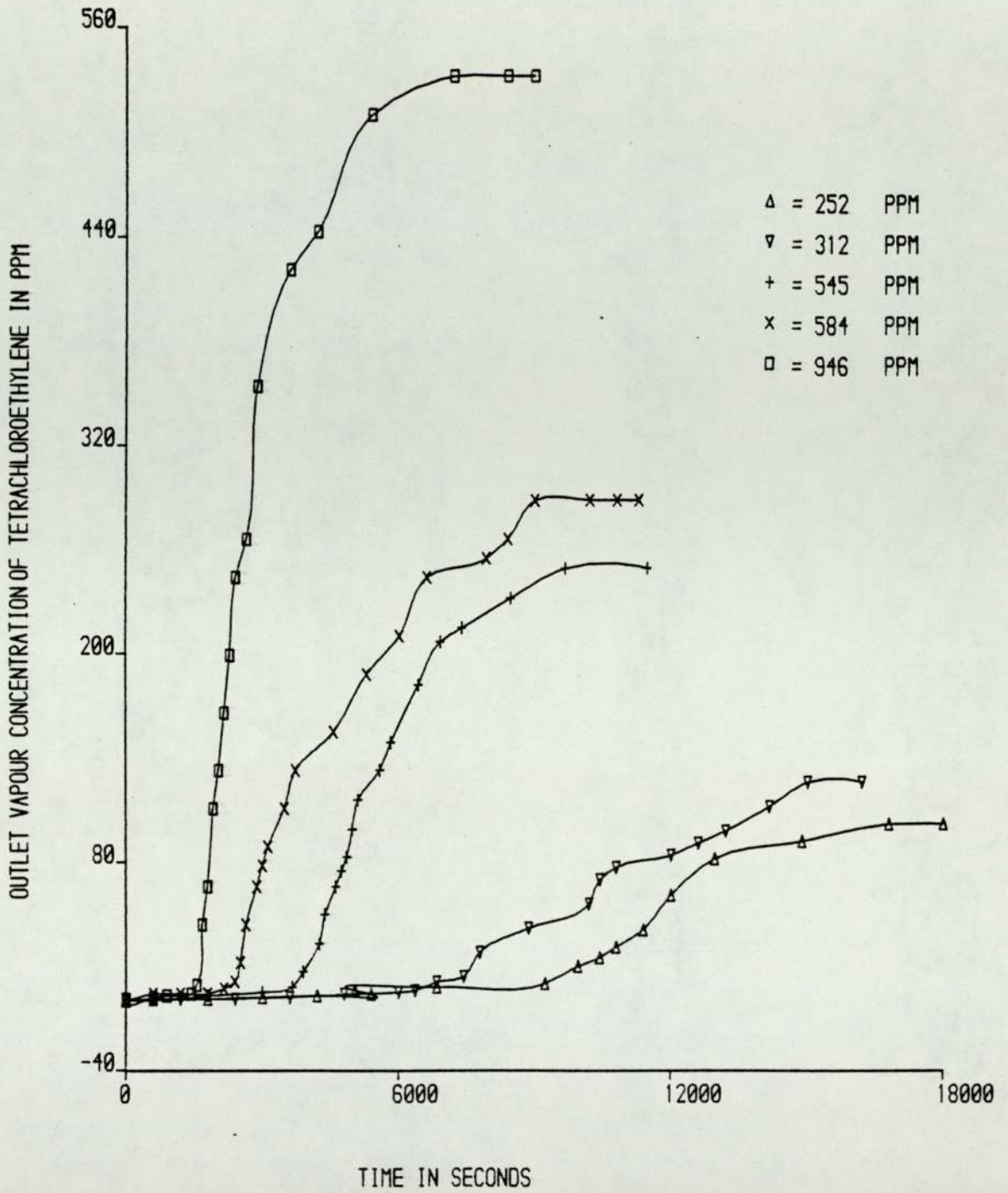


FIGURE 4.9 OUTLET VAPOUR CONCENTRATION VS TIME AT DIFFERENT INLET CONCENTRATION
(35 LAYERS OF CHARCOAL CLOTH)

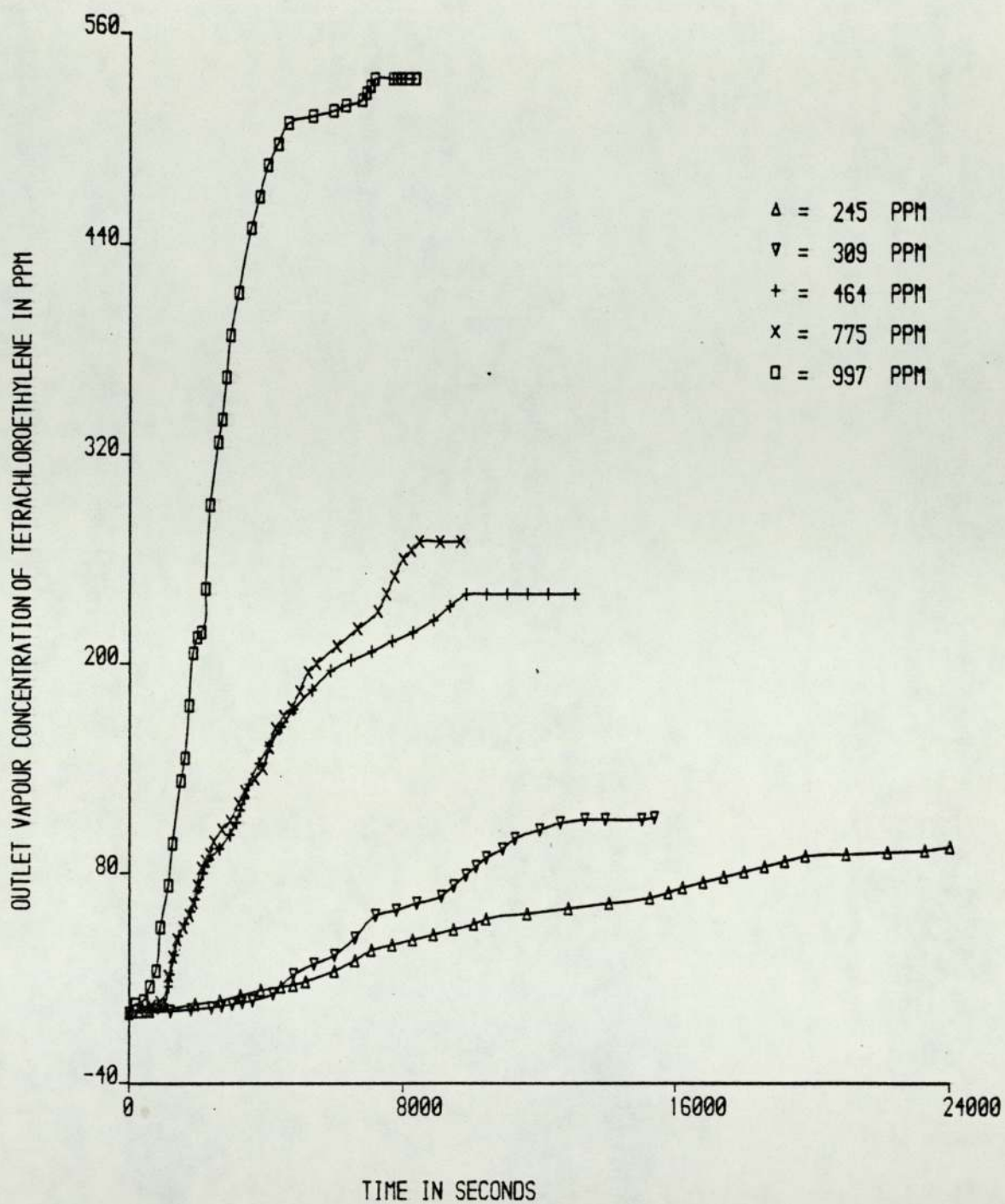


FIGURE 4.10 OUTLET VAPOUR CONCENTRATION VS TIME AT DIFFERENT INLET CONCENTRATION
(45 LAYERS OF CHARCOAL CLOTH)

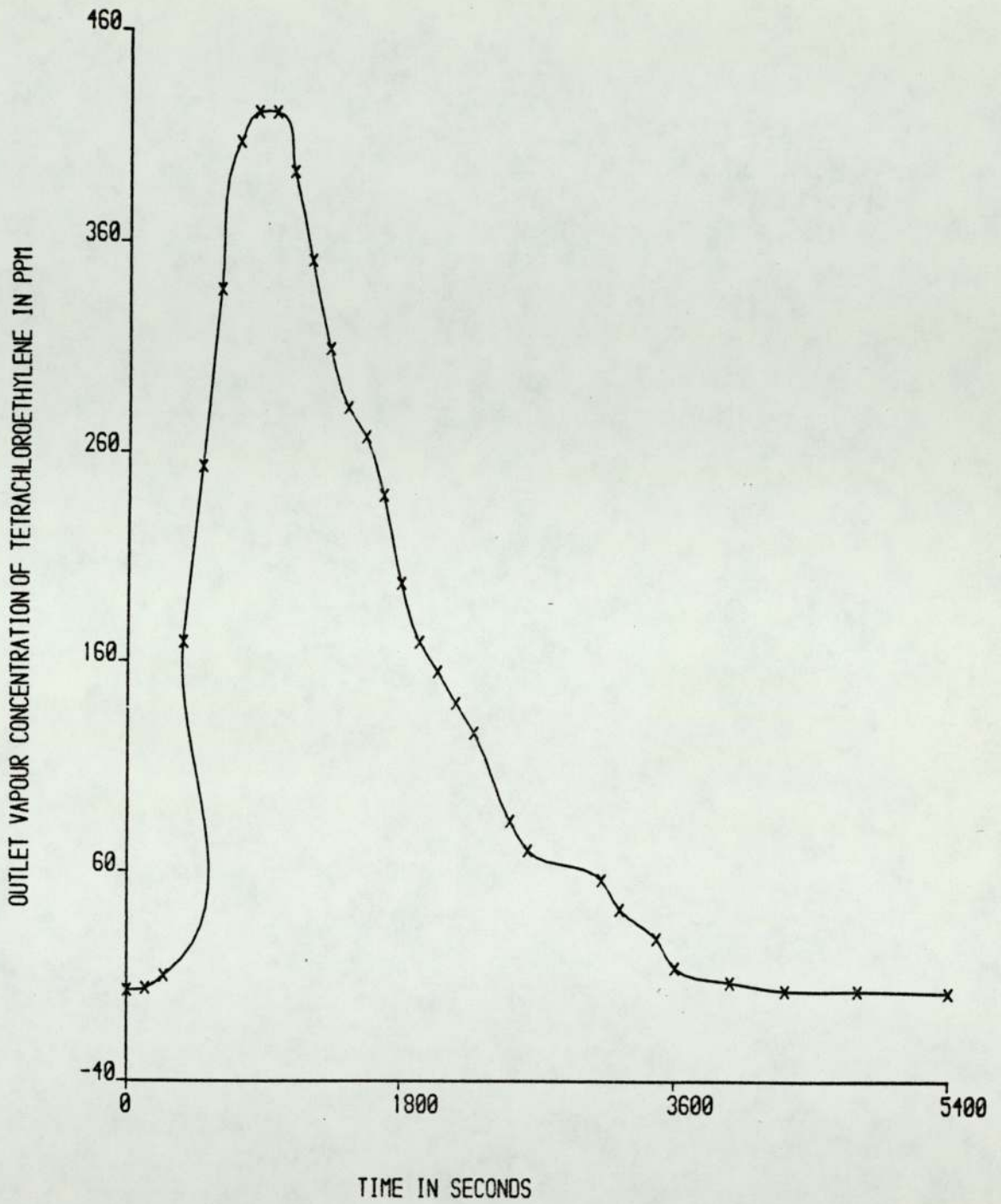


FIGURE 4.11 REGENERATION OF CHARCOAL CLOTH (TETRACHLOROETHYLENE ADSORPTION)

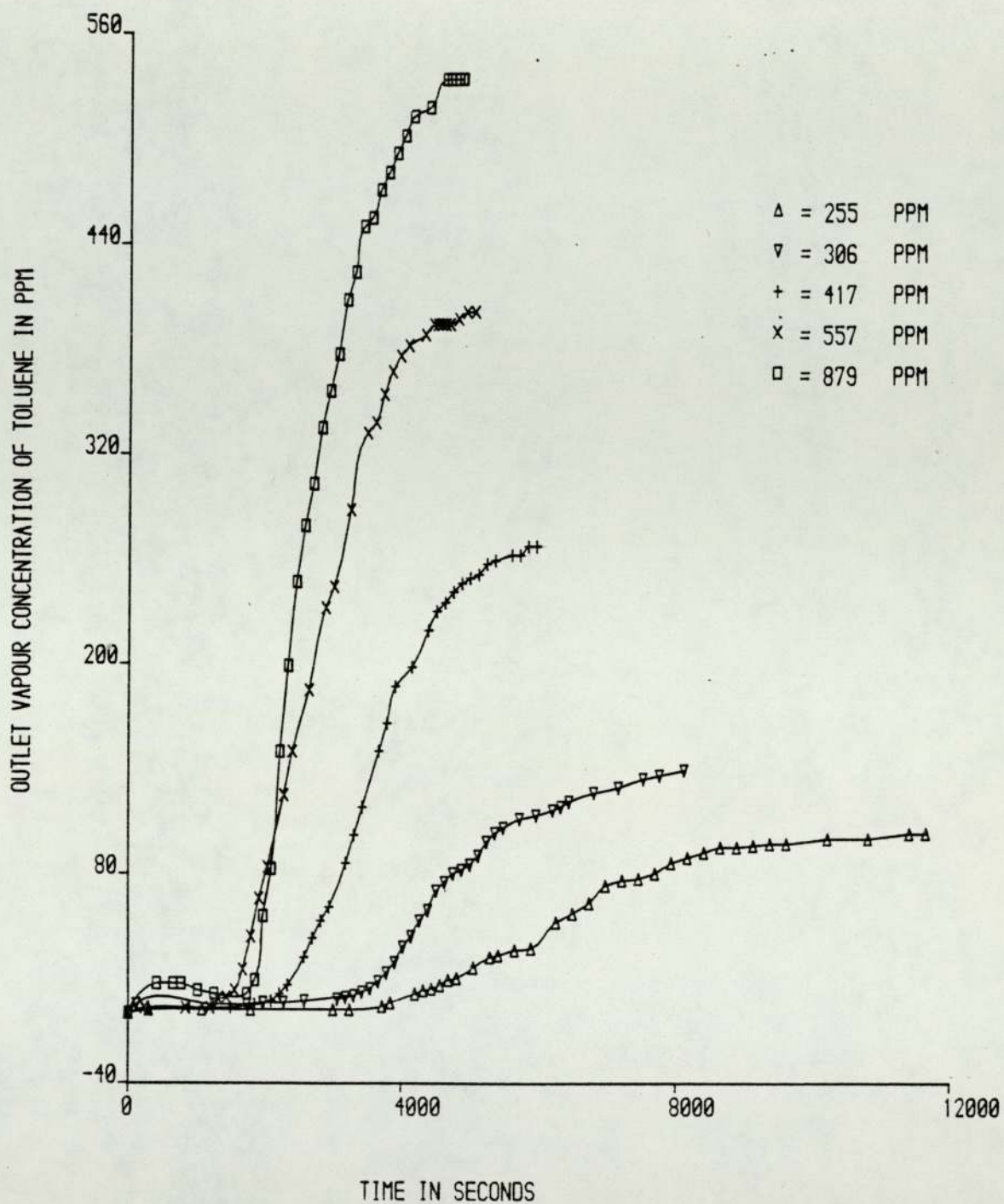


FIGURE 4.12 OUTLET VAPOUR CONCENTRATION VS TIME AT DIFFERENT INLET CONCENTRATION
(25 LAYERS OF CHARCOAL CLOTH)

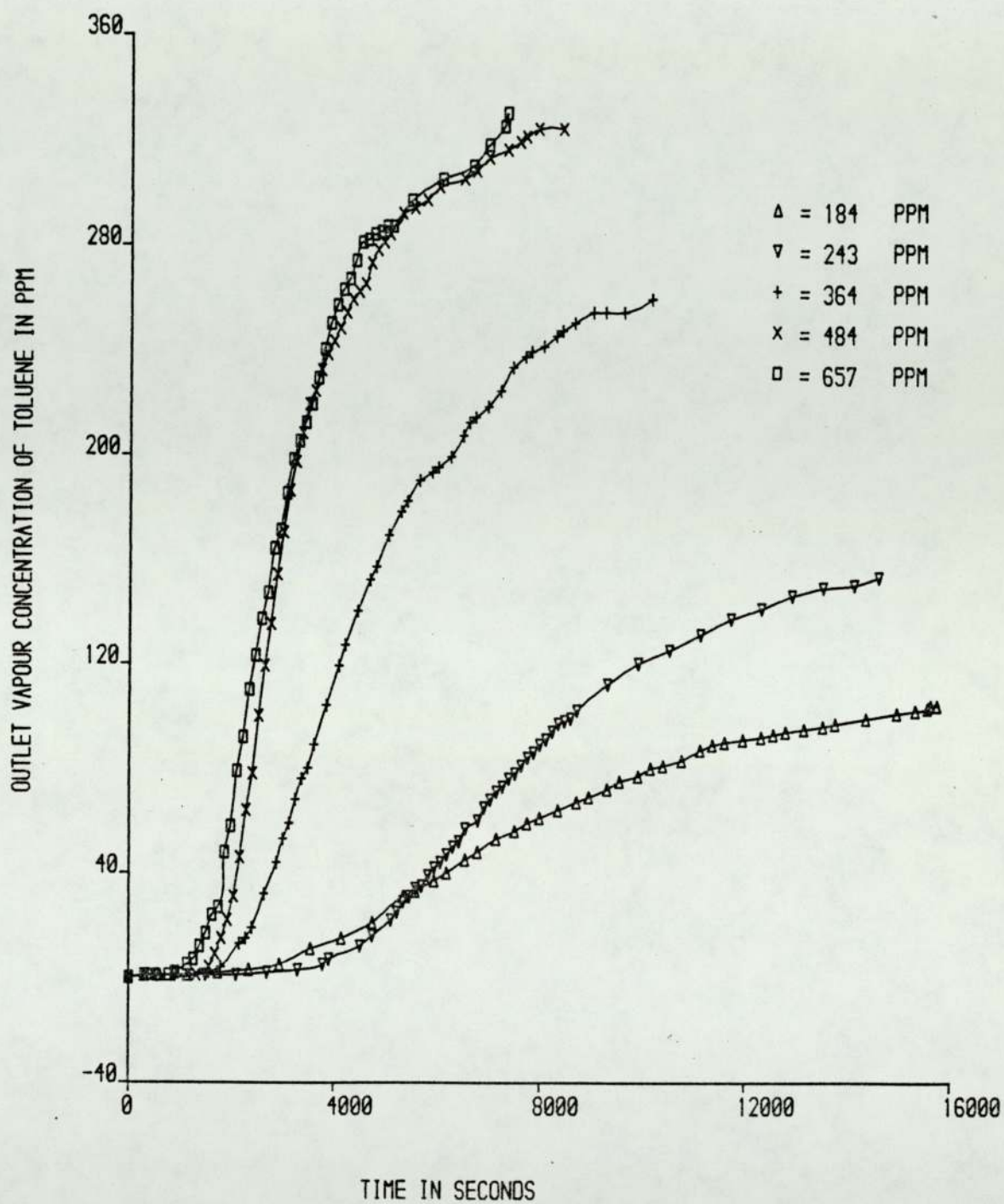


FIGURE 4.13 OUTLET VAPOUR CONCENTRATION VS TIME AT DIFFERENT INLET CONCENTRATION
(35 LAYERS OF CHARCOAL CLOTH)

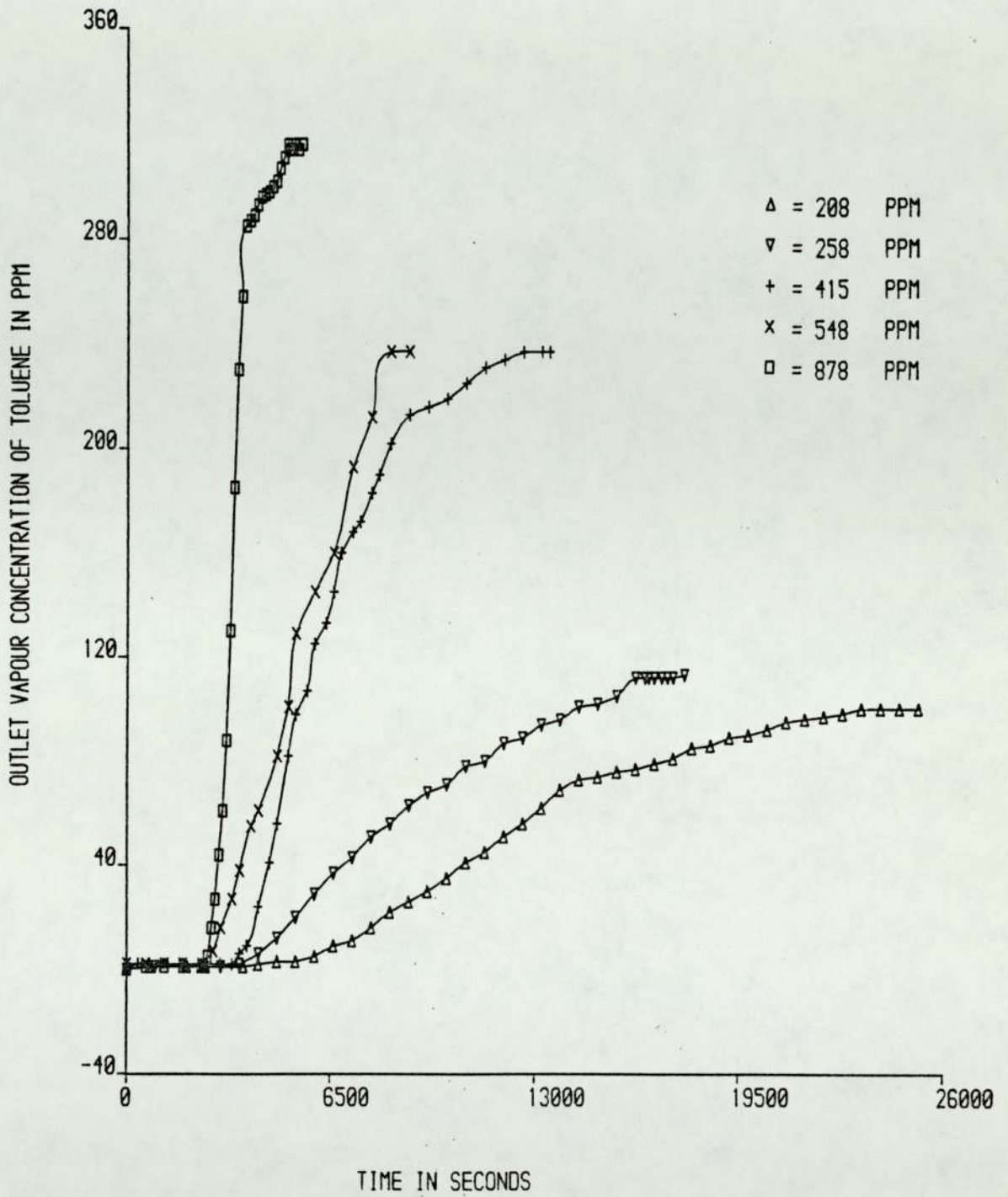


FIGURE 4.14 OUTLET VAPOUR CONCENTRATION VS TIME AT DIFFERENT INLET CONCENTRATION
(45 LAYERS OF CHARCOAL CLOTH)

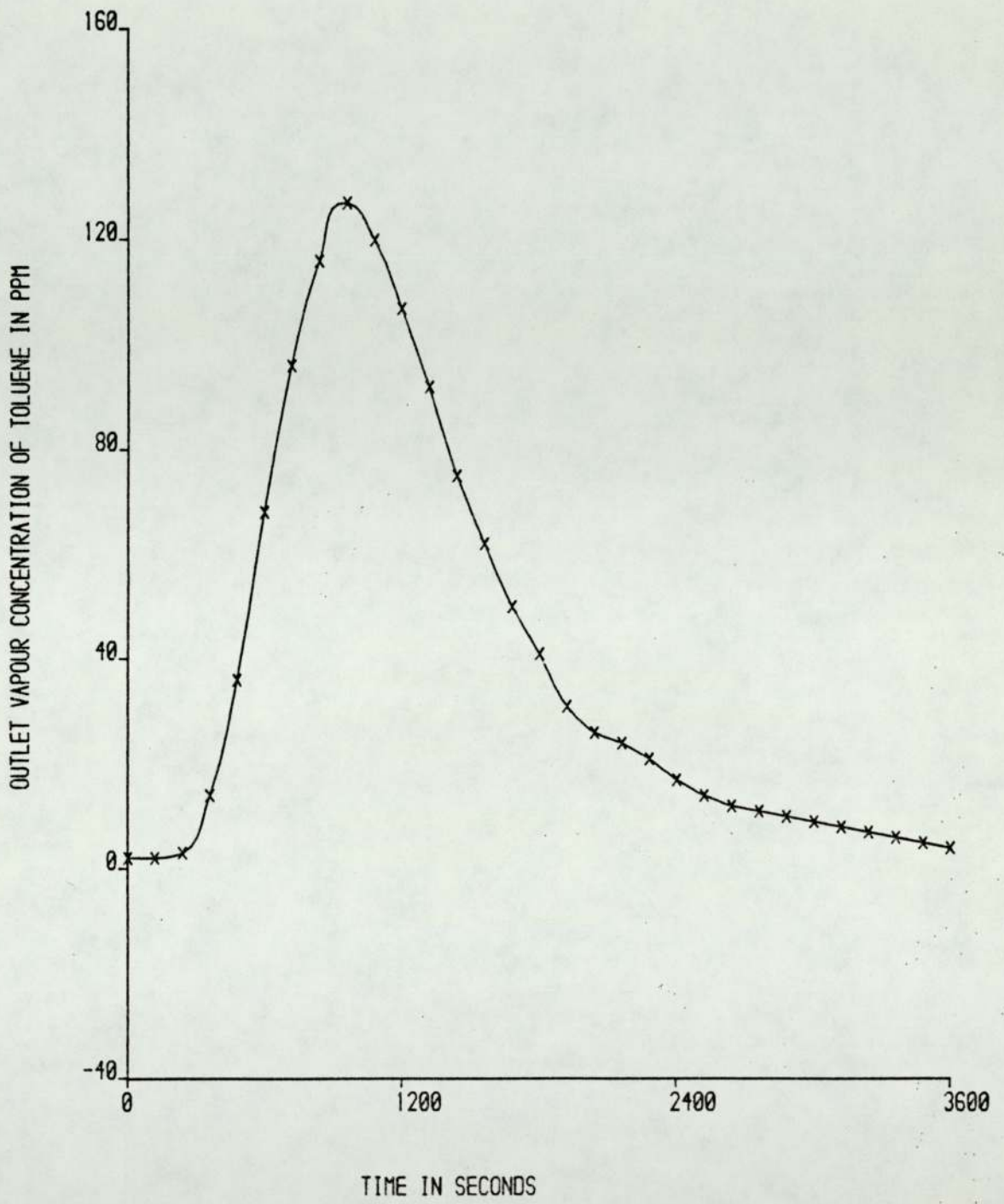


FIGURE 4.15 REGENERATION OF CHARCOAL CLOTH (TOLUENE ADSORPTION)

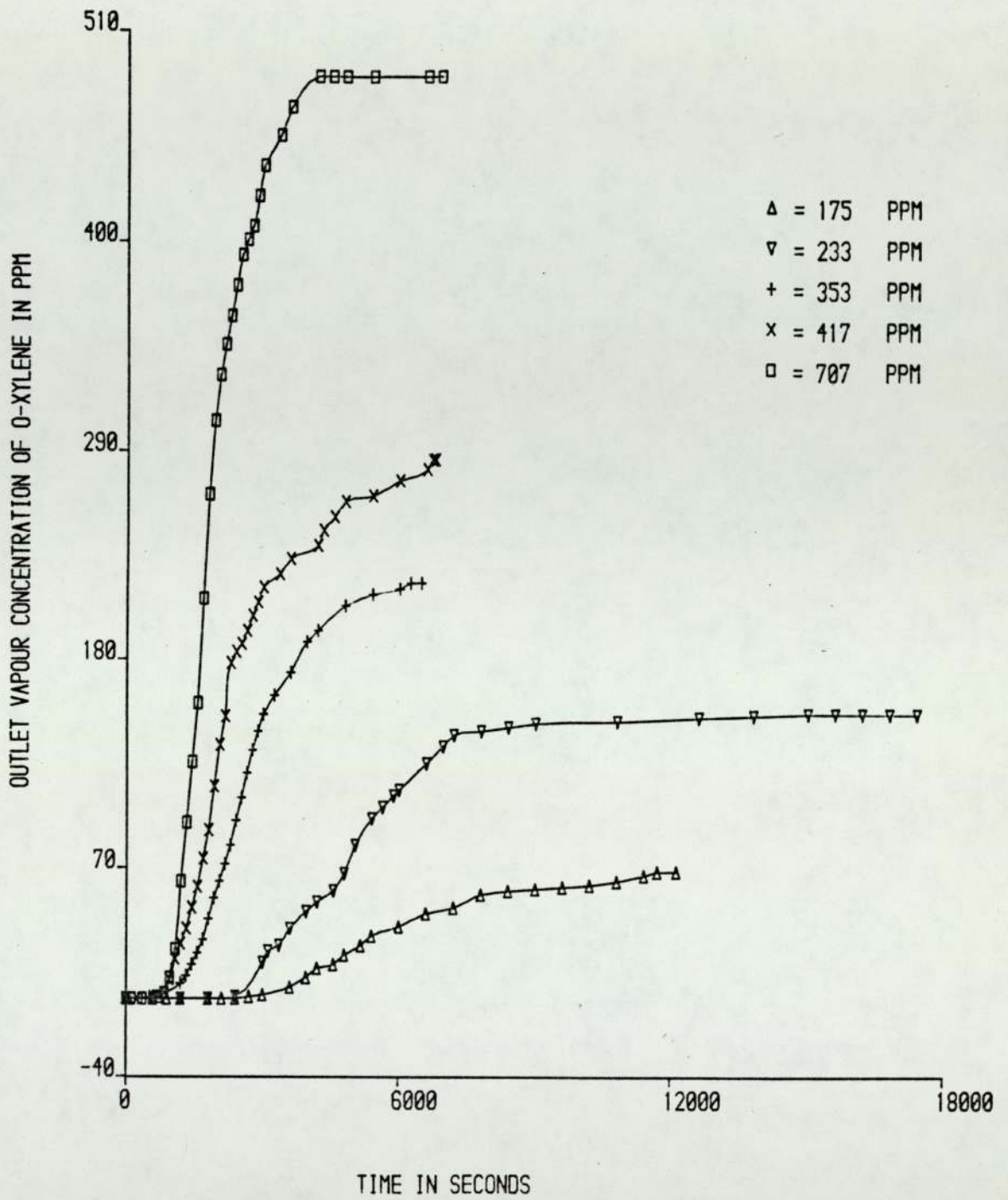


FIGURE 4.16 OUTLET VAPOUR CONCENTRATION VS TIME AT DIFFERENT INLET CONCENTRATION
(25 LAYERS OF CHARCOAL CLOTH)

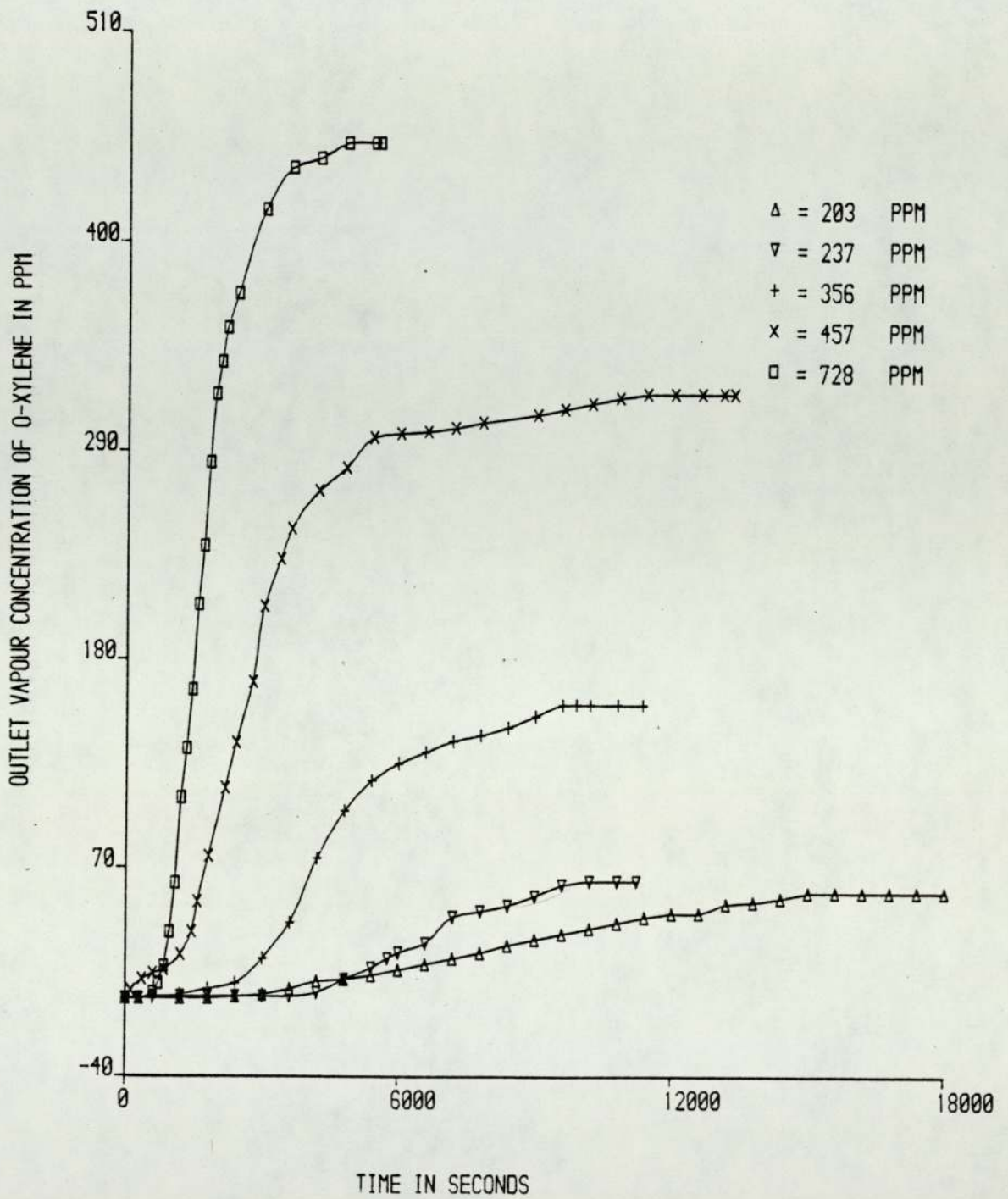


FIGURE 4.17 OUTLET VAPOUR CONCENTRATION VS TIME AT DIFFERENT INLET CONCENTRATION
(35 LAYERS OF CHARCOAL CLOTH)

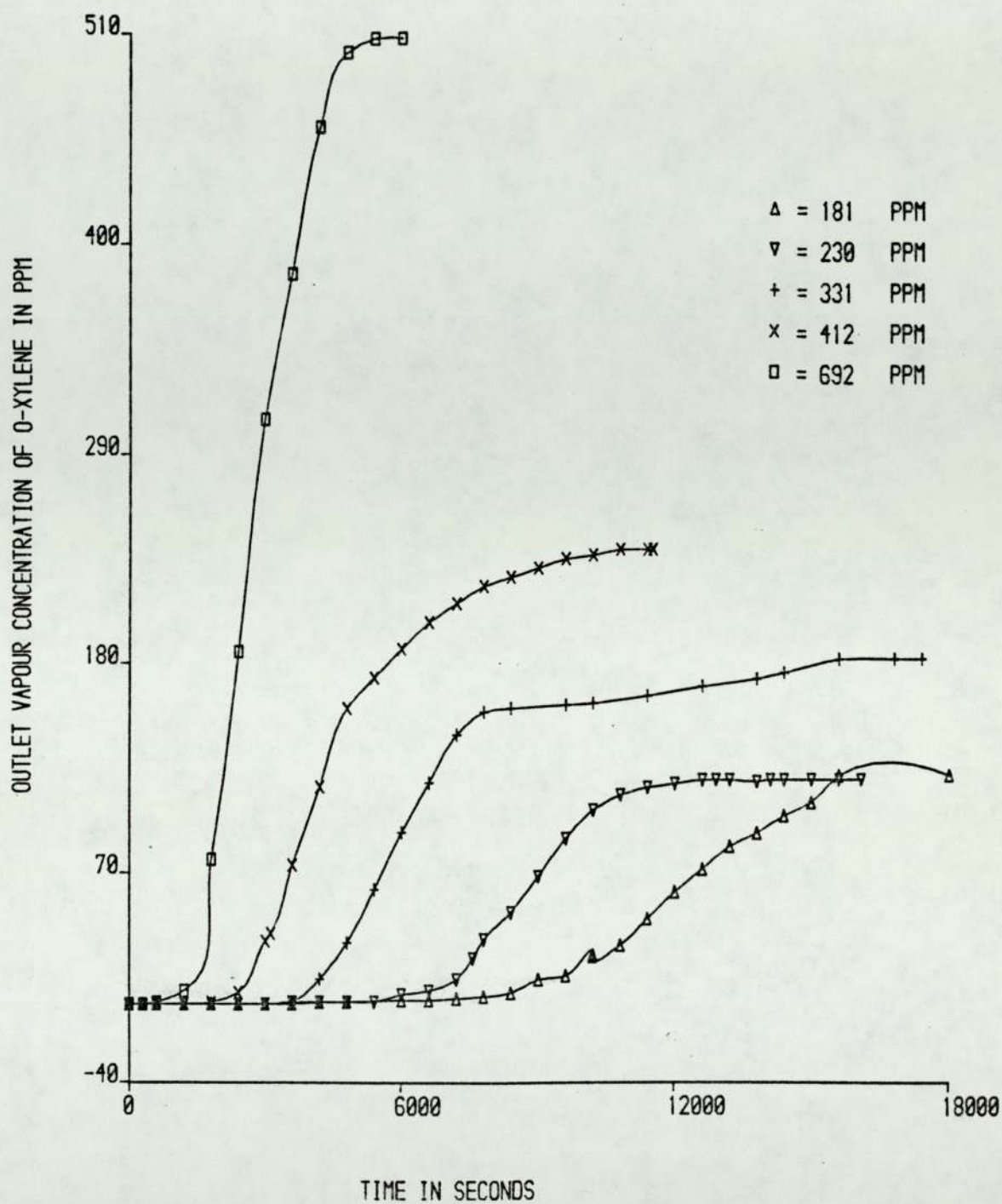


FIGURE 4.18 OUTLET VAPOUR CONCENTRATION VS TIME AT DIFFERENT INLET CONCENTRATION
 (45 LAYERS OF CHARCOAL CLOTH)

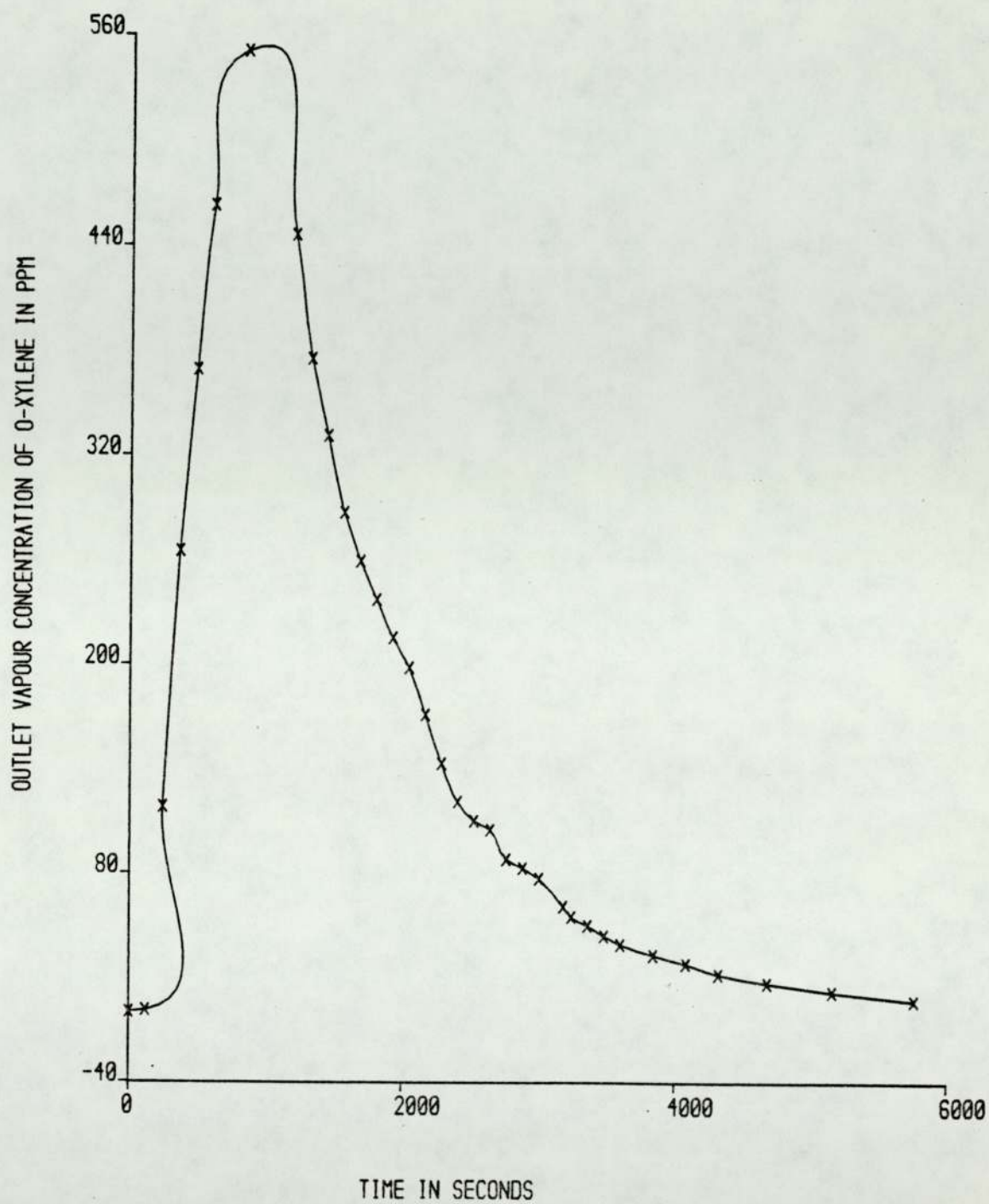


FIGURE 4.19 REGENERATION OF CHARCOAL CLOTH (O-XYLENE ADSORPTION)

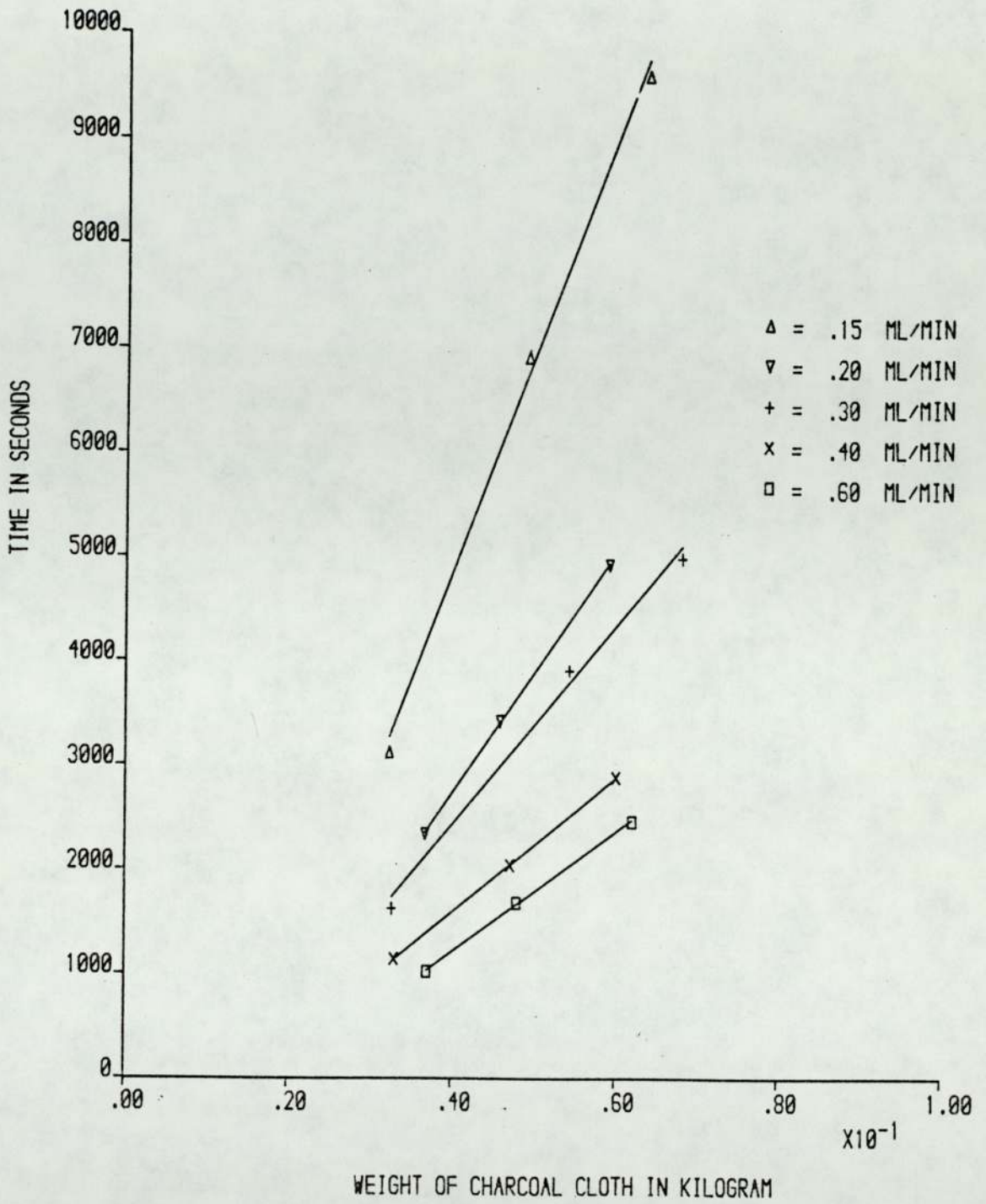


FIGURE 4.20 TIME REQUIRED FOR OUTLET CONCENTRATION TO REACH 10% OF INLET
 CONCENTRATION VS WEIGHT OF CHARCOAL CLOTH (HEPTANE)

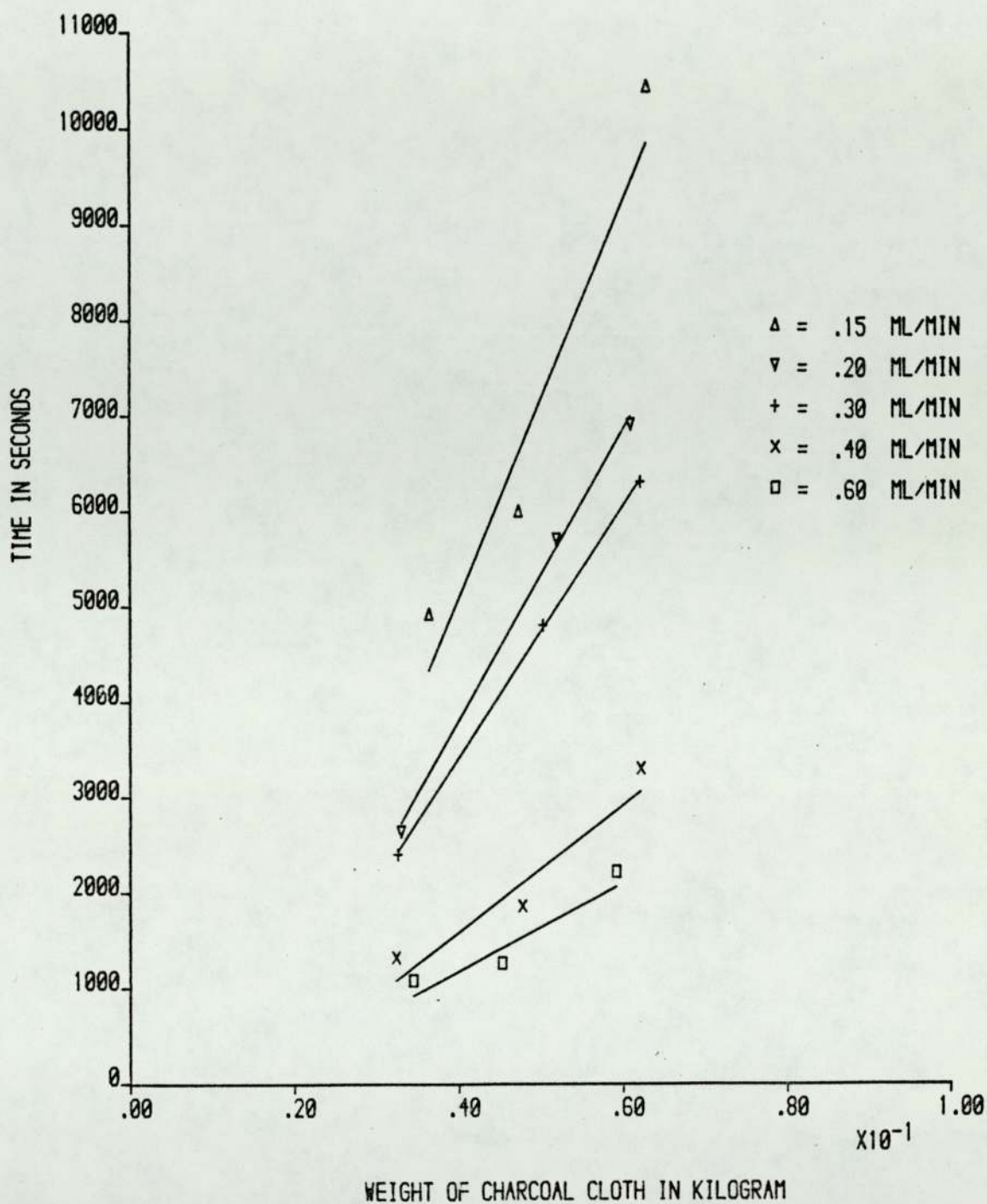


FIGURE 4.21 TIME REQUIRED FOR OUTLET CONCENTRATION TO REACH 10% OF INLET CONCENTRATION VS WEIGHT OF CHARCOAL CLOTH (TETRACHLOROETHYLENE)

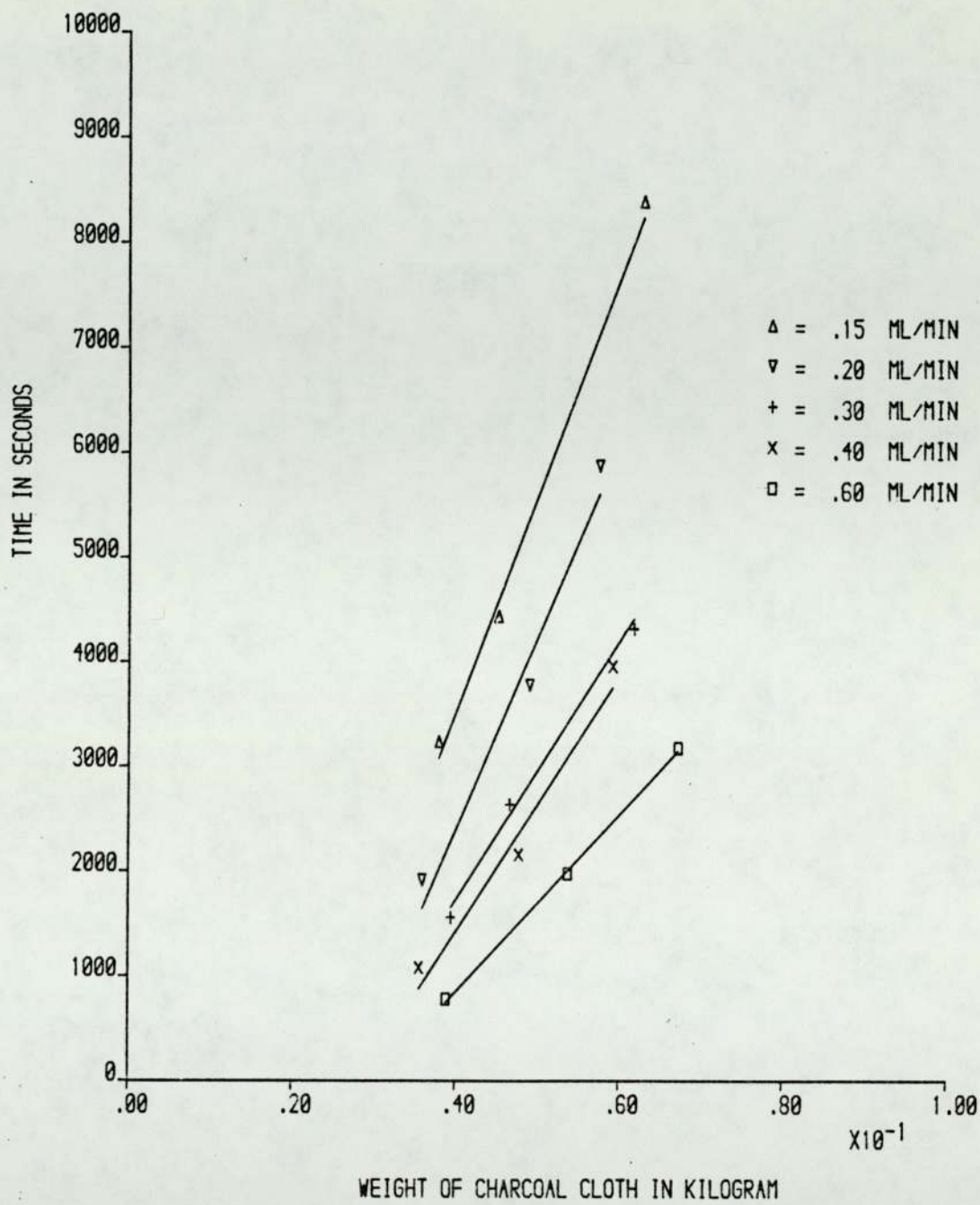


FIGURE 4.22 TIME REQUIRED FOR OUTLET CONCENTRATION TO REACH 10% OF INLET CONCENTRATION VS WEIGHT OF CHARCOAL CLOTH (TOLUENE)

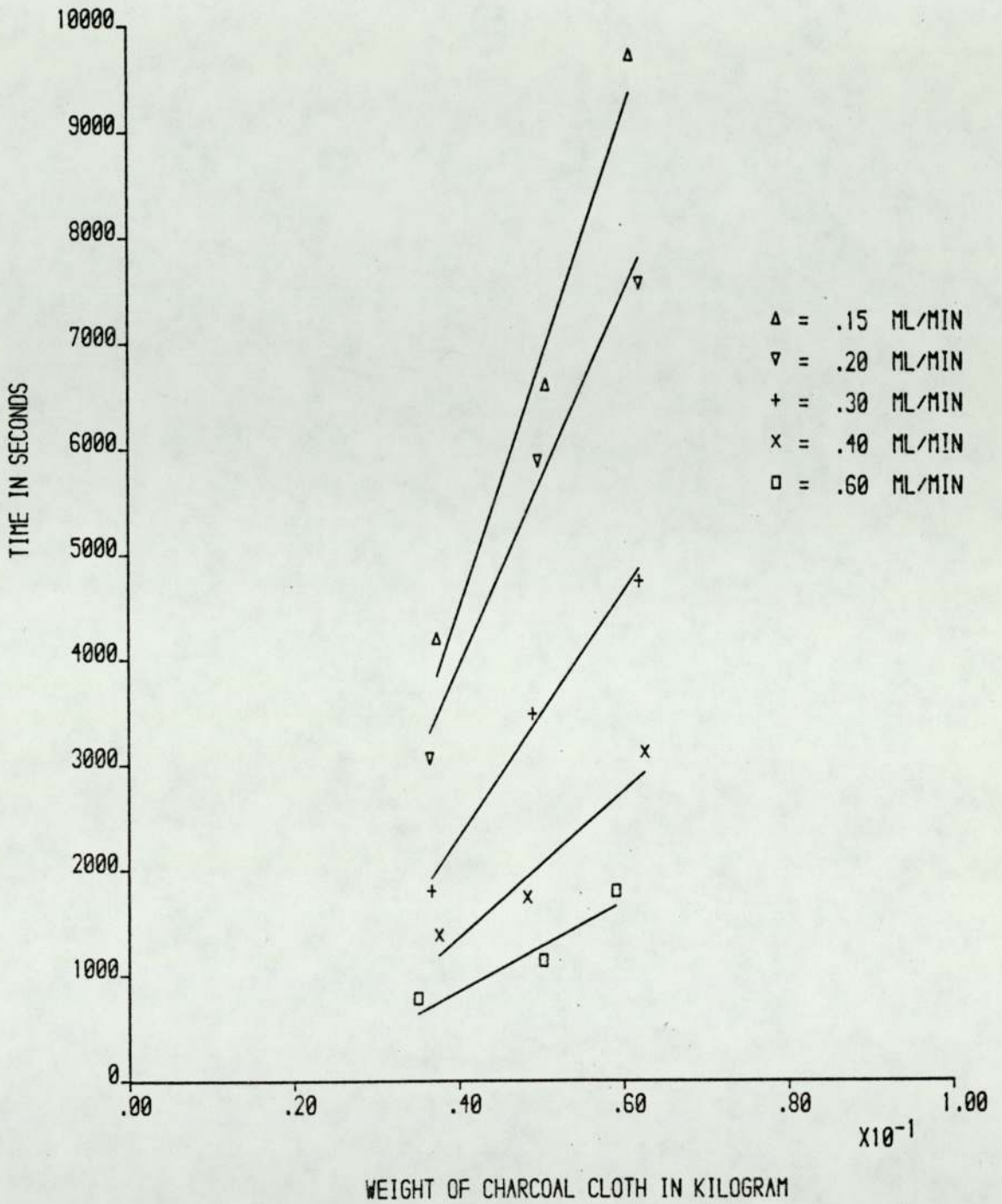


FIGURE 4.23 TIME REQUIRED FOR OUTLET CONCENTRATION TO REACH 10% OF INLET
 CONCENTRATION VS WEIGHT OF CHARCOAL CLOTH (O-XYLENE)

4.6 Effect of Number of Regenerations on the Activity of Charcoal Cloth

To investigate the effects of numerous regeneration cycles, adsorption experiments were carried out using 25 layers of charcoal cloth at a flowrate of $0.25 \times 10^{-8} \text{ m}^3 \text{ s}^{-1}$ of toluene. The outlet vapour concentration was monitored and adsorption continued until the outlet concentration reached 10% of inlet concentration. The charcoal cloth was then removed and heated up in the oven to be used again. This procedure was repeated eight times with the same cloth and the adsorption times recorded did not differ very much. The results are tabulated in Table 4.1.

Expt. No.	Adsorption Time for Outlet Concentration to reach 10% of Inlet Concentration Time (sec)
1	3240
2	3840
3	3720
4	2880
5	3360
6	3240
7	3480
8	3060

Table 4.1 Summary of results of the effect of number of regenerations on the activity of charcoal cloth

CHAPTER 5

DESIGN OF FILTER CANISTER

5 Design of Filter Canister

5.1 Introduction

To design an optimum adsorption system the design engineer must take into consideration many process and equipment factors, besides knowledge of stoichiometry, equilibria, rate and adsorbent life. The factors that influence the performance of an adsorber system need to be considered as a whole after the individual elements have been treated separately. The interaction of these factors is usually complex. The optimization of a process design invariably involves a series of trade-offs within practical limits.

5.1.1 Choice of Adsorbent

The proper choice of the type of adsorbent to be used in a particular application constitutes one of the most important factors in evolving an efficient and economic design. The type of adsorbent chosen depends on its adsorption capacity for the components to be removed, good mass transfer rate, and low deactivation rate. For particulate adsorbents the particle size affects the mass transfer rate and pressure drop in the adsorbent bed as well as the maximum lifting velocity.

Most industrial adsorbents are capable of adsorbing of both inorganic and organic vapours but their preferential adsorption characteristics and other physical properties make certain adsorbents to have a better advantage over the others for a particular adsorbate. Activated alumina, silica gel and molecular sieves will adsorb water

preferentially from a mixture of water vapour and an organic compound whereas charcoal cloth or activated carbon will do just the opposite. It has been reported in the literature (90) that preferential adsorption properties of carbon can be partially regulated by the type of surface oxide induced on the carbon.

In some cases, none of the adsorbents has sufficient retaining adsorption capacity for a particular adsorbate. In cases where adsorption is otherwise minimal, a large surface area adsorbent is impregnated with an inorganic compound or sometimes with a high molecular-weight organic compound which reacts chemically with the adsorbate. Iodine-impregnated carbons are used to remove mercury vapour and bromine-impregnated carbons are used to remove ethylene or propylene. These are examples of catalytic conversion or reaction to a more easily adsorbable compound. An impregnated adsorbent is available for most compounds which are not easily adsorbed by non-impregnated adsorbents.

5.1.2 Flow Rate

The removal of a vapour molecule from the air stream may be regarded as a two step process. The vapour molecule diffuses from the flowing air stream through a motionless air close to the surface and then it is adsorbed on the surface of the adsorbent. The rate of removal will be determined by the slower of these two processes. A linear relationship exists between the

breakdown time and the reciprocal of flow rate (113). The flow rate and column length effects are closely related and change in flow rate alters the critical bed length.

5.1.3 Column Length

The effect of bed depth on adsorption mass transfer is two fold. The bed will have to be deeper than the length of the transfer zone which is not saturated. And any multiplication of the minimum bed depth gives more than proportional increased capacity. It is advantageous to size the adsorbent bed to the maximum length allowed by pressure drop. It is suggested (128) that the length of the mass transfer zone (MTZ) can be experimentally determined

$$MTZ = \frac{\text{Total bed depth}}{\theta_2 / (\theta_2 - \theta_b) - x^*}$$

where

θ_b = Time required to reach breakpoint

θ_2 = Time required to saturate

x^* = Degree of saturation in MTZ

Increasing the length increases the breakthrough time. Danby et al. (113) found a linear relationship between two parameters

$$\theta_b = \frac{N_o}{C_o V_L} [\lambda - \lambda_c]$$

where

θ_b = breakthrough time

N_o = Number of active centres

- V_L = Superficial velocity
 C_0 = Initial concentration
 λ = Bed depth
 λ_c = Critical bed depth

Previously, the design of activated carbon columns has been concerned primarily with hydraulic considerations. Presently, individuals designing activated carbon systems are becoming more aware of the necessity of evaluating the chemical and physical aspects inherent in the adsorption process.

Adsorption is a physico-chemical process, and the design and operation of activated carbon units cannot be optimized unless the physical and chemical aspects of the adsorption process are also considered. A clear understanding of the chemistry and physics inherent in the adsorption process is a prerequisite if the adsorptive characteristics of activated carbon are to be exploited to their fullest extent.

5.2 Design of the Proposed Filter

In constructing gas adsorptive filters it is generally desirable to combine maximum adsorptive capacity with minimum gas flow resistance, minimum overall dimensions and height. Maggs et al. (114) reported that arranging the gas flow substantially parallel, rather than perpendicular to the plane of the charcoal cloth, gives higher adsorption efficiency than the parallel flow. Resistance of charcoal cloth is mainly a function of the weave. Reasonable air

flow is combined in this material with high adsorptive capacity under dynamic conditions.

To demonstrate the advantages of parallel flow arrangement over perpendicular flow, Maggs and Smith (12) did two sets of experiments using 0.2 m^2 of charcoal cloth. They found that the pressure drop was much less in parallel flow than in perpendicular flow. An unusual feature of the parallel flow designs was that with increasing numbers of layers of adsorbent, the pressure drop appeared to reduce. The authors also mentioned that sometimes a combination of both types of mode can contribute to a better filter with a high efficiency than with either of them employed separately.

Maggs and Smith (12) noted that high adsorption efficiency depends on the distance between the two layers of charcoal cloth. They reported 0.0005 m as the best distance. Efficiency decreases with increasing distance. They recommended polyurethane foam as a spacer material between layers of cloth because of its large inter-communicating pores.

In course of the present research polyurethane foam was used as a separating medium. But it did not have any advantages over the polythene mesh used, rather had some handling problems as it took longer time to take the charcoal cloths out of the canister and is liable to give non uniform distribution of flow.

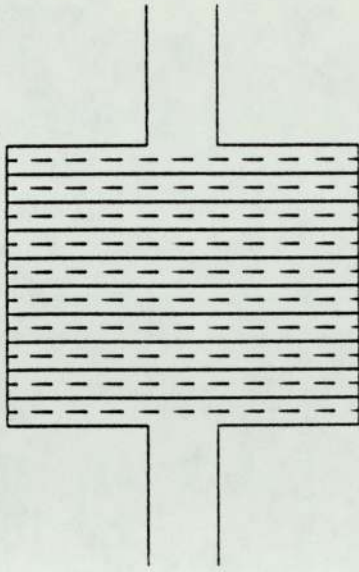
5.2.1. Canister Designs

Four different arrangements of the cloth are used in the canister. Experiments were performed and their relative advantages and disadvantages are discussed in the subsequent sections.

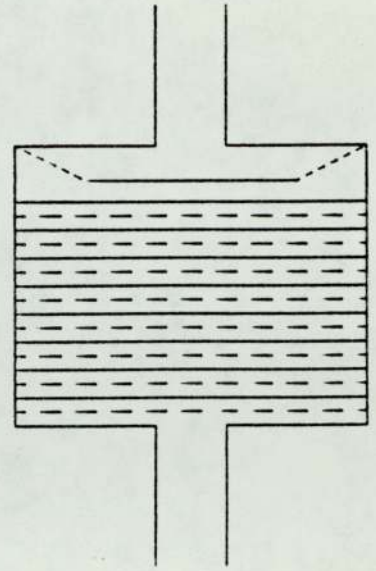
5.2.1.1 DESIGN ONE (See Figure 5.1)

All the sixty experiments tabulated in Appendix II were performed using this design. Charcoal cloth is cut to a size of the canister which is 0.1524 m (6") in diameter. They are stacked one on top of the other with a polythene mesh in between them. Some of the cloths are pulled over the edges to stop the vapour being released without being adsorbed. Three different heights of .0762m (3"), .1016m (4") and 0.1524m (5") are used. 25, 35 and 45 layers of cloth are used. The air-solvent vapour mixture enters the canister through a .0254m (1") hole at the centre of a baffle plate. The exit vapour mixture leaves the canister through a similar hole at the end of the canister and is sucked by the fan connected to the fume cupboard and released to the atmosphere.

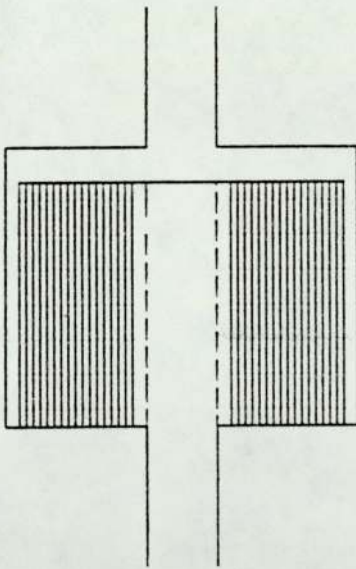
The pressure drop across the bed is measured by a pitot tube and a manometer. The maximum pressure drop for one layer of cloth has been quoted as 1×10^{-2} m water gauge per unit flow rate (m s^{-1}) (15). The present author records less pressure drop than the predicted value. The pressure drop is higher when 0.2286 m (9") diameter canister is used. The velocity ranges from 0.14 m s^{-1} to 0.2 m s^{-1} . There is no change in the velocity



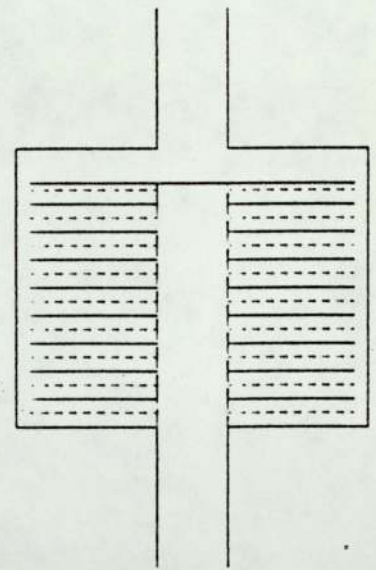
DESIGN ONE



DESIGN TWO



DESIGN THREE



DESIGN FOUR

FIGURE 5.1 CANISTER DESIGNS

range when 0.2286 (9") diameter canister is used.

5.2.1.2 DESIGN TWO

This design is similar to that in design one except that the exit end of the canister is different. Instead of a plate with a hole of 0.0254m (1") diameter in the centre, a circular plate is fixed to the sides of the canister with 0.0127 m (0.5") space all round the plate. Pressure drop was slightly less than in design one, but it did not perform any better than the design one, in fact in some cases it did worse than the design one. This may be due to the fact that the space at the end of the canister all round makes a large amount of vapour to pass through the canister without passing through the charcoal cloth.

5.2.1.3 DESIGN THREE

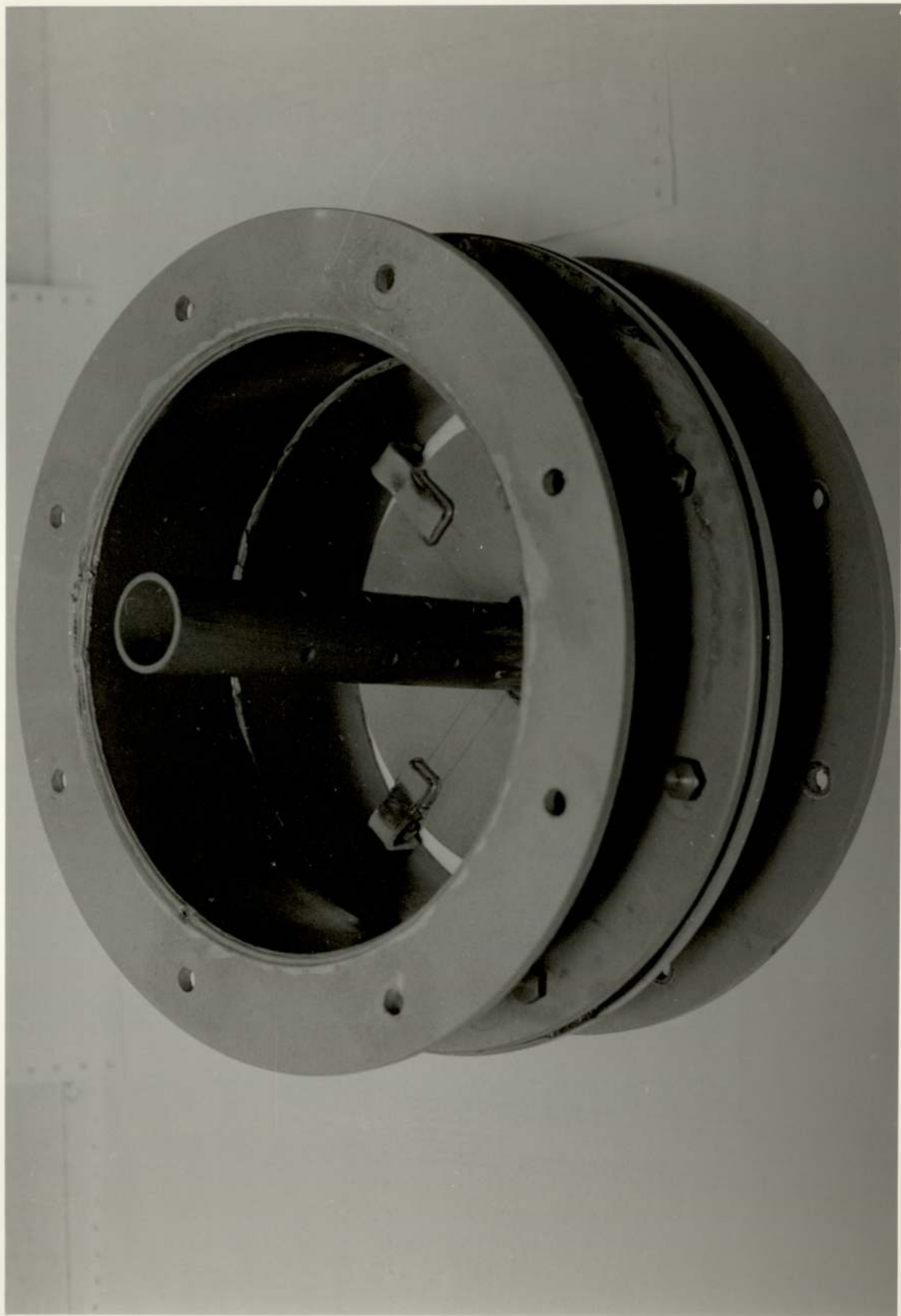
The exit end of this design is same as design two. It only differs in the entrance section. A 0.2032 m (8") long and .0356 (1.4") diameter pipe is welded on the centre of the plate at the exit end. A number of holes are made on the small pipe and charcoal cloth rolled over and over the holes in a spiral "swiss roll" arrangement to fill the canister.

5.2.1.4 DESIGN FOUR

The basic arrangement in this case is the same as the previous one except that the charcoal cloth is arranged in a "pineapple ring" fashion. The objective in this canister is to establish the parallel flow recommended

PLATE 5.1

PARALLEL FLOW CANISTER



by Maggs (12). An equal amount of toluene was adsorbed on an equal amount of charcoal cloth using design three and four. It has been found that both these designs give approximately the same amount of adsorption though design three has much higher pressure drop than design four.

A summary of results using different designs has been tabulated in Table 5.1.

It has been found in the experiments carried out with the 0.1524 m (6") diameter canister with four different designs that design one and design four give relatively better adsorption and less pressure drop than the other two designs (see Table 5.1). Design one and design four were further examined using a 0.2286 m (9") diameter canister with a flowrate of $2.5 \times 10^{-9} \text{ m}^3 \text{ s}^{-1}$ of toluene as solvent, each experiment being continued until equilibrium was attained. Design one took longer time to reach equilibrium than design four though approximately the same weights of cloth were used. The pressure drop in both cases differed very little as was evidenced with the canister of 0.1524 m (6") diameter.

With the parallel arrangement in design four which was recommended by Maggs (12), it has been found that adsorbate concentration was the highest at a point nearest to the small inlet holes and lowest at the edges of the cloth. This decrease in adsorption with increase in

Design	Mass of Charcoal Cloth ($\text{kg} \times 10^3$)	Mass of Inlet Toluene ($\text{kg} \times 10^3$)	Mass of Adsorbed Toluene ($\text{kg} \times 10^3$)	% Adsorption	Pressure (N m^{-2})	Drop (Gauge) (inches water)
1	49.31	30.96	19.83	64.05	208.25	0.84
2	49.33	30.96	14.73	47.58	198.45	0.80
3	48.13	30.96	15.87	51.26	257.25	1.03
4	48.13	30.96	16.85	54.43	200.90	0.81

Table 5.1 Summary of results of adsorption of toluene on charcoal cloth using different canister designs of 0.1524m (6") diameter

Design Number	Mass of Charcoal Cloth ($\text{kg} \times 10^3$)	Time to reach Equilibrium ($\text{kg} \times 10^3$)	Mass of Inlet Toluene ($\text{kg} \times 10^3$)	Mass of Adsorbed Toluene ($\text{kg} \times 10^3$)	Adsorbate Adsorbent (kg kg^{-1})	Pressure Drop (Gauge) N m^{-2} (inches water)
1	65.52	13380	28.77	20.88	0.319	258.23 1.04
4	62.76	6000	12.90	7.12	0.113	257.25 1.03

Table 5.2 Summary of results of adsorption of toluene on charcoal cloth using canister of 0.2286m (9") diameter

Design One	Mass of Charcoal Cloth $(\text{kg} \times 10^3)$	Liquid Solvent Flowrate $(\text{m}^3 \text{ s}^{-1} \times 10^8)$	Time to Reach Equilibrium (sec)	Adsorbate Adsorbed $(\text{kg} \text{ kg}^{-1})$
0.1524 m (6") diameter Canister	62.9	0.25	19800	0.464
0.2286 m (9") diameter Canister	65.52	0.25	13380	0.319

Table 5.3 Summary of results of adsorption of toluene on charcoal cloth using two different canisters

distance of the cloth from the inlet hole could be attributed to the reduction in velocity of the air-vapour mixture beyond the inlet.

5.3 Calculation of Reynold's Number

In view of the results shown in Table 5.1, design one and design four seem to work better than design two and design three. In the following section, Reynold's number has been calculated for design one between two layers of cloth, and in case of design four, Reynold's number is calculated at three different points on the cloth to identify possible variation.

5.3.1 Design One (Between Two Layers of Cloth)

$$u = \frac{u}{e} = \frac{0.2}{0.73} \text{ m s}^{-1}$$

$$\rho = 1.29 \text{ kg m}^{-3}$$

$$d = 2.21 \times 10^{-3} \text{ m}$$

$$\mu = 1.78 \times 10^{-5} \text{ Ns m}^{-2}$$

$$\begin{aligned} \text{Re} &= \frac{\rho u d}{\mu} \\ &= \frac{1.29 \times 0.20 \times 2.21 \times 10^{-3}}{0.73 \times 1.78 \times 10^{-5}} \\ &= 43.88 \end{aligned}$$

5.3.2 Design Four (Along the Cloth Surface)

Reynold's Number at emergence

$$\text{Diameter of a small inlet hole} = 5.5 \times 10^{-3} \text{ m}$$

$$\text{Number of inlet holes} = 10$$

$$u = \frac{\pi \times (9 \times 2.54 \times 10^{-2})^2 \times 0.2}{\pi \times (5.5 \times 10^{-3})^2 \times 10}$$

$$= 34.55 \text{ m s}^{-1}$$

$$\text{Re} = \frac{\rho u d}{\mu}$$

$$= \frac{1.29 \times 34.55 \times 1.71 \times 10^{-3}}{1.78 \times 10^{-5}}$$

$$= 4281.68$$

Reynold's Number at half diameter

$$u = \frac{34.55 \times 0.25 \pi \times (5.5 \times 10^{-3})^2}{2 \pi \times 1.9 \times 2.54 \times 10^{-2} \times 0.5 \times 10^{-3}}$$

$$= 21.66 \text{ m s}^{-1}$$

$$\text{Re} = \frac{\rho u d}{\mu}$$

$$= \frac{1.29 \times 21.66 \times 1.71 \times 10^{-3}}{1.78 \times 10^{-5}}$$

$$= 2684.26$$

Reynold's Number at full diameter

$$u = \frac{34.55 \times 0.25 \pi \times (5.5 \times 10^{-3})^2}{2 \pi \times 3.8 \times 2.54 \times 10^{-2} \times 0.5 \times 10^{-3}}$$

$$= 10.83 \text{ m s}^{-1}$$

$$\text{Re} = \frac{\rho u d}{\mu}$$

$$= \frac{1.29 \times 10.83 \times 1.71 \times 10^{-3}}{1.78 \times 10^{-5}}$$

$$= 1342.13$$

There seems to be no clear correlation between the Reynold's Number and the configuration of charcoal cloth in the filter canister. It is apparent that Maggs' design was on a smaller scale and lower pressure drop was the main objective (12).

In terms of optimum conditions where maximum adsorption is to be attained with minimum amount of adsorbent, the present author believes that a canister of 0.1524 m (6") diameter will do a better job than a canister of 0.2286 m (9") diameter. A perpendicular flow arrangement (Design One) will have slightly higher pressure drop than parallel flow (Design Four), but it will be offset by the higher adsorption capacity encountered by the former.

CHAPTER 6

THEORETICAL DEVELOPMENT
AND MATHEMATICAL MODELLING

6 Theoretical Development and Mathematical Modelling

In the current research programme two mathematical models were required. Firstly, it was required to predict the breakthrough time at a particular effluent concentration in relation to the amount of cloth used and the inlet vapour concentration. Secondly, it was necessary to provide a model which could approximately calculate the length of bed required for a particular adsorption reaction at a fixed effluent concentration.

Although the derived equations describing the adsorption isotherms, adsorption waves and rate of mass transfer expressed in terms of the length of unused bed at a fixed effluent concentration are not universal and will not cover each and every physical and chemical factor responsible for adsorption, it is intended that the theoretical development will provide a basic framework for the adsorption of vapours on charcoal cloth, in particular the four organic vapours used in the present research.

6.1 Adsorption Isotherms

As outlined in Section 3.1 there are three commonly used mathematical expressions used to describe vapour adsorption equilibria by the Langmuir, Freundlich and BET isotherms. The isotherms illustrated by Figures 6.1 to 6.8 corresponding to the equilibrium data with regard to the adsorption of heptane, tetrachloroethylene, toluene and o-xylene vapours on charcoal cloth are similar to those described by Langmuir and Freundlich.

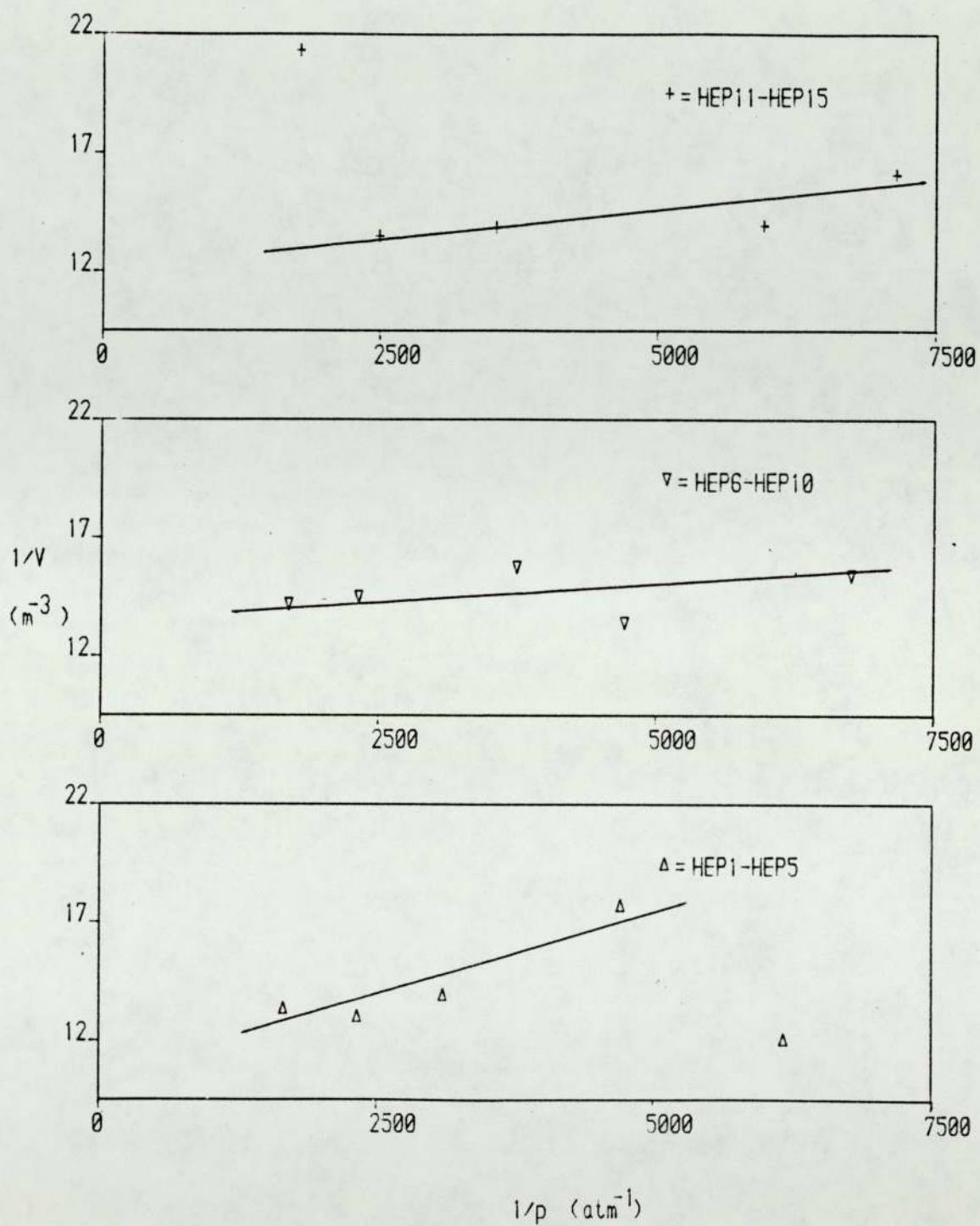


FIGURE 6.1 PLOT OF $1/V$ AGAINST $1/p$ (HEPTANE)

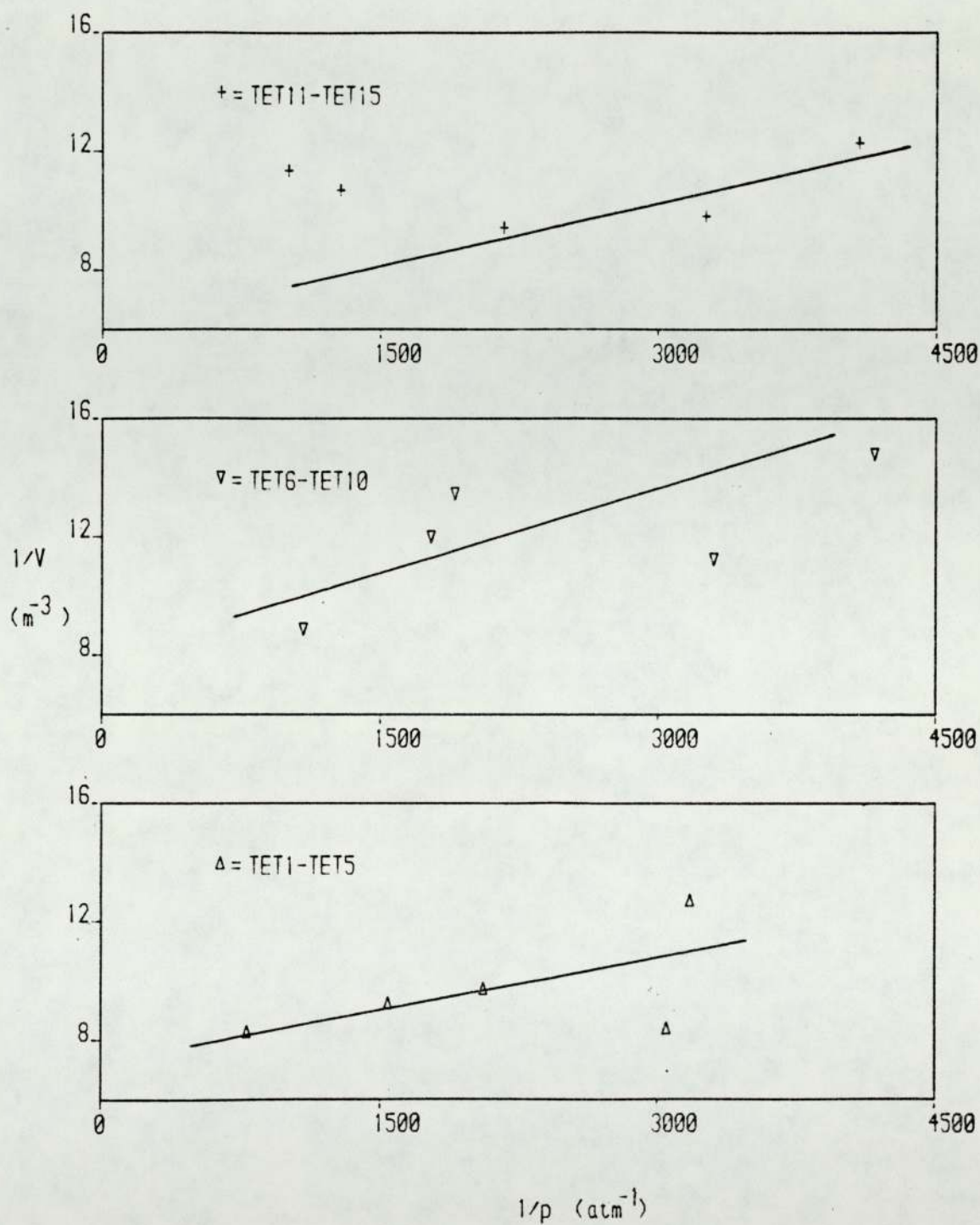


FIGURE 6.2 PLOT OF $1/V$ AGAINST $1/p$ (TETRACHLOROETHYLENE)

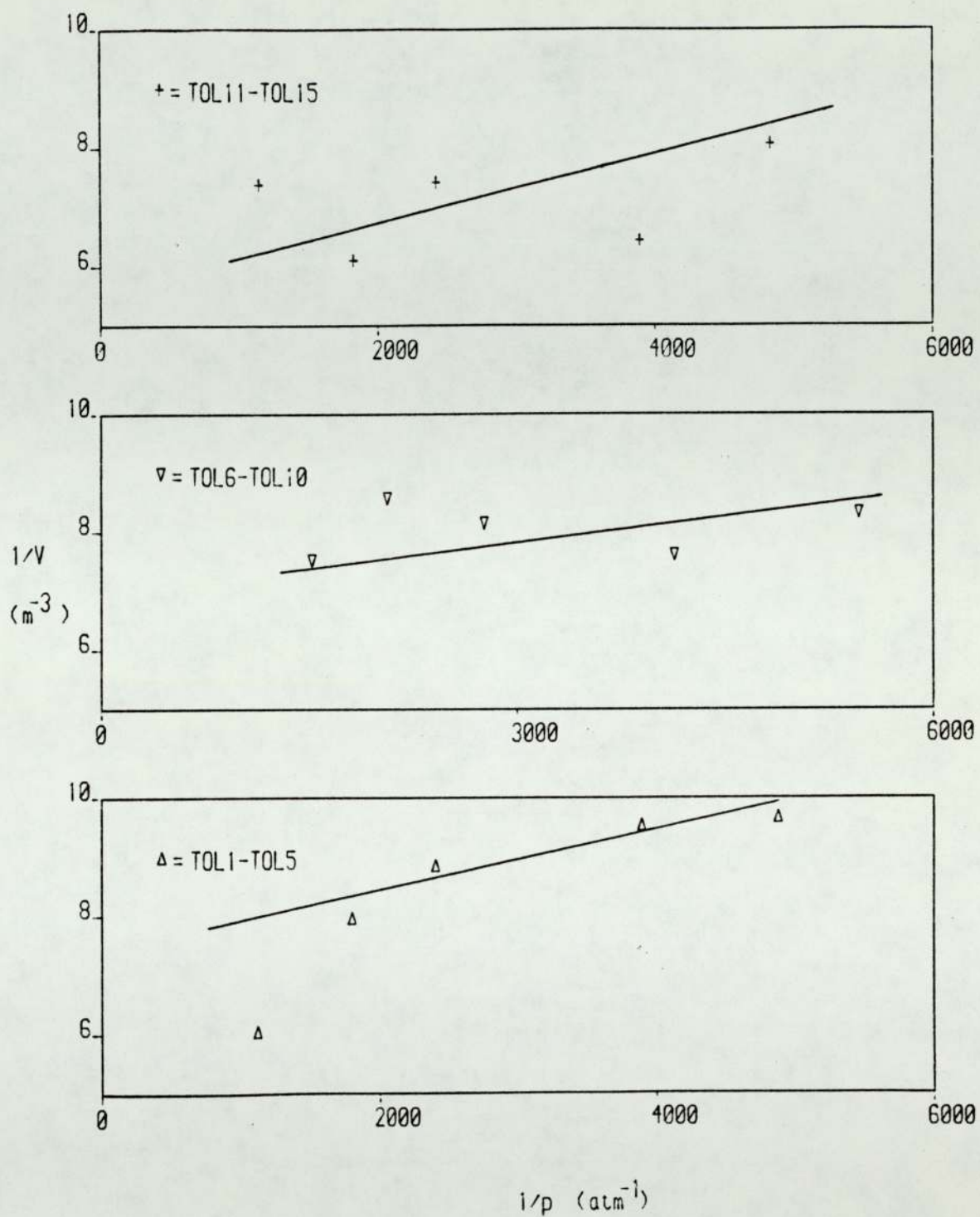


FIGURE 6.3 PLOT OF $1/V$ AGAINST $1/p$ (TOLUENE)

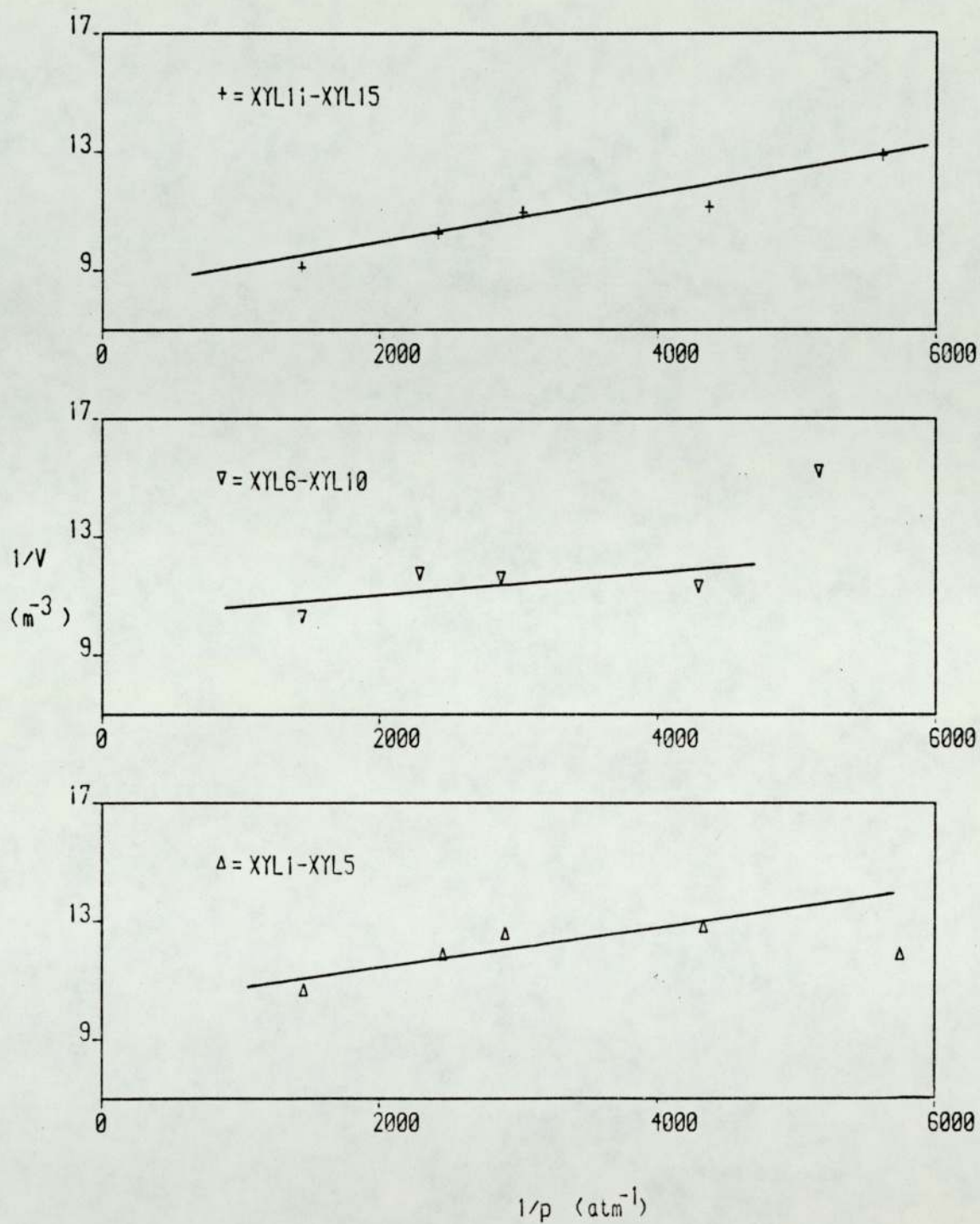


FIGURE 6.4 PLOT OF $1/V$ AGAINST $1/p$ (O-XYLENE)

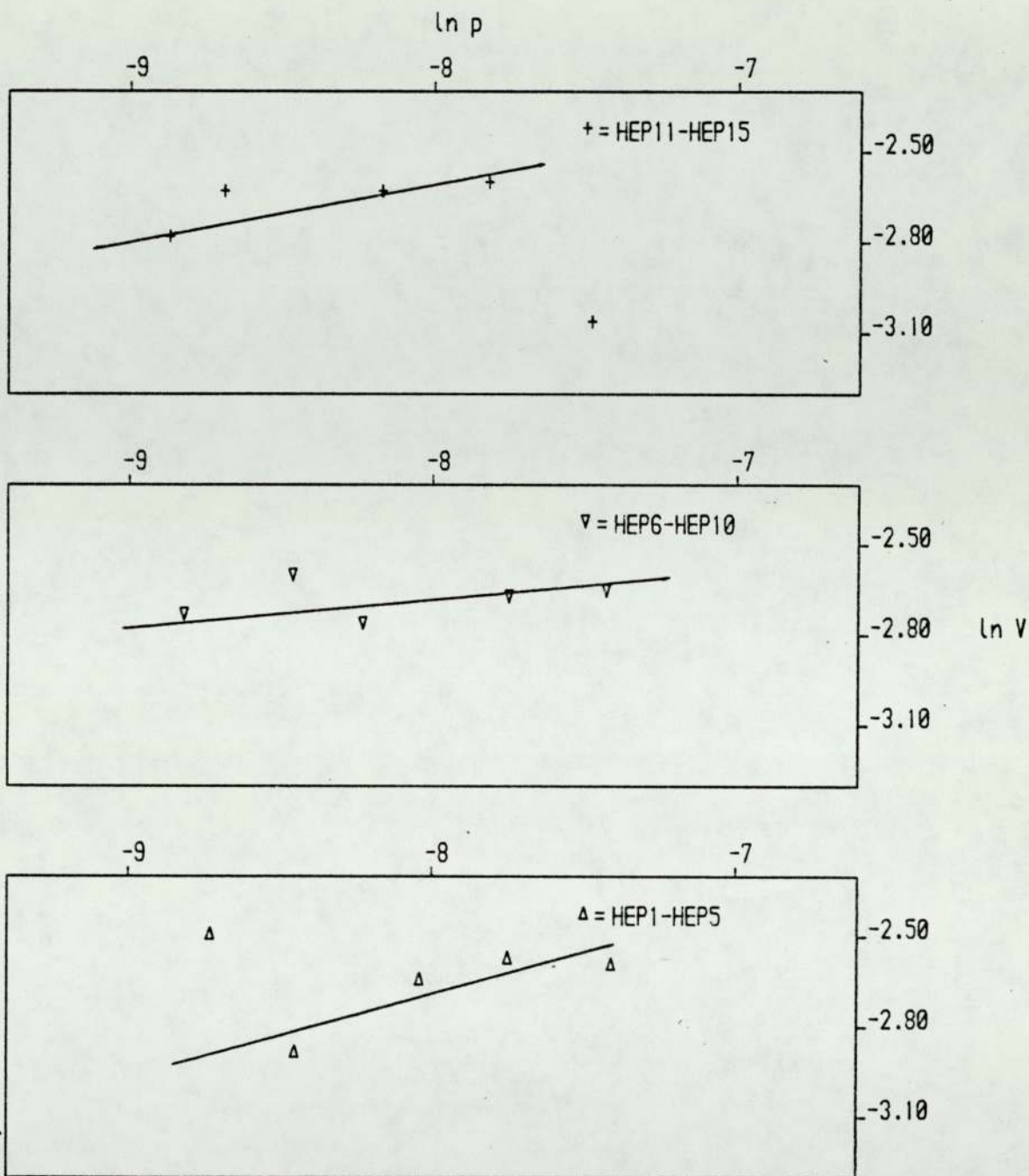


FIGURE 6.5 PLOT OF $\ln V$ AGAINST $\ln p$ (HEPTANE)

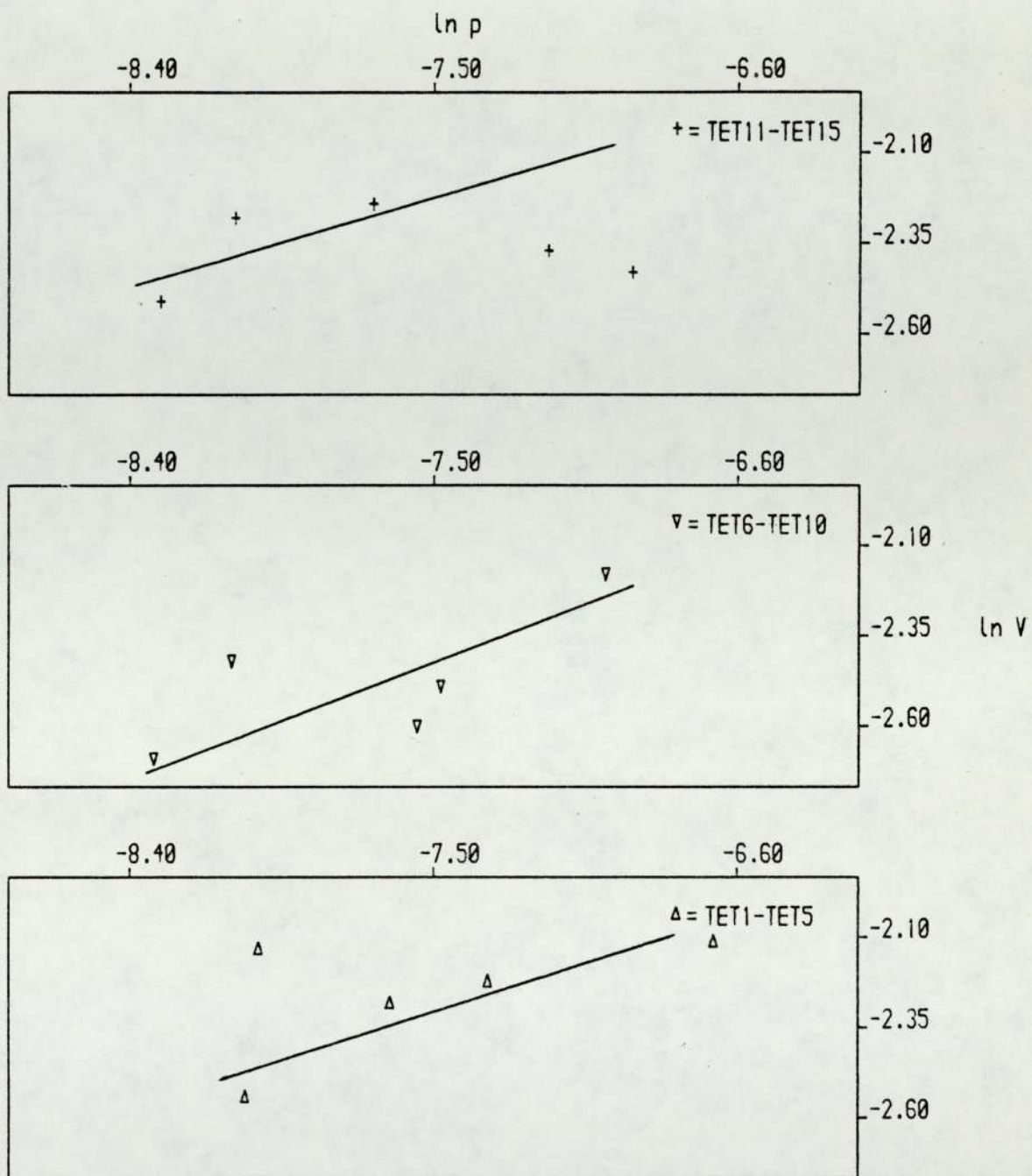


FIGURE 6.6 PLOT OF $\ln V$ AGAINST $\ln p$ (TETRACHLOROETHYLENE)

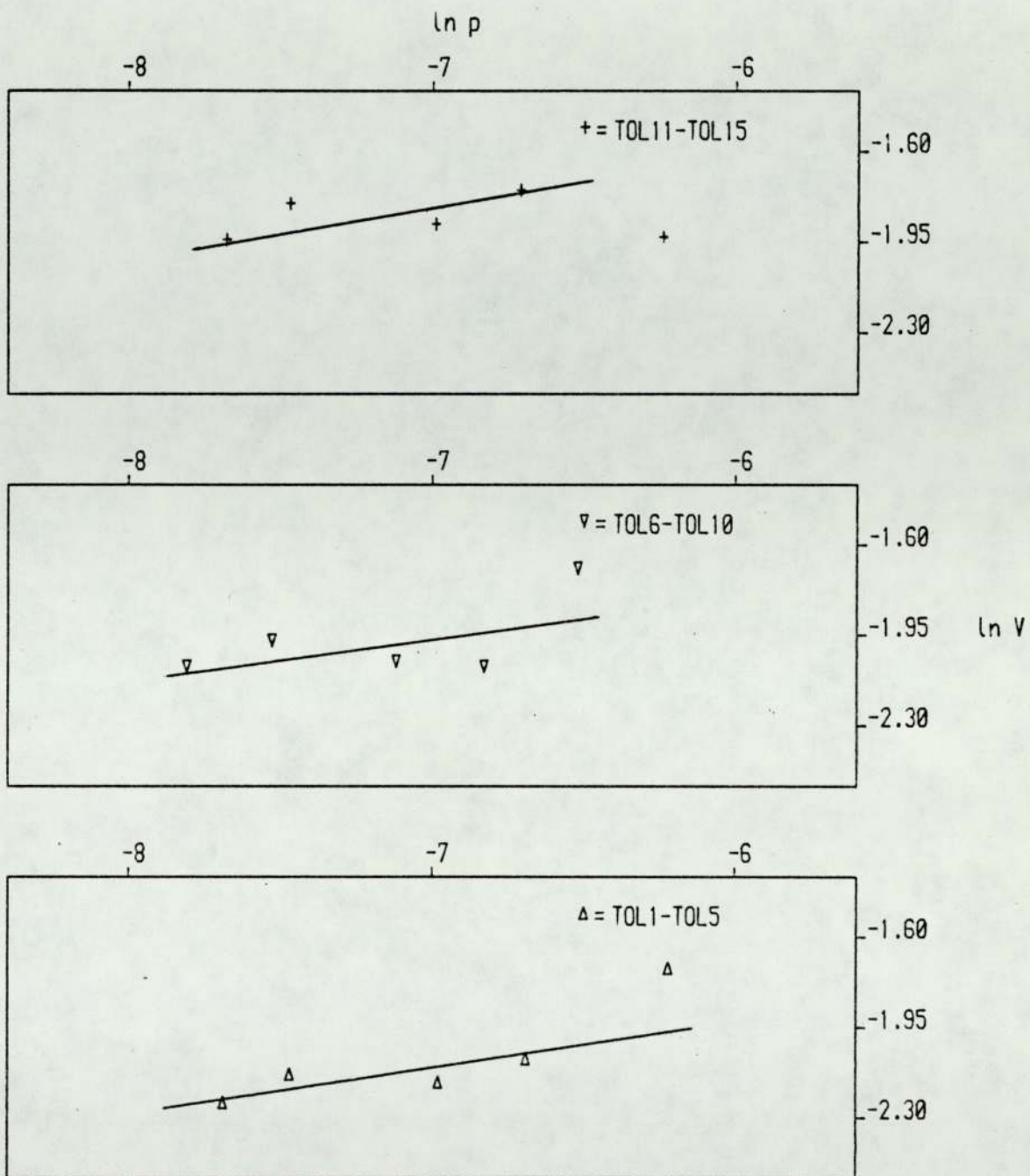


FIGURE 6.7 PLOT OF $\ln V$ AGAINST $\ln p$ (TOLUENE)

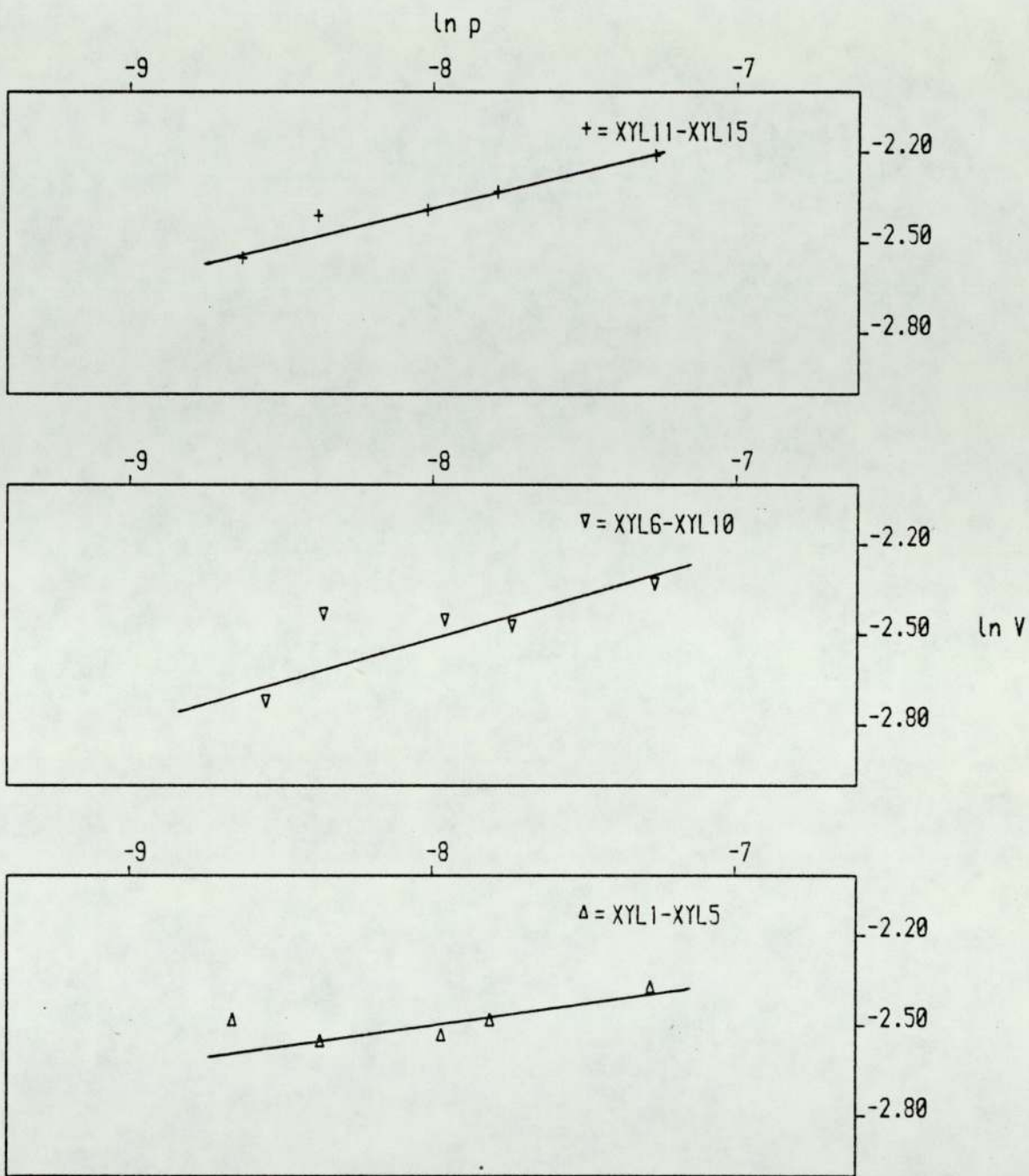


FIGURE 6.8 PLOT OF $\ln V$ AGAINST $\ln p$ (O-XYLENE)

Summaries of the data used to test the application of Langmuir and Freundlich isotherms for each of the four solvents have been tabulated in Appendix III. Since Langmuir's theory suggests that the adsorbed layer is unimolecular, it appears that all the four vapours used in the present research adhere to the surface of charcoal cloth in single layers. But this concept is only valid for the macropore region of the cloth, as the adsorption in micropore region is accompanied by volume filling, the reasons for which are outlined in section 3.4.

6.2 Rate of Mass Transfer

In the interpretation of dynamic adsorption data, and in the design of adsorption systems, it is convenient to view the adsorbent bed as comprised of two sections, the equilibrium section and the LUB (Length of unused bed) section. The adsorbent requirement for the equilibrium section is obtained solely from adsorption equilibrium data. The LUB is an additional quantity of adsorbent added to compensate for the presence of a mass transfer zone during dynamic adsorption. This design approach is best suited to adsorption separations where a stable adsorption mass transfer zone is formed, as is typically the case when drying and/or purifying process streams with molecular sieve adsorbents (115).

6.2.1 LUB and Equilibrium Concept

When a feed containing an adsorbable impurity is fed to an initially activated adsorbent bed, dynamic adsorption occurs across a mass transfer zone (116). The progress of a stable mass transfer wave or front through an adsorbent bed, together with the associated effluent breakthrough curve, is shown graphically in Figure 6.9a. The mass transfer front is the fluid concentration or adsorbent loading profile of the adsorbate over the mass transfer zone. The adsorbate loading through the transfer zone is a linear function of the fluid phase concentration of the adsorbate (116).

At the leading edge of the transfer front, the adsorbate concentration in the carrier fluid is equal to the breakthrough concentration, usually taken as the minimum detectable or minimum allowable concentration in the effluent; the adsorbate loading is substantially equal to that of the initially activated bed. At the trailing edge of the transfer front, the adsorbate concentration in the carrier fluid is substantially equal to that in the feed Y_e , and the adsorbate loading is substantially that which is in equilibrium with the feed. The effluent breakthrough trace is the fluid phase transfer front as it moves past the outlet end of the adsorbent bed as shown in Figure 6.9a. The leading edge of the transfer front exits from the bed at time θ_b , when breakthrough occurs. The trailing edge of the transfer front exits from the bed at time θ_e .

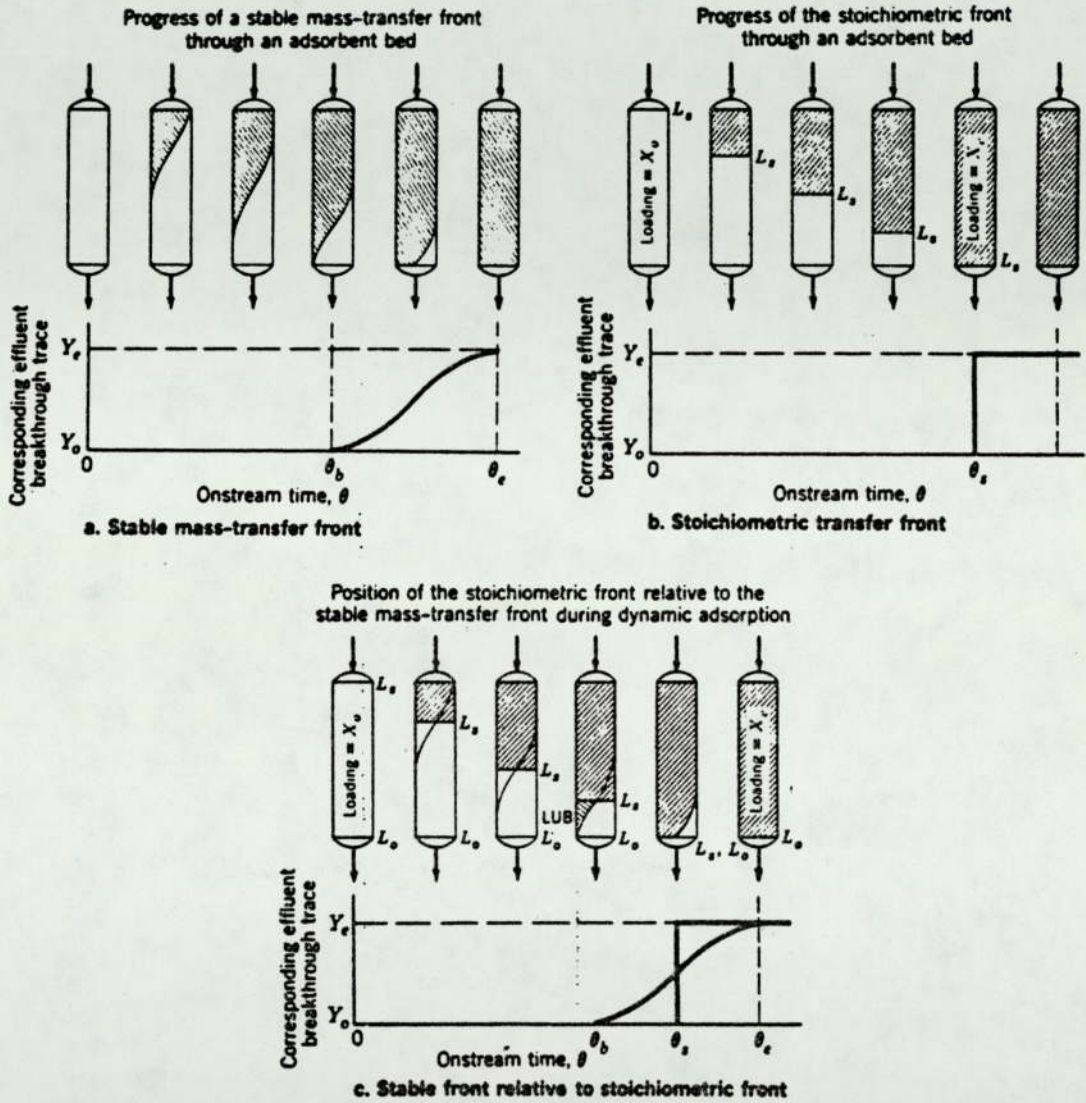


FIGURE 6.9 TRANSFER FRONTS MOVING THROUGH ADSORBER (106)

If adsorption occurs in an infinitely sharp transfer zone, the resulting hypothetical front is called the stoichiometric front and is shown in Figure 6.9b. This shows the progress of a stoichiometric front through an initially activated adsorbent bed similar to Figure 6.9a for a stable mass transfer front. The part of the adsorbent bed behind the stoichiometric front has a uniform adsorption loading X_e , which is in equilibrium with the inlet adsorbate concentration. The part of the adsorbent bed ahead of the stoichiometric front has a uniform adsorption loading X_0 , which is equal to that of the initially activated bed. The distance of the stoichiometric front from the feed end of the adsorbed bed at time θ is shown by L_s . The corresponding effluent breakthrough trace for the stoichiometric front is also given in Figure 6.9b. The stoichiometric front exists from the adsorbent bed at time θ_s . Prior to time θ_s , the adsorbate concentration in the effluent is Y_0 , the concentration in equilibrium with the initial adsorbate loading on the bed X_0 . After time θ_s , the concentration of the adsorbate in the effluent is Y_e , identical to that of the feed.

The position of the hypothetical stoichiometric front relative to the actual stable front during dynamic adsorption is shown in Figure 6.9c. The location of the stoichiometric front must be such that the unused adsorbent bed capacity behind the stoichiometric front is equal to the expended bed capacity ahead of the

stoichiometric front. This is accomplished by positioning the stoichiometric front relative to the actual front so that graphically one area equals the other as noted in Figure 6.9c. It is apparent that the velocity of the stoichiometric front U_1 is identical to that of the stable mass transfer front, since they move through the adsorbent bed together maintaining a fixed position relative to each other. For a constant feed rate G , the velocity of the stoichiometric front will be constant.

When breakthrough occurs, the position of the leading edge of the mass transfer front relative to the stoichiometric front is given by $(L_0 - L_s)$, where L_0 is the length of the adsorbent bed. The length $(L_0 - L_s)$ is called the equivalent length of unused bed, or LUB. At breakthrough, the adsorbent bed can be viewed as the sum of the LUB which compensates for the presence of a mass transfer zone, and an equilibrium section which has a uniform adsorption loading X_e .

At time θ , the position of the stoichiometric front and the length of the equilibrium section is

$$L_s = U_1 \theta \quad 6.1$$

Since at time θ_b ,

$$L_s = U_1 \theta_b \quad 6.2$$

and at time θ_s

$$L_s = L_0 = U_1 \theta_s \quad 6.3$$

Therefore

$$\begin{aligned} L_0 - L_s &= U_1(\theta_s - \theta_b) \\ \therefore LUB &= U_1(\theta_s - \theta_b) \end{aligned} \quad 6.4$$

Combining equations 6.3 and 6.4, U_1 can be eliminated

$$LUB = \frac{(\theta_s - \theta_b)}{\theta_s} L_0 \quad 6.5$$

By material balance across the equilibrium section at time θ , we have

$$\begin{aligned} G(Y_e - Y_0)\theta &= L_s \rho_B (X_e - X_0) \\ L_s &= \frac{G(Y_e - Y_0)}{\rho_B (X_e - X_0)} \theta \end{aligned} \quad 6.6$$

where

G = Feed rate of carrier fluid

Y_e = Concentration of the adsorbate in the carrier fluid

Y_0 = Concentration of the adsorbate in equilibrium with X_0

ρ_B = Bulk density of the adsorbent

θ = Time from the start of adsorption

X_e = Adsorbate loading in equilibrium with the concentration of the adsorbate in the feed

X_0 = Initial adsorbate loading on the adsorbent

θ_b = Breakthrough time

When $\theta = \theta_s$, $L_s = L_0$ and equation 6.6 reduces to

$$(X_e - X_o) = \frac{G \theta_s}{L_o \rho_B} (Y_e - Y_o) \quad 6.7$$

Combining equations 6.1 and 6.6 we get

$$U_1 = \frac{G}{\rho_B} \frac{(Y_e - Y_o)}{(X_e - X_o)} \quad 6.8$$

From equations 6.5 and 6.7, θ_s can be eliminated.

$$LUB = L_o - \frac{G}{\rho_B} \frac{(Y_e - Y_o)}{(X_e - X_o)} \theta_b \quad 6.9$$

To develop the above equation 6.9, several assumptions have been made. They are as follows:

- 1) Holdup of the adsorbate in the adsorbent voids is small compared with X_e .
- 2) The flowrate, temperature and composition of the feed are constant.
- 3) The adsorbent bed has no radial temperature, concentration or flow rate gradients.
- 4) The initial bed temperature and the adsorbate temperature are approximately equal.
- 5) No chemical reaction occurs.
- 6) The feed undergoes no phase change.
- 7) Adsorption heat effects are negligible.

6.2.2 Present Work: Calculation of the length of unused charcoal cloth

In the present studies of adsorption on charcoal cloth, outlet vapour concentration is fixed at 10 p.p.m and the breakthrough time is calculated from the graphs of outlet solvent vapour concentration against time.

The length of the unused bed is calculated using eq. 6.9 for all the four solvent vapours used in the present research. The results are summarized in Appendix IV.

6.3 Rate Controlled Breakthrough

If a single mechanism controls the adsorption rate in a fixed bed, a number of mass transfer units can be defined which will convert the rate equation to non-dimensional form and thus allow it to be evaluated by use of universal solution.

In the course of the present research there is a general pattern among the breakthrough curves regardless of column length used. This indicates that all parts of the exchange zone move through the column at a constant rate. Satterfield (118) has developed the following reaction for a constant separation factor:

$$X = 0.555 [N_{\text{pore}} (\zeta - 1) + 1.22] - 0.077 [N_{\text{pore}} (\zeta - 1) + 1.22]^2 \quad 6.10$$

where

$$N_{\text{pore}} = \psi_{\text{pore}} k_{\text{pore}} a_p \frac{V}{F} \quad 6.11$$

$$k_{\text{pore}} a_p = \frac{60 D_{\text{pore}}}{d_p^2} (1-e) \quad 6.12$$

$$D_{\text{pore}} = \frac{e}{\delta} \left[\frac{3}{2d_p} \left(\frac{\pi M}{2RT} \right)^{0.5} + \frac{1}{D_f} \right]^{-1} \quad 6.13$$

$$\psi_{\text{pore}} = \frac{0.775}{1 - 0.225 R_1^{0.4}} \quad 6.14$$

Here e is the voidage, δ is the tortuosity factor, N_{pore} is the number of transfer units, X is the ratio

of fluid concentration change, ψ_{pore} is the correction factor for R_1 , k_{pore} is the mass transfer coefficient and a_p is the outer surface interfacial area of the pores per unit volume of contacting system (solid plus fluid). D_f is the diffusivity of the fluid in air and can be obtained from the literature (127). v is the volume of the bed and F is the volumetric flow rate. The tortuosity varies between 2.0 and 6.0, but in the present calculation it is taken as 2.0. R is the gas constant, T is the absolute temperature and M is the molecular weight of the adsorbate.

Assumptions inherent in these relations include homogeneous particle size and structure, uniform feed concentration and flow rate and temperature constant enough so as to maintain both the equilibrium and the rate coefficient for adsorption constant.

6.3.1 Method of Calculation

ψ_{pore} is calculated using equation 6.14. R_1 is known as separation factor which identifies the equilibrium between the adsorbate and adsorbent concentration change and taken as 0.0. N_{pore} is calculated using equations 6.11, 6.12 and 6.13. Inlet and outlet concentrations are known and their ratio gives the value of X . Using the value of N_{pore} and X in equation 6.10 the value of ζ can be calculated. The required time for the specific outlet concentration to be reached can be obtained by multiplying the value of ζ by 6000.

ζ can also be obtained from a plot of X versus $N_{\text{pore}}(\zeta - 1)$ at different values of R_1 (117). The symbol R_1 is the same as R in the literature (117, 119).

6.4 Relation of Breakthrough time with Inlet concentration and Number of Layers of Charcoal Cloth

A general equation is proposed relating the breakthrough time and number of layers of charcoal cloth.

$$Z = K_5 + K_6 \theta_{0.1} \quad 6.15$$

where

$\theta_{0.1}$ = Time required in seconds for the outlet solvent vapour concentration to reach 10% of the inlet concentration

K_5, K_6 = Constants

Z = Number of layers of charcoal cloth

The experimental results obtained for each solvent were substituted and the two constant terms were calculated using regression analysis. Depending on the inlet concentration the constants would vary. The constants along with the range of inlet solvent concentration are tabulated in Table 6.1.

For some intermediate concentrations which are not in the range mentioned in Table 6.1, interpolation would have to be used to calculate the value of the constants of equation 6.15.

SOLVENT	K_5	K_6	Correlation Coefficient	Range of Inlet Solvent Vapour Concentration in p.p.m
HEPTANE	15.00	.003056	.9954	100 - 160
	12.20	.006667	.9956	160 - 220
	15.02	.005710	.9794	250 - 320
	11.79	.011490	.9998	390 - 450
	11.17	.013857	.9988	550 - 600
TETRACHLORO ETHYLENE	12.04	.003225	.9434	240 - 310
	12.58	.004414	.9697	310 - 400
	12.33	.005039	.9912	440 - 550
	14.59	.009450	.9624	580 - 780
	11.93	.015176	.9301	920 - 1300
TOLUENE	16.03	.003539	.9555	180 - 240
	15.53	.005044	.9994	240 - 310
	14.74	.007134	.9922	350 - 420
	18.67	.006803	.9897	480 - 560
	18.50	.008333	1.0000	650 - 880
O-XYLENE	10.36	.003603	.9972	170 - 210
	11.07	.004351	.9895	220 - 240
	12.43	.006757	.9966	320 - 370
	13.55	.010313	.9472	400 - 470
	11.37	.019058	.9859	680 - 750

Table 6.1 Values of the constants for different solvents at different inlet concentrations

CHAPTER 7

DISCUSSION

7 Discussion

Charcoal cloth is the first flexible adsorbent available with effectiveness higher than granular charcoal. The cloth has a square form linen weave with 1300 charcoal threads per metre, the threads comprising charcoal filaments of 16×10^{-6} m in diameter. While the cloth has a breaking strength of 150 kg m^{-1} , the calculated tensile strength of the filaments is $400 \times 10^8 \text{ kg m}^{-2}$. The rate of adsorption of vapour by charcoal cloth is at least five times - and often twenty times - greater than that for granular charcoals (15). Consequently the minimum depth of cloth required is smaller by the same factor than that for granular charcoal, and very efficient utilisation of the charcoal cloth is achieved.

7.1 Low Temperature Oxidation

A mass balance was carried out between the inlet solvent vapour adsorbed and the mass of outlet vapour. It has been found that a certain fraction of the inlet vapour cannot be traced and this is shown consistently through all the runs. The amount of this loss depends on the solvent vapour. It is the least with toluene and is the highest with tetrachloroethylene. The loss is ascribed to some reaction on the charcoal cloth surface taking place simultaneously with adsorption and desorption.

Despite a large volume of published information on low temperature oxidation of hydrocarbons, the knowledge is far from complete. The reason lies partly in the fact

that the reaction is markedly sensitive to the experimental conditions, partly to the nature of the surface of the reaction vessel, the influence of trace of impurities and the marked effect on the change of temperature. Despite these difficulties, the oxidation of paraffins and olefins show certain general features. The oxidation has the characteristics of a chain reaction as exemplified by the observation of the sensitivity of the reaction to surface conditions. The dependence of the rate on the concentrations of the reactants is often complex and a small change in initial conditions may cause an abrupt transition from slow reaction to explosion. The active particles responsible for chain propagation are free radicals or atoms and the presence of alkyl, alkoxy, alkylperoxy and hydroxyl radicals and oxygen atoms has been postulated (130) and confirmed by experimental studies.

The rate and products of the oxidation of hydrocarbons show unusual changes with increase in temperature. The high temperature reaction proceeds rapidly giving carbon dioxide and water as the principal product. Liquid and gaseous paraffins react with oxygen at moderate temperatures as has been evidenced in the oxidation of heptane on charcoal cloth in the present research. This low temperature oxidation is very sensitive to the structure of the hydrocarbon and shows the formation of oxygenated products such as alcohols, aldehydes and acids. The low temperature oxidation is associated with the existence of intermediates of different thermal stabilities.

The initiation of the oxidation reaction requires the production of a free radical centre and it is generally agreed (131) that this process is the formation of an alkyl radical (in case of saturated hydrocarbons) and this process takes place by a hydrogen abstraction reaction. The actual structure of the free radical is determined by the point of attack on the paraffin or hydrocarbon by oxygen, and this in turn is determined by the relative C-H bond strength in the hydrocarbon. Thus, the ease of removal increases in the order tertiary > secondary > primary carbon-hydrogen bonds. Straight chain molecules undergo oxidation more readily than branched chain paraffins in direct contrast to the liquid phase behaviour. The rate of oxidation in the gas phase decreases with increasing chain branching and increases with increasing chain length (131). The authors (131) reported that the oxidation rate of heptane is 26.7 times faster than that of hexane and is 200 times faster than that of pentane.

Benzene and its homologues can be oxidized directly with air or oxygen. Reaction occurs well below the ignition point and only the slower type of oxidation is discussed here, complete combustion presumably involving many of the intermediate formulations found in the slow reactions. Both nuclear and side chain oxidation is possible although the benzene nucleus is more resistant to attack than the side chain. The oxidation takes place by a free radical mechanism.

The first stage in a study of free-radical reactions by photochemical methods is to discover the primary products of photolysis of the parent molecules used, and this often proves difficult. In aromatic molecules several primary dissociation processes may occur simultaneously, and the quantum yield of each process is usually low.

The fission of a carbon-hydrogen bond in the side chain of an aromatic molecule always gives a radical which has the possibility of resonance stabilization. In the benzyl radical the resonance energy is responsible for its low reactivity in hydrogen abstraction and similar reactions and a relatively low dissociation energy of the carbon-hydrogen bond of the methyl group in toluene. Although the benzyl radical cannot be prepared in detectable equilibrium concentration, it has been studied more than any other aromatic radical in the vapour phase (130). It has been generally agreed that the quantum yield of dissociation is low and polymers are formed in addition to small quantities of gaseous products. The main products obtained by the vapour phase oxidation of toluene are benzaldehyde, benzoic acid and maleic acid and for the o-xylene, the main products are phthalic anhydride, and maleic anhydride (133).

The pi-electrons of olefins and acetylenes are more loosely held to their carbon nuclei than are the electron pairs of single bonds, and they are accessible to direct attack by electrophilic reagents. However, the two sets of

pi-electrons of acetylenes are held more firmly between the carbon nuclei than are the pi-electrons of olefins. Consequently, acetylenes are less easy to oxidize than olefins. The presence of a double bond in the molecule greatly modifies the susceptibility to oxidation and in simple olefins the initial point of attack is preferentially at the CH_2 group alpha to the double bond (130). The chain is continued by the reaction of the initially formed radical with oxygen to give a peroxy radical and subsequent reactions are determined by the thermal reaction of the peroxy intermediate.

Tetrachloroethylene is an olefin with four chlorine atoms attached to two carbon atoms. The presence of a double bond and four electronegative chlorine atoms makes it less stable than its parent compound, ethylene. It readily reacts with moisture in the air producing halogen acids along with some aldehydes, carbon monoxide and carbon dioxide (130).

7.2 Heat of Adsorption

Since adsorption is a physical process in which work is performed on the molecules, there must be associated with it some change in the thermodynamic state of the adsorbent during the adsorption process. The process is generally exothermic in nature, and the resultant evolution of heat is defined as heat of adsorption.

In support of the theory that the atoms in the surface of an adsorbent possess varying degrees of activity,

Bull et al. (134) reported that the heat of adsorption decreased progressively as successive small increments of adsorbate were adsorbed. The higher initial heats were explained by assuming that the first small amount of adsorbate vapour were adsorbed on the atoms of the adsorbent of relatively high activity as compared to the other atoms on the surface.

There are a few guidelines on the heat of adsorption that can be deduced on the basis of existing experimental data. One is that the heat of adsorption increases with an increase in the boiling point of the adsorbate. An increase in the heat of adsorption of methanol to ethanol and propanol on charcoal was reported in the literature (135).

Although the above rule is usually true, it is by no means rigorous. Thus methyl alcohol boils at 337°K and has a heat of adsorption of 13,100 cal mole⁻¹ whereas dimethyl ether boils at 307°K and has a heat of adsorption of 15500 cal mole⁻¹. To understand the differences encountered in such case, the detailed structures of the molecules, their sizes, polarizabilities and dipole moments would also have to be considered.

Heat of adsorption increases with increasing size of molecule. The addition of successive CH₂ groups causes smaller and smaller increase. Replacement of the hydrogen atoms by chlorine atoms in methane causes an increase in the heat of adsorption. A hydroxyl group replacement causes even a bigger increase. Methyl, ethyl and propyl alcohols have larger heats of adsorption than

the corresponding chlorides (58). This is true in spite of the fact that the chlorides have slightly larger dipole moments. Possibly the main factor accounting for the smaller heats of adsorption of the chlorides is their larger molecular radius which makes the distances of the chloride molecules from the surface larger than the distances of the alcohol molecules.

Branched chain compounds have smaller heats of adsorption than straight chain compounds. Isopropyl chloride has a smaller heat of adsorption than normal propyl chloride. If the organic vapour molecules are assumed to lie flat on the adsorbent, the average distance of the branched chain molecule from the surface will be greater than that of the straight chain molecule, which results in a smaller interaction energy.

Examples of constant heats of adsorption over the entire surface of an adsorbent or even over a large part of the surface, are very rare (58). Ordinarily the heats of adsorption vary considerably with the amount of vapour adsorbed, and often the variation is quite complex. There are two factors that may cause this variation, the nature of the adsorbate and the nature of the adsorbent. Furthermore, variation in the heats of adsorption may be produced by interaction between the adsorbed molecules themselves. If the adsorbed molecules have permanent dipoles, the surface forces may line up these dipoles parallel and oriented in the same direction

resulting in repulsion which will reduce the heat of adsorption. If the molecules are non-polar the heat of adsorption will increase. The attractive or repulsive forces increase as the surface becomes filled with adsorbed molecules, since the average distance between the molecules decreases.

7.3 Discussion of Experimental Results

Experimental conditions and the results are tabulated in Appendix II. The physical parameters of all the runs are included and adsorbate-adsorbent mass ratios are calculated for each run. A series of results is obtained for each of the four solvents ranging from 0.267 to 0.397 for heptane, 0.721 to 1.007 for tetrachloroethylene, 0.406 to 0.696 for toluene and 0.343 to 0.527 in case of o-xylene. These values are higher than the values calculated at breakthrough (Appendix VI) because most of the experiments have been continued long after the equilibrium is established. This is done to make sure all the steps before and after the equilibrium stage can be traced. With a few exceptions, the adsorbate-adsorbent ratio increases with an increase in the inlet solvent flow rate.

Of the four solvents used in the present research, tetrachloroethylene seems to have a much higher adsorbate-adsorbent ratio than the other three. This high value can be attributed to the fact that a hydrogen bond may be created between the moisture of the air and the chlorine atoms of tetrachloroethylene. Maggs (37) reported similar

high values for phosgene and hydrogen chloride adsorption.

Breakthrough time for the outlet concentration to reach 10% of the inlet concentration is plotted against the weight of cloth used. Three different weights of cloth are used for each of the liquid solvent flow rates. A regression analysis is performed and from the intercept and the slope of the straight line the adsorption rate constant is calculated using equation 3.54. The results are summarised in Appendix VII.

Five values of rate constant are obtained for each of the four solvents used in the present research. The difference between the maximum and minimum value is as much as 16.1. This is due to the fact that air-solvent vapour flow rates are different for each run and an average value has to be used. The temperature at which the experiments were carried out were not always the same. The physical conditions of the experiments were not always identical as has been demanded by the original equation 3.54.

The rate constants for some of the vapours adsorbed on granular charcoal are summarised in Table 3.2. The values recorded in the present research are 4 to 5 times higher than the values in Table 3.2 for similar compounds. These higher adsorption rate constants also give evidence that charcoal cloth is a more powerful adsorbent than granular carbon.

The experimental data is plotted in Figures 6.1 to 6.4 to try the applicability of the Langmuir isotherm.

According to the equation the inverse of the slope of the straight line should give the V_m , the volume of vapour necessary to cover the entire surface with a unimolecular adsorbed layer. For any particular vapour the value of V_m should be constant provided the same adsorbent is used. The three sets of values plotted in the three different graphs do not confirm to the constancy of V_m .

One of the fundamental assumptions in the derivation of the Langmuir equation is that the heat of adsorption does not vary with the amount adsorbed. Examples of constant heats of adsorption over the entire surface of an adsorbent, or even over a large part of the surface, are very rare. Ordinarily the heat of adsorption vary considerably with the amount of gas adsorbed, and often the variation is quite complex. Langmuir conducted his experiments at very low pressures, the highest pressure being 0.13×10^{-3} m (0.13 mm). Had he gone to somewhat higher pressures, he would have obtained a more complete covering of the surface (58).

Brunauer (58) concluded that multilayer adsorption takes place at higher pressure. For microporous adsorbents such as charcoal cloth most of the pores are very small and they become inaccessible to molecules of certain adsorbates for sterical reasons. For such pores it is quite difficult to define the concept of surface area. The entire volume of micropores represents a space where an adsorption field exists. In this type of case, it is

natural to expect that adsorption in such pores should lead to their volume filling (17). This may not happen where larger molecule adsorbates are involved.

The theoretical adsorbate-adsorbent mass ratio using Dubinin-Polanyi equation has been calculated for all the four solvents used in the present research and listed in Appendix V. The values seem to be a little higher than the experimental values of adsorbate-adsorbent ratios at breakthrough listed in Appendix VI. One of the main reasons may be that the experimental values have been calculated at the first sign of saturation. Deviation of Dubinin-Polanyi equation has been observed by other workers at low values of (P/P_0) due to capillary condensation in transitional pores or multilayer formation on the walls of macropores (89).

The derivation of the Dubinin-Polanyi equations has been discussed in section 3.7 in detail. It adequately describes over a wide pressure range, the adsorption data of many adsorbates on a wide variety of microporous carbons, both activated and unactivated. The derivation of this equation does not include a detailed analysis of an adsorption process. Nevertheless, there can be no doubt that this particular equation does describe the overall adsorption process. The advantage of the Dubinin-Polanyi equation is that the adsorbate-adsorbent mass ratio can be calculated without doing any experiment.

CHAPTER 8

CONCLUSIONS AND RECOMMENDATIONS

8. Conclusions and Recommendations

The objectives of the experimental programme may be divided approximately into the following main areas:

- i) The study of the adsorption capacity of charcoal cloth.
- ii) The calculation of adsorption rate constants of four different solvents.
- iii) The development and testing of mathematical models to describe the system and enable future workers to scale the system up to process size.
- iv) The design of a canister to enable the maximum adsorption with a minimum pressure drop.

The adsorbate-adsorbent mass ratio (see Appendix VI) decreased in the order of toluene-o-xylene-heptane. Essentially all the three compounds are non-polar. Hence the adsorbate-adsorbent ratio primarily depends on the size and length of C-C bonds in the molecule. The C-C bond length in heptane (1.54 \AA) is higher than the C-C bond length in benzene (1.36 \AA) (138). Moreover size of the heptane molecule is greater than o-xylene and toluene. Wilkins (136) suggested that charcoal cloth contains more micropores than macropores and larger molecules would have difficulty in diffusing into the pores. However, tetrachloroethylene seems to be adsorbed much more on the cloth surface than the three other compounds used in the present research. Due to more electronegativity of chlorine compared to carbon and presence of double bond, partial polarization takes place inside the molecule.

The cloth surface also bears different polar groups. Hence due to electrostatic attraction it is quite likely that C_2Cl_4 is adsorbed in greater amounts compared to the non-polar molecules.

Water vapour is generally present in the atmosphere and an adsorbent filter will usually contain adsorbed water when in use. Filters, however, are still effective in protecting against other vapours, and the reason for this lies in the ability of many vapours to displace the adsorbed water. The efficiency of charcoal cloth is in general reduced by the presence of adsorbed water. Maggs (37) measured the effect of humidity on adsorption of carbon tetrachloride by granular charcoal previously brought to equilibrium with the air stream at a fixed relative humidity. He reported that for an increase in relative humidity from 0% to 95% the breakthrough time was reduced from 4920 seconds to 360 seconds. This reduction in adsorption efficiency due to moisture is much less in charcoal cloth.

In the present research .082 kg of cloth was used in blank tests where air was passed for three hours on different days of varying humidity. The increase in weight due to moisture adsorption ranged from .0024 to 0.0102 kg. The deterioration in the adsorption capacity of charcoal cloth due to moisture is much less in the present research than has been claimed by Maggs (37). The reason lies in the fact that charcoal cloth was heated to

180°C in an oven before an adsorption was carried out. As the adsorption starts, there is a competition between the adsorbate vapour and the moisture in air. Water is held far less strongly on charcoal cloth than on other adsorbents such as silica gel or alumina and displacement of adsorbed water by adsorbate vapours takes place readily at a carbon surface. Nevertheless, the moisture does reduce the adsorption capacity of charcoal cloth and the effect is more in the presaturation period than after saturation as most of the water will be displaced by then.

Various theories of adsorption lead to different expressions for the equilibrium state. As in adsorption equilibria, no one single approach is completely satisfactory. The effective rate of adsorption and desorption is governed by one or more diffusional steps. The mass transport for an adsorbate between the bulk of the fluid phase and the outer surfaces of the adsorbent particles is governed by molecular diffusivity and also by eddy diffusivity in turbulent flow. The solid phase mass transport in the adsorbent is invariably controlled by molecular diffusion through the pores of the solid.

With the mass transfer zone concept, a total resistance is expressed in terms of an amount of unused adsorbent, which must be added to the adsorbent equilibrium requirement. Anderson (106) suggested a formula to calculate the length of unused bed, the details of which are outlined in Section 6.2. The length of the unused bed determined at the breakthrough point can be related

to the total resistance to mass transfer. It follows, therefore, that the greater the length of unused bed, the less effective is the adsorptive system and vice versa.

In the present research, the length of the unused bed has been calculated at a time when the outlet concentration reached 10 p.p.m. Three different heights of bed are used, each bed being used at five different inlet solvent concentrations. The results are summarized in Appendix IV. With a few exceptions, there seems to be a correlation in the percentage of unused bed. The length of unused bed increases as the total length of bed increases from 0.0125 m to 0.0225 m. But the percentage of unused bed does not differ very much. Some of the few discrepancies arise probably due to crude estimation of breakthrough time.

An equation has been developed relating the number of layers of cloth and the time required for the effluent concentration to reach 10% of the inlet concentration. The two constants for the equation at different inlet concentrations are tabulated in section 6.4. It has to be borne in mind that equation 6.15 is developed when the charcoal cloth canister of diameter 0.1524 m (6") is used. For larger sizes, appropriate reduction in the two constants values have to be made.

The time required for the effluent concentration to reach 10% of the inlet concentration has been calculated using equation 6.10 and has been tabulated in Appendix VIII.

The calculated values differ to the experimental values. The reasons may lie in the assumption in the deviation of the equation 6.10. The speed at which adsorption takes place on the charcoal cloth may not be constant all over the surface. The macropore region will have a faster rate than micropore region. Consequently an assumption that a single mechanism controls the adsorption of vapours on charcoal cloth is too much of an over simplification.

Although successful results have been obtained using the current apparatus, future work involving this system would require modifications. The small hole on the PVC plate on the entrance section of the canister can be made bigger than .0254m (1") in diameter. The canister diameter can be reduced to check if there is any improvement in adsorption capacity of the cloth.

The volumetric flow rate of the air-vapour mixture can be increased to check the behaviour of the canister for high capacity. Mixture of different solvents could be tried to meet the need of various industries with different effluent vapours.

Regeneration has been carried out using hot air and a vacuum in an oven. Physical properties of the cloth after regeneration should be monitored. It is then likely that the different oxides which form on the cloth surface would be identified more accurately.

Transparent PVC pipe may be used which would help to

see the position of the anemometer, thermocouples and the probes for mass spectrometer. An analogue computer system connected to the present mass spectrometer would certainly help to measure the peaks more accurately.

NOMENCLATURE

A	Differential molar work of adsorption	Jmol^{-1}
A_1	Area of the bed	m^2
A_s	Differential molar work of adsorption for a standard adsorbate	Jmol^{-1}
a	Adsorption value at equilibrium pressure P	mol
a_0	Adsorption value at saturated pressure P_0	mol
a_1	Parameter of the adsorbate	-
a_2	Constant	-
a_p	Outer surface interfacial area of the pores per unit volume of contacting system	$\text{m}^2 \text{m}^{-3}$
B	Constant for micropores	K^{-2}
B_0	Average value of B	K^{-2}
B_j	Constant for micropore j	K^{-2}
b_1	Parameter of the adsorbate	-
b_2	Constant	-
C	Adsorbate concentration	kg m^{-3}
C_0	Inlet adsorbate concentration	kg m^{-3}
C_{pf}	Specific heat of fluid	$\text{J kg}^{-1} \text{m}^{-2} \text{K}^{-1}$
C_{ps}	Specific heat of adsorbent	$\text{J kg}^{-1} \text{m}^{-2} \text{K}^{-1}$
C_x	Outlet adsorbate concentration at a point x in the bed	kg m^{-3}
c_1	Parameter of the adsorbate	-
c_2	Constant	-
D	Diffusivity	$\text{m}^2 \text{s}^{-1}$
D_1	Constant	-
D_K	Knusden diffusion coefficient	$\text{m}^2 \text{s}^{-1}$
D_e	Effective diffusivity within the adsorbent	$\text{m}^2 \text{s}^{-1}$
D_f	Diffusivity of adsorbate fluid in air	$\text{m}^2 \text{s}^{-1}$
D_{pore}	Pore diffusivity of the adsorbate	$\text{m}^2 \text{s}^{-1}$

d	Distance	m
d_0	Density of liquid adsorbate at 0°C	kg m^{-3}
d_{15}	Density of liquid adsorbate at 15°C	kg m^{-3}
d_p	Pore diameter	m
d_t	Density of liquid adsorbate at t°C	kg m^{-3}
e	Voidage	-
F	Volumetric flow rate of air-solvent vapour mixture	$\text{m}^3 \text{s}^{-1}$
F_1	Ratio of outlet and inlet concentration of the adsorbate	-
ΔG	Differential molar free energy	J mol^{-1}
G	Feed rate of carrier fluid per unit area of adsorbent	$\text{kmol m}^{-2} \text{s}^{-1}$
ΔH	Differential molar enthalpy of adsorption	J mol^{-1}
K	A parameter for each system of adsorbent and adsorbate	$\text{mol}^2 \text{J}^{-2}$
K_1, K_2, K_3))- Constant	-
K_5, K_6)		
K_∞	Adsorption rate constant (mass transfer limiting)	s^{-1}
K_c	External mass transfer coefficient	m s^{-1}
K_s	A parameter for each system of adsorbent and standard adsorbate	$\text{mol}^2 \text{J}^{-2}$
K_v	Adsorption rate constant	s^{-1}
k_{pore}	Mass transfer coefficient in the pores	m s^{-1}
L_0	Adsorbent bed length	m
L_s	Position of the stoichiometric front in the adsorbent bed	m
M	Molecular weight of adsorbate	kg kmol^{-1}
\bar{M}	Average molecular weight of air-vapour mixture	kg kmol^{-1}
N	Refractive index of liquid adsorbate	-

N_0	Number of active centres	-
N_1	Mole fraction of component 1 in the adsorbed phase	-
N_2	Mole fraction of component 2 in the adsorbed phase	-
N_{pore}	Number of transfer units	-
n	Constant	-
n_i	Number of moles of component i in adsorbed phase per unit mass of adsorbent	-
P	Adsorbed vapour pressure	atm
P_0	Saturated vapour pressure	atm
P_1	Adsorbed vapour pressure for component 1	atm
P_2	Adsorbed vapour pressure for component 2	atm
P_e	Electronic polarization	$\text{m}^3 \text{kmol}^{-1}$
P_T	Total pressure	atm
P_{cr}	Critical Pressure	mm Hg
p	Equilibrium partial vapour pressure of adsorbate	mm Hg
Q	Adsorbate-Adsorbent mass ratio	kg kg^{-1}
Q_1	Minimum heat required	J
Q_2	Total heat supplied	J
q	Heat of adsorption	J mol^{-1}
q_i	Rate of heat input	J s^{-1}
R	Gas constant	$\text{Jmol}^{-1} \text{K}^{-1}$
R_1	Constant separation factor	-
r	Radial parameter	m
r_p	Pore radius	m
ΔS	Differential molar entropy of adsorption	$\text{Jmol}^{-1} \text{K}^{-1}$
T	Absolute temperature	K

T_1	Ratio of adsorption temperature to critical temperature	-
t	Adsorption temperature	$^{\circ}\text{C}$
t_f	Inlet temperature of carrier fluid	K
t_s	Initial temperature of adsorbent	K
t_{cr}	Critical temperature	$^{\circ}\text{C}$
U	Internal energy	J mol^{-1}
U_1	Front velocity	m s^{-1}
\bar{U}	Mean molecular velocity	m s^{-1}
u	Velocity of air-vapour mixture	m s^{-1}
V	Volume of vapour adsorbed per unit mass of adsorbent	$\text{m}^3 \text{kg}^{-1}$
V_L	Superficial velocity	m s^{-1}
V_m	Volume of vapour adsorbed per unit mass of adsorbent with a layer one molecule thick	$\text{m}^3 \text{kg}^{-1}$
v	Volume of the bed	m^3
v^*	Molar volume of vapour adsorbed	$\text{m}^3 \text{mol}^{-1}$
W	Amount of vapour adsorbed in liquid volume per unit mass of adsorbent	$\text{m}^3 \text{kg}^{-1}$
W_o	Apparent limiting amount of adsorption for adsorbent	$\text{m}^3 \text{kg}^{-1}$
W_{oj}	Apparent limiting amount of adsorption for micropore j	$\text{m}^3 \text{kg}^{-1}$
W_1	Amount of vapour adsorbed in liquid volume per unit mass of adsorbent for component 1	$\text{m}^3 \text{kg}^{-1}$
W_2	Amount of vapour adsorbed in liquid volume per unit mass of adsorbent for component 2	$\text{m}^3 \text{kg}^{-1}$
W_3	Filled volume of adsorption space	m^3
W_4	Adsorbent weight	kg
W_e	Kinetic adsorption capacity	kg kg^{-1}
$W(x)$	Amount of vapour adsorbed in liquid volume per unit mass of adsorbent at a point x on the bed	$\text{m}^3 \text{kg}^{-1}$

X	Ratio of fluid concentration	-
X_0	Initial adsorbate loading on the adsorbent	kg kg ⁻¹
X_e	Adsorbate loading in equilibrium with the adsorbate concentration in the feed	kg kg ⁻¹
x^*	Degree of saturation in mass transfer zone	-
Y	Bulk vapour phase concentration	kg m ⁻³
Y_0	Concentration of adsorbate in equilibrium with X_0	m ³ m ⁻³
Y_e	Concentration of adsorbate in carrier fluid	m ³ m ⁻³
Y_p	Concentration of adsorbate in the pores	kg m ⁻³
Z	Number of layers of cloth	-
α	Thermal coefficient of liquid expansion	kg m ⁻³ K ⁻¹
α_1	Thermal coefficient of limiting adsorption	K ⁻¹
β	Affinity coefficient	-
β_1	Affinity coefficient for component 1	-
β_2	Affinity coefficient for component 2	-
γ	Surface tension at 15°C	N m ⁻¹
δ	Tortuosity factor	-
θ	Time	s
$\theta_{0.1}$	Time required for outlet vapour concentration to reach 10% of the inlet vapour concentration	s
θ_1	Degree of volume filling	s
θ_2	Saturation time	s
θ_b	Breakthrough time	s
θ_e	Equilibrium time	s
θ_s	Stoichiometric time	s
λ	Bed thickness	m
λ_c	Critical bed thickness	m
λ_1	Ratio of adsorbed vapour pressure to saturated vapour pressure	-

ρ	Density of air-vapour mixture	kg m^{-3}
ρ_B	Bulk density of the adsorbent	kg m^{-3}
μ	Viscosity	Ns m^{-2}
μ_i	Chemical potential of component i	J mol^{-1}
π	Spreading pressure	$\text{J mol}^{-1} \text{m}^{-2}$
Δ	Distribution width	-
τ	Throughput parameter based on concentration changes	-
$v_{3.2}$	Volume of the micropores smaller than $3.2 \times 10^{-9} \text{ m}$ in diameter	$\text{m}^3 \text{kg}^{-1}$
ψ_{pore}	Correction factor	-

REFERENCES

- 1) P.N. CHEREMISINOFF and F. ELLERBUSCH,
Carbon Adsorption Handbook, Ann Arbor Science,
Michigan, 1, 1978.
- 2) V.R. DEITZ, Bibliography of Solid Adsorbents,
United States Cane Sugar Refiners and Bone Char
Manufacturers and National Bureau of Standards,
Washington D.C., 689-696, 1944.
- 3) LOWITZ, Crell's Chem Ann, 1, 211, 1786.
- 4) J. STENHOUSE, Chem. News, 3, 78, 1861.
- 5) U.K. PATENT 1,301,101.
- 6) U.K. PATENT 1,001,606.
- 7) M.E. SMITH and J. DAVIES, Dynamic Adsorption of
Chlorobenzene on Charcoal Cloth and Nutshell
Charcoal, Lab Report No 582, Charcoal Laboratories,
CDE Porton Down, 1977.
- 8) M.E. SMITH and J. DAVIES, Dynamic Adsorption of
Chloroform on Charcoal Cloth and Nutshell Charcoal,
Lab Report No. 587, Charcoal Laboratories, CDE
Porton Down, 1977.
- 9) M.E. SMITH and J. DAVIES, Dynamic Adsorption
of Trichloroethylene on Charcoal Cloth and Nutshell
Charcoal, Lab Report No. 588 Charcoal Laboratories,
CDE Porton Down, 1978.

- 10) M.E. SMITH and J. DAVIES. Dynamic Adsorption of Carbon Tetrachloride on Charcoal Cloth and Nutshell Charcoal, Lab Report No. 605, Charcoal Laboratories, CDE Porton Down, 1978.
- 11) M.E. SMITH and J. DAVIES, Dynamic Adsorption of Penthrane on Charcoal Cloth and Nutshell Charcoal, Lab. Report No. 609, Charcoal Laboratories, CDE Porton Down, 1978.
- 12) F.A.P. MAGGS and M.E. SMITH, Respiratory Protection, ed. Brian Bwlantyne and Paul H. Schwabe, Chapman & Hall, London, 189-203, 1981.
- 13) J.A. CLARK, The Recovery of Valuable Vapour Phase Solvents using Activated Charcoal Cloth, PhD Thesis, Aston University, 1983.
- 14) R.G. DORMAN and F.A.P. MAGGS, Chemical Engineer, 671-674, 1976.
- 15) CHARCOAL CLOTH LTD, Technical Notes.
- 16) WALTER J. WEBER JR., Physico-Chemical Processes For Water Quality Control, Wiley Interscience, New York, 207, 1972.
- 17) B.P. BERING, M.M. DUBININ and V.V. SERPINSKY J. Colloid Interface Sci, 21, 378-393, 1966.
- 18) S. GLASTONE^S, Textbook of Physical Chemistry, (2nd edition) Macmillan, London, 1197-1205, 1946.

- 19) S. BRUNAUER, P.H. EMMETT and E. TELLER,
J. Am. Chem. Soc., 60, 309-319, 1938.
- 20) D.M. YOUNG and A.D. CROWELL, Physical Adsorption
of Gases, Butterworths, London, 156, 1962.
- 21) C.J. GORTER and H.P.R. FREDERIKSE, Physica, 's Grav,
15, 891, 1949.
- 22) WALTER J. WEBER JR., Physico-Chemical Processes
For Water Quality Control, Wiley Interscience,
New York, 237, 1972.
- 23) J.S. JAIN and V.L. SNOEYINK, Jou Wat Poll
Control Fed, 45 (12), 2463-2479, 1973.
- 24) J.A.V. BUTLER and C. OKRENT, J. Phys. Chem,
34, 2841, 1930.
- 25) C.J. RADKE and J.M. PRAUSNITZ, AIChE J, 18 (4),
761, 1972.
- 26) L. JOSSENS, J.M. PRAUSNITZ, W. FRITZ, E.U.
SCHLUNDER and A.L. MYERS, Chem. Eng. Sci, 33,
1097-1106, 1978.
- 27) J.R. ARNOLD, J. Am. Chem. Soc, 71, 104-110, 1949.
- 28) M.M. DUBININ, Chemistry and Physics of Carbon,
ed. P.C. Walker Jr., Marcel Dekker, New York,
2, 51-120, 1966.
- 29) J.P. HOBSON, The Solid Gas Interface, ed. E.A.
Flood, Arnold, London, 1, 11-75, 1967.

- 30) B.P. BERING, M.M. DUBININ and V.V. SERPINSKY,
J. Colloid Interface Sci, 38 (1), 185-194, 1972.
- 31) M.M. DUBININ, Progress in Surface and Membrane
Science, ed. D.A. Cadenhead, Academic Press,
New York, 9, 1-70, 1975.
- 32) M.M. DUBININ, Adsorption Desorption Phenomena
Proceedings, 2nd Int. Conf, 3-17, 1972.
- 33) A.L. MYERS and J.M. PRAUSNITZ, AIChE J, 11 (1),
121, 1965.
- 34) M.M. DUBININ, Quarterly Rev (London), 9, 101-114,
1955.
- 35) WALTER J. WEBER JR., Physico-Chemical Processes
For Water Quality Control, Wiley Interscience,
New York, 236, 1972.
- 36) R.L. DEDRICK and R.B. BECKMANN, Chem. Eng. Prog.
Symp. Series, 63 (74), 68-78, 1967.
- 37) F.A.P. MAGGS, Filtration & Separation, 10,
413-417, 1973.
- 38) JAMES S MATTSON, HARRY B. MARK JR., MICHAEL
D. MALBIN, WALTER J. WEBER, JR. and JOHN C.
CRITTENDEN, J. Colloid Interface Sci, 31 (1),
116-130, 1969.
- 39) HENRY G. SCHWARTZ JR., Environ Sci & Tech, 1 (4),
332-337, 1967.

- 40) THOMAS M. WARD and FORREST W. GETZEN,
Environ Sci & Tech, 4 (1), 64-67, 1970.
- 41) ROBERT S. COUGHLIN and FOUAD S. EZRA,
Environ Sci & Tech, 2 (4), 291-297, 1968.
- 42) R.S. DRAGO, R.J. NIEDZIELSKI and R.L. MIDDAGH,
J. Am. Chem. Soc, 86, 1694, 1964.
- 43) R.A. SMITH, Proc. Roy. Soc. (London), 12, 425,
1863.
- 44) T.F.E. RHEAD and R.V. WHEELER, J. Chem. Soc,
101, 846, 1912.
- 45) R.N. SMITH, Quarterly Rev(London), 13, 287, 1959.
- 46) S.W. WEDLER and T.F. YOUNG, J. Am. Chem. Soc, 71,
4155, 1948.
- 47) B.R. PURI, Chemistry and Physics of Carbon,
ed. P.C. Walker Jr., Marcel Dekker, New York,
6, 191-282, 1970.
- 48) B.R. PURI and R.C. BANSAL, Carbon, 5, 169, 1967.
- 49) B.R. PURI and K.C. SEHGAL, Indian J Chem,
5, 379, 1967.
- 50) B.R. PURI and R.C. BANSAL,
Indian J Chem, 5, 381, 1967.

- 51) D. RIVIN and J. ARON, Proceedings of the seventh conference on Carbon, Cleveland (Ohio), U.S.A. 1965.
- 52) B.R. PURI and N.K. SANDLE, Indian J Chem, 6, 267, 1968.
- 53) B.R. PURI and R.S. HAZRA, Carbon, 9, 123, 1971.
- 54) B.R. PURI, D.D. SINGH and B.C. KAISTHA, Carbon, 10, 481, 1972.
- 55) WALTER J. WEBER JR., Physico-Chemical Processes For Water Quality Control, Wiley Interscience, New York, 230, 1972.
- 56) WALTER J. WEBER JR., Physico-Chemical Processes For Water Quality Control, Wiley Interscience, New York, 234, 1972.
- 57) J.H. DE BOER, Adv Catalysis, 8, 17-161, 1956.
- 58) STEPHEN BRUNAUER, The Adsorption of Gases and Vapours, Oxford University Press, London, 240-364, 1944.
- 59) S. BRUNAUER and P.H. EMMETT, J Am Chem Soc, 62, 1732, 1940.
- 60) J. MCGARACK and W.A. PATRICK, J Am Chem Soc, 42, 946, 1920.
- 61) WALTER J. WEBER JR., Physico-Chemical Processes For Water Quality Control, Wiley Interscience, New York, 239-243, 1972.

- 62) K.J. LAIDLER, Chemical Kinetics (2nd edition) Mcgraw-Hill, New York, 256-320, 1965.
- 63) J.H. DE BOER, The Mechanism of Heterogeneous Catalysis, ed. J.H. De Boer, Elsevier, Amsterdam, 1, 1960.
- 64) J.J. ZELINSKI, PhD Thesis, The Pennsylvania State University, 1950.
- 65) D.J.E. INGRAM and D.E. G. AUSTEN, Industrial Carbon and Graphite, Society of Chemical Industry, London, 19, 1957.
- 66) WALTER J. WEBER JR., Physico-Chemical Processes For Water Quality Control, Wiley Interscience, New York, 200, 1972.
- 67) I. LANGMUIR, Trans. Faraday Soc., 17, 621, 1921.
- 68) C.N. HINSHELWOOD, Kinetics of Chemical Change, Clarendon Press, Oxford, 145, 1926; 187, 1940.
- 69) A. PARKER, Industrial Air Pollution Handbook, Mcgraw-Hill, U.K., 184-189, 1978.
- 70) WALTER J. WEBER JR., Physico-chemical Processes For Water Quality Control, Wiley Interscience, New York, 215, 1972.
- 71) J. DE ACETIS and G. THODOS, Ind Eng Chem, 52, 1003, 1960.
- 72) M. KNUSDEN, Annin Physik, 35, 389, 1911.

- 73) J.O. HIRSCHFELDER, R.O. BIRD and E.L. SPOTZ,
Trans ASME, 71, 921, 1949.
- 74) E.N. FULLER, J.C. GIDDINS and P.D. SCHETLER,
Ind. Eng. Chem, 58 (5), 19, 1966.
- 75) T. VERMEULEN, Adv in Chem Eng, 2, 147-208, 1958.
- 76) R.G. PEEL, A. BENEDEK and C.M. CREWE,
AIChE J, 27 (1), 26-32, 1981.
- 77) DE SAUSSURE, Gilbert's Ann der Physik, 47, 113,
1814.
- 78) A. EUCKEN, Verh deut physik Ges, 16, 345, 1914.
- 79) M. POLANYI, Verh deut physik Ges, 16, 1012, 1914.
- 80) M.M. DUBININ, Chem Rev, 60, 235-241, 1960.
- 81) K. URANO, S.OMORI and E.YAMAMATO, Environ
Sci & Tec, 16 (1), 10-14, 1982.
- 82) G.G. JAYSON, T.A. LAWLESS and D. FAIRHURST,
J. Colloid Interface Sci, 86 (2), 397-410, 1982.
- 83) N.A. LANGE, Handbook of Chemistry, McGraw Hill,
New York, 10-31, 1961.
- 84) J. TIMMERMAN, Physicochemical constants of Pure
Organic Compounds, Elsevier, Amsterdam,
Netherlands, 150-153, 1950.

- 85) E. W. WASHBURN, International Critical Tables, McGraw Hill, New York, 3, 28, 1926.
- 86) M.M. DUBININ, J. Colloid Interface Sci, 23 (4), 487-499, 1967.
- 87) J. P. HOBSON and P.A. ARMSTRONG, J. Phys Chem, 67, 2000, 1967.
- 88) M. G. KAGANER, Rus Jou Phys Chem, 33 (10), 352-356, 1959.
- 89) H. MARSH and B. RAND, J. Colloid Interface Sci, 33 (1), 101-116, 1970.
- 90) H. MARSH and T. SIEMIENIEWSKA, Fuel, 46, 441-457, 1967.
- 91) S.J. GREGG and K.S.W. SING, Adsorption Surface Area and Porosity, Academic Press, London, 5, 1967.
- 92) H.F. STOECKLI, J. PH HOURIET, A PERRET and U. HUBER, Characterisation of Porous Solids, Society of Chemical Industry, London, 31-39, 1979.
- 93) H.F. STOECKLI, J. Coll Interface Sci, 59 (1), 184-185, 1977.
- 94) P.J. REUCROFT, W.H. SIMPSON and L.A. JONAS, J. Phys Chem, 75 (23), 3526-3531, 1971.
- 95) A.D. CROWELL, J. Chem Phys, 49, 892, 1968.

- 96) B.RAND, J. Coll Interface Sci, 56 (2), 336-346, 1976.
- 97) U. HUBER, F. STOECKLI and J. PH HOURIET, J. Colloid Interface Sci, 67 (2), 195-203, 1978.
- 98) M.M. DUBININ, Carbon, 17 (6), 506, 1979.
- 99) N.K. HIESTER and T. VERMEULEN, Chem Eng Prog, 48, 505-516, 1952.
- 100) S. MASAMUNE and J.M. SMITH, AIChE J, 10, 246-252, 1964.
- 101) L.A. JONAS and W.J. SVIRBELY, J Catalysis, 24 (3), 446-459, 1972.
- 102) A. WHEELER and A.J. ROBELL, J Catalysis, 13, 299-305, 1969.
- 103) L.A. JONAS, Y.B. TEWARI and E.B. SANSONE, Carbon, 17 (4), 345-349, 1979.
- 104) A. WHEELER, Catalysis, ed. P.H. EMMETT, Reinhold, New York, 2, 150, 1955.
- 105) L.A. JONAS and J.A. REHRMANN, Carbon, 11 (1), 59-64, 1973.
- 106) R.A. ANDERSON, Encyclopaedia of Chemical Processing & Design, ed. J.J. MCKETTA, Marcel Dekker, New York, 2, 174-213, 1977.

- 107) N.K. CHANEY, A.B. RAY and ANCEL ST. JOHN,
Ind. Eng. Chem, 15 (12), 1244, 1923.
- 108) H.N. HOLMES and J.B. MCKELVY, J. Phys Chem,
32, 1522, 1928.
- 109) E.F. LUNDELIUS, Kolloid Z, 26, 145, 1920.
- 110) R.S. HANSEN and R.P. CRAIG, J. Phys Chem, 58,
211, 1954.
- 111) W.J. WEBER JR. and J.C. MORRIS, J. Sanit Eng
Div, ASCE, 90, SA3, 79-107, 1964a.
- 112) A.H. ANDERSON, Acta Pharmacol Toxicol, 3, 199-
218, 1947.
- 113) C.J. DANBY, J.G. DAVOUD, D.H. EVERETT, C.N. HINSHELWOOD
and R.M. LODGE, J. Chem. Soc Trans, 918-934, 1946.
- 114) U.K. PATENT 1,429,476.
- 115) J.J. COLLINS and B.D. PHILIPS, "Single Component
Dynamic Adsorption" paper presented at AIChE
Pittsburgh meeting, November 5, 1965.
- 116) R.E. TREYBAL, Mass Transfer Operations (2nd
edition) McGraw Hill Kogakusha Ltd, Tokyo,
491-568, 1968.
- 117) T. VERMEULEN, G. KLEIN and N.K. HIESTER,
Chemical Engineers Handbook, ed. Robert H. Perry
and Cecil H. Chilton, McGraw Hill Kogakusha Ltd,
Tokyo, Chapter 16, 1973.

- 118) CHARLES N. SATTERFIELD, Mass Transfer in Heterogeneous Catalysis, M.I.T. Press, Cambridge, Massachusetts, 41-54, 1970.
- 119) K.R. HALL, L.C. EAGLETON, A. ACRIVOS and T. VERMEULEN, Ind Eng Chem Fundamentals, 5, 212-223, 1966.
- 120) D. ATKINSON, A.I. MCLEOD, K.S.W. SING and A. CAPON, Carbon, 20 (4), 339-343, 1982.
- 121) T.M. ROVINSKAYA and A.M. KOGANOVSKII, Kolloid Zh, 23 (6), 739-748, 1961.
- 122) J. CRANK, Phil Mag, 39, 140-149, 1948.
- 123) V. SNOEYINK, Environ Sci & Tech, 3, 918, 1969.
- 124) J.S. ZOGORSKI, S.D. FAUST and J.H. HASS, J. Colloid Interface Sci, 55, 329, 1976.
- 125) R.E. BECK and J.S. SCHULTZ, Science, 170, 1302, 1970.
- 126) C.N. SATTERFIELD, C.K. COLTON and W.H. PITCHER, AIChE J, 19, 628, 1973.
- 127) EDWARD W. WASHBURN, International Critical Tables, McGraw Hill Book Co. Inc, New York, 5, 62-63, 1929.
- 128) P.R. CHEREMISINOFF and F. ELLERBUSCH Carbon Adsorption Handbook, Ann Arbor Science, Michigan, 327-349, 1978.

- 129) A. CORNU and R. MASSOT, Compilation of Mass Spectral Data, Heyden and Son Ltd., London, 2, 1966.
- 130) Reactions of free radicals in the gas phase, Special Publication No. 9, The Chemical Society, London, 65-145, 1957.
- 131) C.F. CULLIS, C.N. HINSHELWOOD and M.F.A. MULCANY, Proc Roy Soc, A196, 160, 1949.
- 132) J.W. HASSLER, Purification with Activated Carbon (2nd edition), Chemical Publishing Co Inc, New York, 2-212, 1974.
- 133) E.H. RODD, Rodd's chemistry of carbon compounds, Elsevier Publishing Co, Amsterdam, 2nd ed., 3, 186-195, 1971.
- 134) H.I. BULL, M.H. HALL and W.E. GARNER, J. Chem. Soc, 837-847, 1931.
- 135) A.B. LAMB and A.S. COOLIDGE, J Am Chem Soc, 42, 1146, 1920.
- 136) M.J. WILKINS, The Removal of Trace Organic Impurities from Water using Activated Charcoal Cloth, PhD Thesis, Aston University, 1979.
- 137) I. LANGMUIR, J. Am Chem Soc, 40, 1361, 1918.
- 138) I.L. FINAR, Organic Chemistry, (4th Ed.) Longmans, London, 1, 508, 1961.

APPENDIX I

SAMPLE CALCULATIONS

Calculation of Inlet Solvent Vapour Concentration

(Ref. Run HEP 1)

$$\text{Diameter of the pipe} = 0.1524 \text{ m}$$

$$\text{Velocity of air-solvent vapour mixture} = 0.15 \text{ m s}^{-1}$$

$$\begin{aligned} \text{Volumetric flow rate} &= \frac{\pi}{4} \times (.1524)^2 \times 0.15 \\ &= 273.62 \times 10^{-5} \text{ m}^3 \text{ s}^{-1} \end{aligned}$$

Mass flow rate of liquid solvent

$$\begin{aligned} &= \frac{0.15}{60} \times 10^{-6} \frac{\text{m}^3}{\text{s}} \times 680 \frac{\text{kg}}{\text{m}^3} \\ &= 17 \times 10^{-7} \text{ kg s}^{-1} \end{aligned}$$

Volume of 1 kmol of Heptane at 17°C and 763 mm Hg

$$\begin{aligned} &= \frac{22.4 \times 760 \times (273 + 17)}{273 \times 763} \text{ m}^3 \\ &= 23.684 \text{ m}^3 \end{aligned}$$

Density of Heptane vapour

$$\begin{aligned} &= \frac{100}{23.684} \frac{\text{kg}}{\text{m}^3} \\ &= 4.222 \text{ kg m}^{-3} \end{aligned}$$

Volumetric flowrate of Heptane vapour

$$\begin{aligned} &= \frac{17 \times 10^{-7} \text{ kg s}^{-1}}{4.222 \text{ kg m}^{-3}} \\ &= 4.0265 \times 10^{-7} \text{ m}^3 \text{ s}^{-1} \end{aligned}$$

Inlet solvent vapour concentration

$$\begin{aligned} &= \frac{\text{Volumetric flowrate of Heptane vapour}}{\text{Volumetric flowrate of air-solvent vapour mixture}} \\ &= \frac{4.0265 \times 10^{-7} \text{ m}^3 \text{ s}^{-1}}{273.62 \times 10^{-5} \text{ m}^3 \text{ s}^{-1}} \\ &= 147 \text{ p.p.m (by volume)} \end{aligned}$$

Calculation of Outlet Solvent Vapour Concentration

(Ref. Run HEP 1)

Inlet solvent vapour concentration

$$= 147 \text{ p.p.m}$$

Height of peak of Inlet vapour on

mass spectrometer = 0.176m

Height of peak of Outlet vapour on

mass spectrometer = 0.0108 m

Outlet solvent vapour concentration

$$= \frac{147}{0.176} \times 0.0108 \text{ p.p.m}$$

$$= 9 \text{ p.p.m}$$

Calculation of Adsorption Rate Constant

Breakthrough time for outlet concentration to reach 10% of the inlet concentration was determined from the outlet vapour concentration vs time graph for three different weights of charcoal cloth. A regression analysis was performed between three values. (Reference HEP 1, HEP 6 and HEP 11)

$$\text{Slope} = 207500.4 \text{ s kg}^{-1}$$

$$\text{Intercept} = -3489.2 \text{ sec}$$

$$\theta_b = \frac{W_e C_o}{F} \left[W_4 - \frac{\rho_B F}{K_V} \ln\left(\frac{C_o}{C_x}\right) \right]$$

$$\text{slope} = \frac{W_e C_o}{F}$$

$$\text{Intercept} = - \frac{W_e C_o}{F} \times \frac{\rho_B F}{K_V} \ln\left(\frac{C_o}{C_x}\right)$$

$$-3489.2 = - \frac{207500.4 \times 275 \times 2.736 \times 10^{-3} \times \ln 10}{K_V}$$

$$K_V = 103.0 \text{ s}^{-1}$$

Calculation of Length of Unused Bed (Ref. Run HEP 1)

Length of Unused Bed (LUB)

$$\begin{aligned} &= L_o - \frac{G(Y_e - Y_o)}{\rho_B (X_e - X_o)} \theta_b \\ &= .0125 - \frac{6.248 \times 10^{-3}}{275} \frac{(159 \times 10^{-6} - 10 \times 10^{-6})}{(.09875 \times 10^{-2} - 0)} \times 2400 \\ &= .0125 - .0082 \\ &= .0043 \text{ m} \end{aligned}$$

APPENDIX II

TABLES OF THE EXPERIMENTAL CONDITIONS AND
THE RESULTS OF ADSORPTION

Expt No.	Mass of Fresh Cloth (kg x 10 ³)	Liquid Solvent Flowrate (m ³ s ⁻¹ x 10 ⁸)	Superficial Gas Velocity (m s ⁻¹)	Temperature (K)	Atmospheric Pressure (m Hg)	Volumetric Concentration (p.p.m)
HEP1	32.3	0.25	0.14	295	0.772	159
HEP2	36.7	0.33	0.14	293	0.771	210
HEP3	32.7	0.50	0.14	295	0.771	318
HEP4	33.0	0.67	0.14	295	0.772	423
HEP5	34.7	1.00	0.15	295	0.770	596
HEP6	49.1	0.25	0.15	290	0.763	147
HEP7	45.8	0.33	0.14	292	0.754	214
HEP8	54.2	0.50	0.17	297.5	0.764	266
HEP9	47.1	0.67	0.14	295	0.754	433
HEP10	47.9	1.00	0.15	290	0.764	588
HEP11	63.6	0.25	0.16	291.5	0.764	139
HEP12	59.1	0.33	0.18	295.5	0.768	166
HEP13	68.0	0.50	0.16	295	0.767	279
HEP14	60.0	0.67	0.15	295	0.764	399
HEP15	62.0	1.00	0.16	295.5	0.762	563

TABLE 1: EXPERIMENTAL CONDITIONS FOR THE ADSORPTION OF HEPTANE VAPOUR ON CHARCOAL CLOTH

Expt No.	Total Time of the Experiment (sec)	Weight of the Inlet Solvent ($\text{kg} \times 10^3$)	Weight of the Outlet Solvent ($\text{kg} \times 10^3$)	Weight of the Adsorbed Solvent ($\text{kg} \times 10^3$)	Weight of the Solvent Adsorbed Per Unit Weight of Cloth ($\text{kg} \text{ kg}^{-1}$)	%Loss
HEP1	14700	24.99	8.10	12.0	0.372	19.57
HEP2	10200	23.12	7.71	9.8	0.267	24.22
HEP3	9120	31.01	12.97	11.4	0.397	21.41
HEP4	7440	33.73	13.21	12.1	0.367	24.96
HEP5	5400	36.72	16.52	12.2	0.352	21.79
HEP6	36000	61.20	29.36	16.3	0.332	25.39
HEP7	14640	33.18	10.73	15.9	0.347	19.74
HEP8	12840	43.66	16.92	15.7	0.290	25.29
HEP9	8040	36.45	9.74	14.5	0.308	33.50
HEP10	7440	50.59	17.38	18.2	0.380	29.67
HEP11	36000	61.20	24.74	23.3	0.366	21.51
HEP12	26580	60.37	23.62	22.6	0.382	23.44
HEP13	12000	40.80	8.71	21.9	0.322	24.98
HEP14	10680	48.42	13.09	22.2	0.370	27.12
HEP15	10140	79.15	15.82	20.4	0.329	54.00

TABLE 2: ADSORPTION RESULTS FOR THE ADSORPTION OF HEPTANE VAPOUR ON CHARCOAL CLOTH

Expt No.	Mass of Fresh Cloth ($\text{kg} \times 10^3$)	Liquid Solvent Flowrate ($\text{m}^3 \text{s}^{-1} \times 10^8$)	Superficial Gas Velocity (m s^{-1})	Temperature (K)	Atmospheric Pressure (m Hg)	Volumetric Concentration (p.p.m)
TET1	36.4	0.25	0.10	291	0.756	317
TET2	33.0	0.33	0.13	300	0.734	336
TET3	32.6	0.50	0.13	291	0.746	495
TET4	32.4	0.67	0.13	291	0.747	659
TET5	34.5	1.00	0.10	290	0.749	1292
TET6	47.3	0.25	0.13	288	0.724	252
TET7	51.9	0.33	0.14	292	0.734	312
TET8	50.3	0.50	0.12	291	0.733	545
TET9	47.8	0.67	0.15	292.5	0.734	584
TET10	45.3	1.00	0.14	295	0.738	946
TET11	62.9	0.25	0.13	291	0.762	245
TET12	60.9	0.33	0.14	294.5	0.756	309
TET13	62.1	0.50	0.14	294.5	0.756	464
TET14	62.2	0.67	0.11	292	0.762	775
TET15	59.2	1.00	0.13	294	0.757	997

TABLE 3: EXPERIMENTAL CONDITIONS FOR THE ADSORPTION OF TETRACHLOROETHYLENE VAPOUR ON CHARCOAL CLOTH

Expt No.	Total Time of the Experiment (sec)	Weight of the Inlet Solvent ($\text{kg} \times 10^3$)	Weight of the Outlet Solvent ($\text{kg} \times 10^3$)	Weight of the Adsorbed Solvent ($\text{kg} \times 10^3$)	Weight of the Solvent Adsorbed Per Unit Weight of Cloth ($\text{kg} \text{ kg}^{-1}$)	% Loss
TET1	20880	84.57	20.23	28.3	0.777	42.62
TET2	10980	59.29	21.89	27.8	0.842	16.19
TET3	17460	141.43	59.40	32.6	1.000	34.95
TET4	12960	139.97	70.30	30.4	0.938	28.06
TET5	6180	100.12	38.12	34.4	0.997	27.57
TET6	28200	114.21	27.05	31.0	0.655	49.17
TET7	15360	82.94	14.81	37.4	0.721	37.05
TET8	13020	105.46	32.82	36.6	0.728	34.17
TET9	9660	104.33	25.98	38.3	0.801	38.39
TET10	8340	135.11	53.97	45.6	1.007	26.30
TET11	28800	116.64	29.36	47.5	0.755	34.10
TET12	18000	97.20	16.78	51.8	0.851	29.44
TET13	11460	92.83	25.29	53.1	0.855	15.56
TET14	11280	121.82	26.68	57.6	0.926	30.82
TET15	9000	145.80	52.77	43.4	0.733	34.04

TABLE 4: ADSORPTION RESULTS FOR THE ADSORPTION OF TETRACHLOROETHYLENE VAPOUR ON CHARCOAL CLOTH

Expt No.	Mass of Fresh Cloth (kg x 10 ³)	Liquid Solvent Flowrate (m ³ s ⁻¹ x 10 ⁸)	Superficial Gas Velocity (m s ⁻¹)	Temperature (K)	Atmospheric Pressure (m Hg)	Volumetric Concentration (p.p.m)
TOL1	38.0	0.25	0.12	293.5	0.767	255
TOL2	36.0	0.33	0.20	293.5	0.758	306
TOL3	39.5	0.50	0.15	297	0.759	417
TOL4	35.6	0.67	0.15	297.5	0.759	557
TOL5	38.9	1.00	0.14	298	0.774	879
TOL6	45.3	0.25	0.17	295	0.755	184
TOL7	49.1	0.33	0.17	295	0.756	243
TOL8	46.7	0.50	0.17	293	0.756	364
TOL9	47.8	0.67	0.17	295.5	0.762	486
TOL10	53.8	1.00	0.19	298	0.763	657
TOL11	62.9	0.25	0.15	296	0.757	208
TOL12	57.6	0.33	0.16	293.5	0.756	258
TOL13	61.9	0.50	0.15	294.5	0.756	415
TOL14	59.3	0.67	0.15	294	0.762	548
TOL15	67.3	1.00	0.14	293	0.762	878

TABLE 5: EXPERIMENTAL CONDITIONS FOR THE ADSORPTION OF TOLUENE VAPOUR ON CHARCOAL CLOTH

Expt No.	Total Time of the Experiment (sec)	Weight of the Inlet Solvent ($\text{kg} \times 10^3$)	Weight of the Outlet Solvent ($\text{kg} \times 10^3$)	Weight of the Adsorbed Solvent ($\text{kg} \times 10^3$)	Weight of the Solvent Adsorbed Per Unit Weight of Cloth ($\text{kg} \text{ kg}^{-1}$)	% Loss
TOL1	11640	25.03	4.65	17.49	0.460	11.53
TOL2	8100	23.22	6.58	14.62	0.406	8.72
TOL3	5840	25.54	6.55	17.11	0.433	7.37
TOL4	5040	28.90	9.45	16.98	0.477	8.54
TOL5	4860	41.80	11.38	26.55	0.683	9.27
TOL6	15720	33.80	9.84	21.69	0.478	6.73
TOL7	14580	41.80	12.25	25.99	0.529	8.52
TOL8	10140	43.60	16.73	22.89	0.490	9.13
TOL9	8400	48.16	19.26	23.05	0.482	12.13
TOLL0	7320	62.95	17.13	37.47	0.696	12.37
TOLL1	25200	13.19	13.19	34.18	0.543	12.56
TOLL2	17760	10.93	10.93	36.30	0.630	7.23
TOLL3	13440	17.39	17.39	35.66	0.576	8.21
TOLL4	8400	5.43	5.43	39.54	0.667	6.63
TOLL5	5580	6.76	6.76	37.36	0.555	8.13

TABLE 6: ADSORPTION RESULTS FOR THE ADSORPTION OF TOLUENE VAPOUR ON CHARCOAL CLOTH

Expt No.	Mass of Fresh Cloth (kg x 10 ³)	Liquid Solvent Flowrate (m ³ s ⁻¹ x 10 ⁸)	Superficial Gas Velocity (m s ⁻¹)	Temperature (K)	Atmospheric Pressure (m Hg)	Volumetric Concentration (p.p.m)
XYL1	37.32	0.25	0.16	298	0.754	175
XYL2	36.45	0.33	0.16	297	0.754	233
XYL3	36.65	0.50	0.16	296	0.741	353
XYL4	37.53	0.67	0.18	294.4	0.742	417
XYL5	35.00	1.00	0.16	295	0.740	707
XYL6	50.62	0.25	0.14	291.5	0.726	203
XYL7	49.66	0.33	0.16	298.5	0.746	237
XYL8	49.00	0.50	0.16	298	0.743	356
XYL9	48.30	0.67	0.17	298	0.726	457
XYL10	50.26	1.00	0.16	297	0.724	728
XYL11	60.84	0.25	0.15	298	0.754	181
XYL12	61.91	0.33	0.16	300.5	0.756	230
XYL13	61.91	0.50	0.17	300.5	0.758	331
XYL14	62.68	0.67	0.18	299	0.762	412
XYL15	59.07	1.00	0.16	298	0.764	692

TABLE 7: EXPERIMENTAL CONDITIONS FOR THE ADSORPTION OF O-XYLENE VAPOUR ON CHARCOAL CLOTH

Expt No.	Total Time of the Experiment (sec)	Weight of the Inlet Solvent (kg x 10 ³)	Weight of the Outlet Solvent (kg x 10 ³)	Weight of the Adsorbed Solvent (kg x 10 ³)	Weight of the Solvent Adsorbed Per Unit Weight of Cloth (kg kg ⁻¹)	%Loss
XYL1	12120	26.66	5.21	13.79	0.370	28.73
XYL2	17400	51.04	23.43	15.55	0.427	23.63
XYL3	6048	28.51	10.25	14.95	0.408	11.61
XYL4	6780	39.78	17.05	15.47	0.412	18.25
XYL5	6900	60.72	30.10	16.14	0.461	23.85
XYL6	18000	39.60	5.91	17.38	0.343	41.19
XYL7	11220	32.91	3.68	20.85	0.420	25.46
XYL8	11340	48.90	12.82	22.81	0.466	27.14
XYL9	13320	78.14	42.33	23.86	0.494	15.29
XYL10	5520	48.58	20.48	21.79	0.434	12.99
XYL11	36000	79.20	35.33	25.41	0.418	23.31
XYL12	16080	47.17	11.51	26.35	0.426	19.74
XYL13	17400	76.50	25.83	32.60	0.537	23.62
XYL14	11520	68.58	23.16	32.30	0.523	18.50
XYL15	6000	52.80	20.49	29.42	0.498	5.47

TABLE 8: ADSORPTION RESULTS FOR THE ADSORPTION OF O-XYLENE VAPOUR ON CHARCOAL CLOTH

APPENDIX III

DATA USED TO TEST THE APPLICATION OF THE
LANGMUIR AND FREUNDLICH ISOTHERMS

Expt No.	Mass of Heptane Adsorbed per Unit Mass of charcoal cloth (kg kg ⁻¹)	Partial pressure of Heptane in Air		ln p	Volume of Heptane Adsorbed per Unit Mass of Charcoal Cloth		ln V
		p (atm)	$\frac{1}{p}$ (atm ⁻¹)		V (m ³)	$\frac{1}{V}$ (m ⁻³)	
HEP 1	0.348	.000162	6172.8	-8.73	.0829	12.07	-2.49
HEP 2	0.238	.000213	4694.8	-8.45	.0564	17.73	-2.88
HEP 3	0.300	.000323	3095.9	-8.04	.0716	13.97	-2.64
HEP 4	0.322	.000430	2325.6	-7.75	.0767	13.03	-2.57
HEP 5	0.312	.000604	1655.6	-7.41	.0748	13.37	-2.59
HEP 6	0.274	.000148	6756.8	-8.82	.0649	15.41	-2.73
HEP 7	0.309	.000212	4716.9	-8.46	.0746	13.40	-2.60
HEP 8	0.261	.000267	3745.3	-8.23	.0635	15.75	-2.76
HEP 9	0.283	.000430	2325.6	-7.75	.0690	14.49	-2.67
HEP 10	0.298	.000591	1692.0	-7.43	.0705	14.18	-2.65
HEP 11	0.261	.000140	7142.8	-8.87	.0621	16.10	-2.78
HEP 12	0.299	.000168	5952.4	-8.69	.0718	13.93	-2.63
HEP 13	0.301	.000282	3546.1	-8.17	.0722	13.85	-2.63
HEP 14	0.308	.000401	2493.8	-7.82	.0742	13.48	-2.60
HEP 15	0.194	.000564	1773.0	-7.48	.0769	21.32	-3.06

TABLE 1 SUMMARY OF DATA USED TO TEST THE APPLICATION OF LANGMUIR AND FREUNDLICH ISOTHERMS FOR THE ADSORPTION OF HEPTANE ON ACTIVATED CHARCOAL CLOTH

Expt No.	Mass of Tetrachloroethylene Adsorbed per Unit mass of Charcoal Cloth (kg kg ⁻¹)	Partial Pressure of Tetrachloroethylene in air p(atm)	$\frac{1}{p}$ (atm ⁻¹)	lnp	Volume of Tetrachloroethylene Adsorbed per Unit Mass of charcoal cloth $\frac{1}{V}$ (m ⁻³)	lnV
TET1	0.550	.000315	3174.6	-8.06	0.0786	12.72
TET2	0.807	.000328	3048.8	-8.02	0.1189	8.41
TET3	0.709	.000486	2057.6	-7.63	0.1027	9.74
TET4	0.748	.000648	1543.2	-7.34	0.1082	9.24
TET5	0.830	.001273	785.5	-6.67	0.1207	8.29
TET6	0.458	.000240	4166.7	-8.33	0.0676	14.79
TET7	0.602	.000303	3300.3	-8.10	0.0889	11.25
TET8	0.504	.000526	1901.1	-7.55	0.0743	13.46
TET9	0.563	.000564	1773.0	-7.48	0.0833	12.00
TET10	0.761	.000919	1088.1	-6.99	0.1126	8.88
TET11	0.568	.000245	4081.6	-8.31	0.0815	12.27
TET12	0.695	.000307	3257.3	-8.09	0.1018	9.82
TET13	0.725	.000462	2164.5	-7.68	0.1061	9.43
TET14	0.650	.000777	1287.0	-7.16	0.0936	10.68
TET15	0.604	.000993	1007.0	-6.91	0.0881	11.35

TABLE 2: SUMMARY OF DATA USED TO TEST THE APPLICATION OF LANGMUIR AND FREUNDLICH ISOTHERMS FOR THE ADSORPTION OF TETRACHLOROETHYLENE ON ACTIVATED CHARCOAL CLOTH

Expt No.	Mass of Toluene Adsorbed per Unit Mass of Charcoal Cloth (kg kg ⁻¹)	Partial Pressure of Toluene in Air p(atm)	$\frac{1}{p}$ (atm ⁻¹)	lnp	Volume of Toluene Adsorbed per Unit Mass of Charcoal Cloth V(m ³)	$\frac{1}{V}$ (m ⁻³)	lnV
TOL1	0.404	.000259	3891.1	-8.27	0.1048	9.54	-2.26
TOL2	0.394	.000205	4878.0	-8.49	0.1034	9.67	-2.27
TOL3	0.426	.000416	2403.8	-7.78	0.1130	8.85	-2.18
TOL4	0.473	.000556	1798.6	-7.49	0.1257	7.96	-2.07
TOL5	0.633	.000895	1117.3	-7.02	0.1652	6.05	-1.80
TOL6	0.454	.000183	5464.5	-8.61	0.1202	8.32	-2.12
TOL7	0.500	.000242	4132.2	-8.33	0.1314	7.61	-2.03
TOL8	0.467	.000362	2762.4	-7.92	0.1227	8.15	-2.10
TOL9	0.444	.000485	2061.9	-7.63	0.1167	8.57	-2.15
TOL10	0.502	.000660	1515.2	-7.32	0.1329	7.52	-2.02
TOL11	0.468	.000207	4830.9	-8.48	0.1240	8.06	-2.09
TOL12	0.591	.000257	3891.1	-8.27	0.1555	6.43	-1.86
TOL13	0.511	.000413	2421.3	-7.79	0.1349	7.41	-2.00
TOL14	0.627	.000549	1821.5	-7.51	0.1640	6.10	-1.81
TOL15	0.520	.000880	1136.4	-7.04	0.1355	7.38	-2.00

TABLE 3 : SUMMARY OF DATA USED TO TEST THE APPLICATION OF LANGMUIR AND FREUNDLICH ISOTHERMS FOR THE ADSORPTION OF TOLUENE ON ACTIVATED CHARCOAL CLOTH

Expt No.	Mass of O-Xylene Adsorbed per Unit Mass of charcoal cloth (kg kg ⁻¹)	Partial pressure of O-Xylene in Air		lnp	Volume of O-Xylene Adsorbed per Unit Mass of Charcoal Cloth		lnV
		p(atm)	$\frac{1}{p}$ (atm ⁻¹)		V(m ³)	$\frac{1}{V}$ (m ⁻³)	
XYL1	0.361	.000174	5747.1	-8.66	.0840	11.90	-2.48
XYL2	0.336	.000231	4329.0	-8.37	.0779	12.84	-2.55
XYL3	0.339	.000344	2907.0	-7.97	.0794	12.59	-2.53
XYL4	0.360	.000407	2457.0	-7.81	.0841	11.89	-2.48
XYL5	0.399	.000688	1453.5	-7.28	.0936	10.68	-2.37
XYL6	0.278	.000194	5154.6	-8.55	.0657	15.22	-2.72
XYL7	0.375	.000233	4291.8	-8.36	.0883	11.33	-2.43
XYL8	0.365	.000348	2873.6	-7.96	.0861	11.61	-2.45
XYL9	0.352	.000437	2288.3	-7.74	.0850	11.76	-2.47
XYL10	0.402	.000694	1440.9	-7.27	.0970	10.31	-2.33
XYL11	0.344	.000178	5618.0	-8.63	.0777	12.87	-2.55
XYL12	0.384	.000229	4366.8	-8.38	.0898	11.14	-2.41
XYL13	0.391	.000330	3030.3	-8.02	.0912	10.96	-2.39
XYL14	0.423	.000413	2421.3	-7.79	.0976	10.25	-2.33
XYL15	0.479	.000696	1436.8	-7.27	.1099	9.10	-2.21

TABLE 4: SUMMARY OF DATA USED TO TEST THE APPLICATION OF LANGMUIR AND FREUNDLICH ISOTHERMS FOR THE ADSORPTION OF O-XYLENE ON ACTIVATED CHARCOAL CLOTH

APPENDIX IV

SUMMARY OF DATA USED IN EVALUATING
THE LENGTH OF UNUSED ADSORBENT BED
AT AN OUTLET VAPOUR CONCENTRATION
OF 10 p.p.m.

Outlet Solvent Vapour Concentration (Y_0) = 10 p.p.m

Expt No.	Total Length of Bed L_0 (m)	Air-solvent Vapour Flowrate G ($\text{kmol m}^{-2} \text{s}^{-1} \times 10^3$)	Bulk Density of Adsorbent (kg m^{-3})	Inlet Solvent Concentration in air Y_e (mole $\text{mole}^{-1} \times 10^6$)	Time (s)	Adsorbate Adsorbent X_e ($\text{kmol kg}^{-1} \times 10^2$)	Length of Unused Bed LUB (m)
HEP 1	.0125	6.248	275	159	2400	.09875	.0043
HEP 2	.0125	6.248	275	210	1440	.06604	.0026
HEP 3	.0125	6.248	275	318	1140	.09775	.0043
HEP 4	.0125	6.248	275	423	660	.06724	.0033
HEP 5	.0125	6.695	275	596	300	.04548	.0031
HEP 6	.0175	6.695	275	147	6000	.15067	.0037
HEP 7	.0175	6.248	275	214	2400	.09309	.0056
HEP 8	.0175	7.588	275	266	1920	.08782	.0020
HEP 9	.0175	6.248	275	433	1080	.06838	.0023
HEP 10	.0175	6.695	275	588	1080	.10680	.0033
HEP 11	.0225	7.141	275	139	3600	.05679	.0013
HEP 12	.0225	8.034	275	166	2400	.06822	.0065
HEP 13	.0225	7.141	275	279	3000	.11081	.0036
HEP 14	.0225	6.695	275	399	1800	.09839	.0052
HEP 15	.0225	7.141	275	563	1980	.15098	.0037

TABLE 1: DATA USED IN EVALUATING THE LENGTH OF UNUSED ADSORBENT BED (HEPTANE)

Expt No.	Total Length of Bed L_o (m)	Air-solvent Vapour Flowrate G ($\text{kmol m}^{-2}\text{s}^{-1}\times 10^3$)	Bulk Density of Adsorbent (kg m^{-3})	Inlet Solvent Concentration Y_e (mole $\text{mole}^{-1}\times 10^6$) in air	Time (s)	Outlet Solvent Vapour Concentration (Y_o) = 10 p.p.m	
						Adsorbate Adsorbent X_e ($\text{kmol kg}^{-1}\times 10^2$)	Length of Unused Bed LUB (m)
TET 1	.0125	4.463	275	317	1800	.00076	.0007
TET 2	.0125	5.802	275	336	2040	.00164	.0039
TET 3	.0125	5.802	275	495	1860	.00178	.0018
TET 4	.0125	5.802	275	659	1320	.00188	.0029
TET 5	.0125	4.463	275	1292	780	.00157	.0021
TET 6	.0175	5.802	275	252	3240	.00101	.0011
TET 7	.0175	6.249	275	312	4200	.00171	.0006
TET 8	.0175	5.356	275	545	1140	.00072	.0010
TET 9	.0175	6.695	275	585	1020	.00084	.0005
TET 10	.0175	6.249	275	946	600	.00094	.0039
TET 11	.0225	5.802	275	245	9240	.00226	.0022
TET 12	.0225	6.249	275	309	6840	.00252	.0041
TET 13	.0225	6.249	275	464	3660	.00247	.0072
TET 14	.0225	4.910	275	775	2400	.00170	.0032
TET 15	.0225	5.802	275	997	1560	.00167	.0030

TABLE 2: DATA USED IN EVALUATING THE LENGTH OF UNUSED ADSORBENT BED (TETRACHLOROETHYLENE)

Outlet Solvent Vapour Concentration (Y_0) = 10 p.p.m

Expt No.	Total Length of Bed L_0 (m)	Air-solvent Vapour Flowrate G ($\text{kmol m}^{-2}\text{s}^{-1}\times 10^3$)	Bulk Density of Adsorbent (kg m^{-3})	Inlet Solvent Concentration in air Y_e (mole $\text{mole}^{-1}\times 10^6$)	Time (s)	Adsorbate Adsorbent X_e ($\text{kmol kg}^{-1}\times 10^2$)	Length of Unused Bed LUB (m)
TOL 1	.0125	5.356	275	255	4200	.00226	.0036
TOL 2	.0125	6.927	275	306	3300	.00262	.0031
TOL 3	.0125	6.695	275	417	2200	.00241	.0033
TOL 4	.0125	6.695	275	557	1440	.00229	.0041
TOL 5	.0125	6.249	275	879	1260	.00270	.0033
TOL 6	.0175	7.588	275	184	3540	.00167	.0033
TOL 7	.0175	7.588	275	243	3900	.00225	.0064
TOL 8	.0175	7.588	275	364	2040	.00184	.0068
TOL 9	.0175	7.588	275	486	1680	.00192	.0060
TOL 10	.0175	8.480	275	657	1260	.00189	.0042
TOL 11	.0225	6.695	275	208	6600	.00212	.0075
TOL 12	.0225	7.141	275	258	4800	.00239	.0076
TOL 13	.0225	6.695	275	415	3840	.00264	.0082
TOL 14	.0225	6.695	275	548	2760	.00270	.0091
TOL 15	.0225	6.249	275	878	2580	.00329	.0070

TABLE 3: DATA USED IN EVALUATING THE LENGTH OF UNUSED ADSORBENT BED (TOLUENE)

Expt No.	Total Length of Bed L_o (m)	Air-solvent Vapour Flowrate G ($\text{kmol m}^{-2} \text{s}^{-1} \times 10^3$)	Bulk Density of Adsorbent (kg m^{-3})	Inlet Solvent Concentration in air Y_e (mole $\text{mole}^{-1} \times 10^6$)	Time (s)	Adsorbate Adsorbent X_e ($\text{kmol kg}^{-1} \times 10^2$)	Length of Unused Bed LUB (m)
XYL 1	.0125	7.141	275	175	3600	.00141	.0016
XYL 2	.0125	7.141	275	233	2700	.00155	.0020
XYL 3	.0125	7.141	275	353	1200	.00119	.0035
XYL 4	.0125	8.034	275	417	960	.00115	.0026
XYL 5	.0125	7.141	275	707	960	.00173	.0025
XYL 6	.0175	6.249	275	203	4200	.00109	.0006
XYL 7	.0175	7.141	275	237	4200	.00172	.0031
XYL 8	.0175	7.141	275	356	2400	.00146	.0027
XYL 9	.0175	7.585	275	457	360	.00034	.0044
XYL 10	.0175	7.141	275	728	720	.00103	.0045
XYL 11	.0225	6.695	275	181	8400	.00216	.0063
XYL 12	.0225	7.141	275	230	6600	.00234	.0064
XYL 13	.0225	7.585	275	331	4200	.00213	.0050
XYL 14	.0225	8.034	275	412	2400	.00175	.0064
XYL 15	.0225	7.141	275	692	1200	.00159	.0091

TABLE 4: DATA USED IN EVALUATING THE LENGTH OF UNUSED ADSORBENT BED (O-XYLENE)

APPENDIX V

DATA USED TO CALCULATE THEORETICAL ADSORBATE-
ADSORBENT RATIO USING DUBININ-POLANYI EQUATION

Solvent	a_1	b_1	c_1	d_0 (kg m^{-3})	α ($\text{kg m}^{-3}\text{K}^{-1}$)	γ ($\text{N m}^{-1} \times 10^3$)	d_{15} (kg m^{-3})	β
Benzene	-	-	-	-	-	29.55	884.2	-
Heptane	6.897	1265	217	700	0.82	20.85	687.8	1.51
Tetrachloro -ethylene	6.977	1387	218	1656	1.65	32.86	1631.1	1.91
Toluene	6.955	1345	220	885	0.93	29.10	871.6	1.19
O-Xylene	6.999	1475	214	897	0.84	30.75	884.3	1.37

TABLE 1: DATA USED TO CALCULATE THEORETICAL ADSORPTION CAPACITY USING

DUBININ-POLANYI EQUATION

Expt No.	$\frac{\text{Adsorbate}}{\text{Adsorbent}}$ (kg kg ⁻¹)	Expt. No.	$\frac{\text{Adsorbate}}{\text{Adsorbent}}$ (kg kg ⁻¹)	Expt. No.	$\frac{\text{Adsorbate}}{\text{Adsorbent}}$ (kg kg ⁻¹)	Expt No.	$\frac{\text{Adsorbate}}{\text{Adsorbent}}$ (kg kg ⁻¹)
HEP1	0.387	TET1	0.819	TOL1	0.459	XYL1	0.437
HEP2	0.386	TET2	0.843	TOL2	0.459	XYL2	0.435
HEP3	0.387	TET3	0.820	TOL3	0.463	XYL3	0.435
HEP4	0.387	TET4	0.820	TOL4	0.464	XYL4	0.433
HEP5	0.387	TET5	0.817	TOL5	0.463	XYL5	0.433
HEP6	0.386	TET6	0.814	TOL6	0.461	XYL6	0.429
HEP7	0.385	TET7	0.824	TOL7	0.461	XYL7	0.438
HEP8	0.388	TET8	0.821	TOL8	0.459	XYL8	0.437
HEP9	0.387	TET9	0.825	TOL9	0.461	XYL9	0.438
HEP10	0.385	TET10	0.831	TOL10	0.464	XYL10	0.437
HEP11	0.386	TET11	0.818	TOL11	0.462	XYL11	0.424
HEP12	0.387	TET12	0.828	TOL12	0.459	XYL12	0.440
HEP13	0.387	TET13	0.828	TOL13	0.461	XYL13	0.440
HEP14	0.387	TET14	0.821	TOL14	0.460	XYL14	0.438
HEP15	0.387	TET15	0.827	TOL15	0.459	XYL15	0.436

TABLE 2: SUMMARY OF THEORETICAL ADSORBATE-ADSORBENT RATIO USING DUBININ-POLANYI EQUATION

APPENDIX VI

DATA USED TO CALCULATE ADSORBATE-ADSORBENT
RATIO AT BREAKTHROUGH

Expt No.	Time to Attain Breakthrough (sec)	Weight of the Inlet Solvent ($\text{kg} \times 10^3$)	Weight of the Outlet Solvent ($\text{kg} \times 10^3$)	Weight of the Lost Solvent ($\text{kg} \times 10^3$)	Weight of the Adsorbed Solvent ($\text{kg} \times 10^3$)	Weight of the Solvent Adsorbed per Unit Weight of Cloth at Breakthrough (kg kg^{-1})
HEP1	12600	21.42	5.98	4.19	11.25	0.348
HEP2	7740	17.54	4.55	4.24	8.75	0.238
HEP3	6780	23.05	8.29	4.94	9.82	0.300
HEP4	5700	25.84	8.75	6.45	10.64	0.322
HEP5	4020	27.34	10.54	5.96	10.84	0.312
HEP6	15600	26.52	6.32	6.73	13.47	0.274
HEP7	11400	25.84	6.57	5.10	14.17	0.309
HEP8	9600	32.64	10.23	8.25	14.16	0.261
HEP9	6900	31.28	7.46	10.48	13.34	0.283
HEP10	4440	30.19	6.95	8.96	14.28	0.298
HEP11	19200	32.64	9.05	7.02	16.57	0.261
HEP12	16200	36.72	10.44	8.61	17.67	0.299
HEP13	10800	36.72	7.11	9.17	20.44	0.301
HEP14	7680	34.82	6.89	9.44	18.49	0.308
HEP15	5460	37.13	4.98	20.14	12.00	0.194

TABLE 1: DATA USED TO CALCULATE ADSORBATE-ADSORBENT RATIO AT BREAKTHROUGH (HEPTANE)

Expt No.	Time to Attain Breakthrough (sec)	Weight of the Inlet Solvent ($\text{kg} \times 10^3$)	Weight of the Outlet Solvent ($\text{kg} \times 10^3$)	Weight of the Lost Solvent ($\text{kg} \times 10^3$)	Weight of the Adsorbed Solvent ($\text{kg} \times 10^3$)	Weight of the Solvent Adsorbed per Unit Weight of Cloth at Breakthrough (kg kg^{-1})
TET1	12480	50.54	8.98	21.54	20.02	0.550
TET2	9600	51.84	16.82	8.39	26.63	0.809
TET3	6600	53.46	11.67	18.68	23.11	0.709
TET4	4680	50.54	12.11	14.18	24.25	0.748
TET5	3780	61.24	15.73	16.88	28.63	0.830
TET6	14040	56.86	7.24	27.96	21.66	0.458
TET7	11280	60.91	7.09	22.57	31.25	0.602
TET8	7080	57.35	12.40	19.60	25.35	0.504
TET9	5460	58.97	9.43	22.64	26.90	0.563
TET10	4620	74.84	20.70	19.68	34.46	0.761
TET11	16800	68.04	9.13	23.20	35.71	0.568
TET12	12600	68.04	5.70	20.03	42.31	0.695
TET13	8460	68.04	12.44	10.59	45.01	0.725
TET14	6600	71.28	8.88	21.97	40.43	0.650
TET15	5400	87.48	21.96	29.78	35.74	0.604

TABLE 2: DATA USED TO CALCULATE ADSORBATE-ADSORBENT RATIO AT BREAKTHROUGH (TETRACHLOROETHYLENE)

Expt No.	Time to Attain Breakthrough (sec)	Weight of the Inlet Solvent ($\text{kg} \times 10^3$)	Weight of the Outlet Solvent ($\text{kg} \times 10^3$)	Weight of the Lost Solvent ($\text{kg} \times 10^3$)	Weight of the Adsorbed Solvent ($\text{kg} \times 10^3$)	Weight of the Solvent Adsorbed per Unit Weight of Cloth at Breakthrough (kg kg^{-1})
TOL1	9600	20.64	2.92	2.38	15.34	0.404
TOL2	7500	21.50	5.45	1.87	14.18	0.394
TOL3	5700	24.51	5.89	1.81	16.81	0.426
TOL4	4920	28.21	8.97	2.41	16.83	0.473
TOL5	4140	35.60	7.68	3.30	24.62	0.633
TOL6	14340	30.83	8.21	2.07	20.55	0.454
TOL7	12900	36.98	9.29	3.15	24.54	0.500
TOL8	9000	38.70	13.29	3.53	21.88	0.467
TOL9	6960	39.90	13.83	4.84	21.23	0.444
TOL10	4500	38.70	6.55	5.14	27.01	0.502
TOL11	19800	42.57	7.78	5.35	29.44	0.468
TOL12	16200	46.44	8.99	3.38	34.07	0.591
TOL13	10800	46.44	11.00	3.81	31.63	0.511
TOL14	7800	44.72	4.58	2.96	37.18	0.627
TOL15	5100	43.86	5.27	3.57	35.02	0.520

TABLE 3: DATA USED TO CALCULATE ADSORBATE-ADSORBENT RATIO AT BREAKTHROUGH (TOLUENE)

Expt No.	Time to Attain Breakthrough (sec)	Weight of the Inlet Solvent ($\text{kg} \times 10^3$)	Weight of the Outlet Solvent ($\text{kg} \times 10^3$)	Weight of the Lost Solvent ($\text{kg} \times 10^3$)	Weight of the Adsorbed Solvent ($\text{kg} \times 10^3$)	Weight of the Solvent Adsorbed per Unit Weight of Cloth at Breakthrough (kg kg^{-1})
XYL1	11700	25.74	4.85	7.40	13.49	0.361
XYL2	8400	24.64	6.56	5.82	12.26	0.336
XYL3	5700	25.08	9.75	2.91	12.42	0.339
XYL4	4800	28.14	9.49	5.14	13.51	0.360
XYL5	3600	31.68	10.16	7.56	13.96	0.399
XYL6	13200	29.04	3.03	11.96	14.05	0.278
XYL7	9600	28.14	2.38	7.16	18.60	0.375
XYL8	7200	31.68	5.18	8.60	17.90	0.365
XYL9	6000	35.20	13.05	5.38	16.99	0.352
XYL10	4800	42.24	16.54	5.49	20.21	0.402
XYL11	15600	34.32	5.41	8.00	20.91	0.344
XYL12	12600	36.96	5.89	7.30	23.77	0.384
XYL13	9600	42.24	8.06	9.98	24.20	0.391
XYL14	7800	45.76	10.83	8.47	26.46	0.423
XYL15	5400	47.52	16.62	2.60	28.30	0.479

TABLE 4: DATA USED TO CALCULATE ADSORBATE-ADSORBENT RATIO AT BREAKTHROUGH (O-XYLENE)

APPENDIX VII

SUMMARY OF DATA USED TO CALCULATE ADSORPTION
RATE CONSTANT

Expt. No.	Liquid Solvent Rate ($\text{m}^3\text{s}^{-1}\times 10^8$)	Weight of Charcoal Cloth ($\text{kg}\times 10^3$)	Time to reach Outlet Concentration = .1 Inlet Concentration (sec)	Average Air-Solvent Vapour Flowrate ($\text{m}^3\text{s}^{-1}\times 10^3$)	Bulk Density of the Adsorbent (kg m^{-3})	Slope (s kg^{-1})	Intercept (sec)	Adsorption Rate Constant (s^{-1})
HEP1	0.25	32.3	3120					
HEP6	0.25	49.1	6900	2.736	275	207500.4	-3489.2	103.0
HEP11	0.25	63.6	9600					
HEP2	0.33	36.7	2340					
HEP7	0.33	45.8	3420	2.797	275	115002.8	-1868.1	109.0
HEP12	0.33	59.1	4920					
HEP3	0.50	32.7	1620					
HEP8	0.50	54.2	3900	2.858	275	96131.2	-1463.6	118.9
HEP13	0.50	68.0	4980					
HEP4	0.67	33.0	1140					
HEP9	0.67	47.1	2040	2.615	275	64434.9	-989.1	107.9
HEP14	0.67	60.0	2880					
HEP5	1.00	34.7	1020					
HEP10	1.00	47.9	1680	2.797	275	52776.4	-823.8	113.5
HEP15	1.00	62.0	2460					

TABLE 1: DATA USED TO CALCULATE ADSORPTION RATE CONSTANT OF HEPTANE ON CHARCOAL CLOTH

Expt. No.	Liquid Solvent Rate ($\text{m}^3\text{s}^{-1}\times 10^8$)	Weight of Charcoal Cloth ($\text{kg}\times 10^3$)	Time to reach Outlet Concentration = 0.1 Inlet Concentration (sec)	Average Air-Solvent Vapour Flowrate ($\text{m}^3\text{s}^{-1}\times 10^3$)	Bulk Density of the Adsorbent (kg m^{-3})	Slope (s kg^{-1})	Intercept (sec)	Adsorption Rate Constant (s^{-1})
TET1	0.25	36.4	4920					
TET6	0.25	47.3	6000	2.189	275	213558.6	-3315.9	89.3
TET11	0.25	62.9	10440					
TET2	0.33	33.0	2640					
TET7	0.33	51.9	5700	2.493	275	154105.6	-2409.5	101.0
TET12	0.33	60.9	6900					
TET3	0.50	32.6	2400					
TET8	0.50	50.3	4800	2.371	275	132471.0	-1902.8	104.5
TET13	0.50	62.1	6300					
TET4	0.67	32.4	1320					
TET9	0.67	47.8	1860	2.371	275	66080.3	-976.6	101.6
TET14	0.67	62.2	3300					
TET5	1.00	34.5	1080					
TET10	1.00	45.3	1260	2.25	275	47227.0	-668.2	100.7
TET15	1.00	59.2	2220					

TABLE 2: DATA USED TO CALCULATE ADSORPTION RATE CONSTANT OF TETRACHLOROETHYLENE ON CHARCOAL CLOTH

Expt. No.	Liquid Solvent Rate ($m^3s^{-1} \times 10^8$)	Weight of Charcoal Cloth ($kg \times 10^3$)	$\frac{\text{Time to reach Outlet Concentration}}{\text{Inlet Concentration}} = .1$ (sec)	Average Air-Solvent Vapour Flowrate ($m^3s^{-1} \times 10^3$)	Bulk Density of the Adsorbent ($kg m^{-3}$)	Slope ($s kg^{-1}$)	Intercept (sec)	Adsorption Rate Constant (s^{-1})
TOL1	0.25	38.0	3240					
TOL6	0.25	45.3	4440	2.675	275	210506.0	-4898.7	72.8
TOL11	0.25	62.9	8400					
TOL2	0.33	36.0	1920					
TOL7	0.33	49.1	3780	3.162	275	179826.0	-4693.7	76.7
TOL12	0.33	57.6	5880					
TOL3	0.50	39.5	1560					
TOL8	0.50	46.7	2640	2.858	275	121248.0	-3145.6	69.8
TOL13	0.50	61.9	4320					
TOL4	0.67	35.6	1080					
TOL9	0.67	47.8	2160	2.858	275	121184.7	-3364.3	65.2
TOL14	0.67	59.3	3960					
TOL5	1.00	38.9	780					
TOL10	1.00	53.8	1980	2.858	275	84438.6	-2523.4	60.6
TOL15	1.00	67.3	3180					

TABLE 3: DATA USED TO CALCULATE ADSORPTION RATE CONSTANT OF TOLUENE ON CHARCOAL CLOTH

Expt. No.	Liquid Solvent Rate ($\text{m}^3\text{s}^{-1}\times 10^8$)	Weight of Charcoal Cloth ($\text{kg}\times 10^3$)	Time to reach Outlet Concentration = .1 Inlet Concentration (sec)	Average Air-Solvent Vapour Flowrate ($\text{m}^3\text{s}^{-1}\times 10^3$)	Bulk Density of the Adsorbent (kg m^{-3})	Slope (s kg^{-1})	Intercept (sec)	Adsorption Rate Constant (s^{-1})
XYL1	0.25	37.32	4200	2.736	275	232031.3	-4667.2	86.1
XYL6	0.25	50.62	6600					
XYL11	0.25	60.84	9720					
XYL2	0.33	36.45	3060	2.919	275	177226.6	-3244.4	101.0
XYL7	0.33	49.66	5880					
XYL12	0.33	61.91	7560					
XYL3	0.50	36.65	1800	2.979	275	116247.6	-2377.8	92.2
XYL8	0.50	49.00	3480					
XYL13	0.50	61.91	4740					
XYL4	0.67	37.53	1380	3.222	275	70898.9	-1427.4	101.3
XYL9	0.67	48.30	1740					
XYL14	0.67	62.58	3120					
XYL5	1.00	35.00	780	2.918	275	40298.5	-698.8	106.5
XYL10	1.00	50.26	1140					
XYL15	1.00	59.07	1800					

TABLE 4: DATA USED TO CALCULATE ADSORPTION RATE CONSTANT OF O-XYLENE ON CHARCOAL CLOTH

APPENDIX VIII

CALCULATED THEORETICAL BREAKTHROUGH
TIME USING EQUATION 6.10

Expt No.	Fluid Diffusivity D_f ($m^2 s^{-1} \times 10^4$)	Pore Diffusivity D_{pore} ($m^2 s^{-1} \times 10^8$)	Number of Transfer Units N_{pore}	Throughput Parameter τ	Calculated Time (s)	Experimental Time (sec)
HEP 1	.0505	184	3.14	0.67	4020	3120
HEP 6	.0505	184	4.11	0.75	4500	6900
HEP 11	.0505	184	4.95	0.79	4740	9600
TET 1	.0636	232	5.55	0.81	4860	4920
TET 6	.0636	232	5.98	0.83	4980	6000
TET 11	.0636	232	7.68	0.87	5220	10440
TOL 1	.0709	259	5.16	0.80	4800	3240
TOL 6	.0709	259	5.10	0.82	4920	4440
TOL 11	.0709	259	7.44	0.86	5160	8400
XYL 1	.0620	226	3.46	0.70	4200	4200
XYL 6	.0620	226	5.40	0.81	4860	6600
XYL 11	.0620	226	7.43	0.86	5160	9720

TABLE 1: CALCULATED THEORETICAL BREAKTHROUGH TIME USING EQUATION 6.10

APPENDIX IX

SUMMARY OF RESULTS SHOWING OXIDATION DURING
ADSORPTION OF SOLVENT VAPOURS ON CHARCOAL CLOTH

Expt. No	Weight of Charcoal Cloth (kg x 10 ³)	Liquid Solvent Flow Rate (m ³ s ⁻¹ x 10 ⁸)	Total Time (s)	Weight of Inlet Vapour (kg x 10 ³)	Weight of adsorbed vapour (kg x 10 ³)	Weight of Outlet vapour (kg x 10 ³)	%Loss
HEP A	36.03	0.25	5400	9.18	6.52	1.24	15.47
HEP B	38.68	1.00	1800	12.24	8.61	1.21	19.77
TET A	36.18	0.25	5400	21.87	14.29	0.98	30.18
TET B	38.77	1.00	1800	29.16	17.25	2.53	32.17
TOL A	38.62	0.25	5400	11.61	9.51	1.13	8.35
TOL B	34.92	1.00	1800	15.48	11.12	3.44	6.00
XYL A	38.14	0.25	5400	11.88	9.71	0.41	14.81
XYL B	35.61	1.00	1800	15.84	11.08	1.74	19.07

TABLE 1: SUMMARY OF RESULTS SHOWING OXIDATION DURING ADSORPTION OF SOLVENT

VAPOURS ON CHARCOAL CLOTH

APPENDIX X
LIST OF COMPUTER PROGRAMS

C A COMPUTER PROGRAM TO DRAW A GRAPH OF
 C OUTLET VAPOUR CONCENTRATION OF HEPTANE
 C IN PPM AGAINST TIME IN SECONDS
 C AT DIFFERENT INLET CONCENTRATION

```

    INTEGER Z
    DIMENSION A(30),B(30),C(20),D(20),G(43),
1    H(43),Q(43),R(43),X(30),Y(30),Z(5)
    DO 10 I=1,30
    READ(12,-) A(I),B(I)
    A(I)=A(I)*60.0
10   CONTINUE
    DO 20 I=1,20
    READ(22,-) C(I),D(I)
    C(I)=C(I)*60.0
20   CONTINUE
    DO 30 I=1,43
    READ(32,-) G(I),H(I)
    G(I)=G(I)*60.0
30   CONTINUE
    DO 40 I=1,43
    READ(42,-) Q(I),R(I)
    Q(I)=Q(I)*60.0
40   CONTINUE
    DO 50 I=1,30
    READ(52,-) X(I),Y(I)
    X(I)=X(I)*60.0
50   CONTINUE
    CALL GINO
    CALL CHASWI(1)
    CALL SCALE(1.0)
    CALL CHASIZ(2.0,3.0)
    CALL SHIFT2(50.0,70.0)
    CALL AXIPOS(1,0.0,0.0,140.0,1)
    CALL AXIPOS(1,0.0,0.0,180.0,2)
    CALL AXISCA(3,3,0.0,18000.0,1)
    CALL AXISCA(3,5,-40.0,510.0,2)
    CALL AXIDRA (1,1,1)
    CALL AXIDRA(-1,-1,2)
    CALL GRASYM (A,B,30,1,0)
    CALL GRASYM (C,D,20,2,0)
    CALL GRASYM (G,H,43,3,0)
    CALL GRASYM (Q,R,43,4,0)
    CALL GRASYM (X,Y,30,5,0)
    CALL GRACUR(A,B,30)
    CALL GRACUR (C,D,20)
    CALL GRACUR (G,H,43)
    CALL GRACUR (Q,R,43)
    CALL GRACUR (X,Y,30)
    CALL MOVTO2(40.0,-20.0)
    CALL CHAHOL(17HTIME IN SECONDS*.)
    CALL MOVTO2(-17.0,-50.0)
    CALL CHAHOL(42HFIGURE 4.4  OUTLET VAPOUR CONCENTRATION*.)
    CALL MOVTO2(67.0,-50.0)
    CALL CHAHOL(42HVS TIME AT DIFFERENT INLET CONCENTRATION*.)
  
```

```
CALL MOVTO2(27.0,-60.0)
CALL CHAHOL(31H(25 LAYERS OF CHARCOAL CLOTH)*.)
CALL MOVTO2(-17.0,50.0)
CALL CHAANG(90.0)
CALL CHAHOL(47HOUTLET VAPOUR CONCENTRATION OF HEPTANE IN PPM*.)
P=110.0
S=150.0
DO 60 J=1,5,1
  READ (62,-) Z(J)
  CALL MOVTO2(P,S)
  CALL CHAANG(0.0)
  CALL SYMBOL(J)
  CALL MOVTO2(P+2.0,S-2.0)
  CALL CHAHOL(5H = *.)
  CALL CHAINT(Z(J),3)
  CALL MOVTO2(P+20.0,S-2.0)
  CALL CHAHOL(5HPPM*.)
  S=S-7.0
60 CONTINUE
  CALL DEVEND
  STOP
  END
```

C A COMPUTER PROGRAM TO CALCULATE
C THE AREA UNDER A CURVE

```
    DIMENSION X(7),Y(7)
    DO 10 I=1,7
    READ(12,-) X(I),Y(I)
10  CONTINUE
    WRITE(25,90)
90  FORMAT((9X,4HX(I),9X,4HY(I),8X,1HA,15X,1HB))
    B=0.0
    DO 55 I=1,6
    A=ABS((X(I+1)-X(I))*Y(I))+0.5*ABS((X(I+1)-X(I))*
1  (Y(I+1)-Y(I)))
    B=A+B
65  WRITE(25,100) X(I),Y(I),A,B
100 FORMAT(3X,F9.2,4X,F9.2,5X,F9.2,6X,F9.2)
55  CONTINUE
    STOP
    END
```

```

C A COMPUTER PROGRAM TO CALCULATE THE ADSORPTION
C CAPACITY OF A SOLVENT ON CHARCOAL CLOTH USING
C DUBININ-POLANYI EQUATION
C  $R = \log(Q)$  IN DUBININ-POLANYI EQUATION
C Q=CALCULATED ADSORPTION CAPACITY
C M=MOLECULAR WEIGHT OF THE SOLVENT
      REAL T,P,V,D,P1,P2,D1,R,Q
      REAL V,D,P1,P2,D1,R,Q
      REAL T(15),P(15)
      INTEGER I
      WRITE(13,110)
110  FORMAT(//,T7,2HD1,T17,2HD3,T30,2HD4,
1  T41,1HR,T51,1HQ)
      DO 150 I=1,15
      READ (7,-) T(I),P(I)
       $V = 760.0 * 22.4 * (273.0 + T(I)) / (273.0 * P(I))$ 
      M=106
       $D = M * 1000 / V$ 
       $P0 = 0.062 * (273.0 + T(I)) * D / 106.0$ 
       $P1 = \text{ALOG10}(P0)$ 
       $P2 = 6.999 - 1475 / (214.0 + T(I))$ 
       $D1 = 0.897 - 0.0084 * T(I)$ 
       $D2 = 0.615 * D1$ 
       $D3 = \text{ALOG10}(D2)$ 
       $D4 = 0.00000046 * ((273.0 + T(I)) / 1.37) ** 2$ 
1   $((P1 - P2) ** 2)$ 
       $R = D3 - D4$ 
       $Q = 10.0 ** R$ 
      WRITE(13,120) D1,D3,D4,R,Q
120  FORMAT(2X,F8.3,3X,F8.3,4X,F8.3,2X,
1  F8.3,3X,F8.3)
150  CONTINUE
      STOP
      END

```

```

C A COMPUTER PROGRAM TO PLOT THE BREAKTHROUGH
C TIME IN SECONDS AGAINST WEIGHT OF CHARCOAL
C CLOTH IN KILOGRAM AND CALCULATE THE SLOPE AND
C INTERCEPT USING CURVE FITTING METHOD
      INTEGER N,M,I,J,D
      REAL X(3),Y(3),A(4),REF,Z(3),S(3),T(3),K(5),H,L
      CALL GINO
      CALL CHASWI(1)
      CALL SCALE(1.0)
      CALL CHASIZ(2.0,3.0)
      CALL SHIFT2(50.0,70.0)
      CALL AXIPOS(0,0.0,0.0,140.0,1)
      CALL AXIPOS(0,0.0,0.0,180.0,2)
      CALL AXISCA(3,5,0.0,0.1,1)
      CALL AXISCA(3,11,0.0,11000.0,2)
      CALL AXIDRA (1,1,1)
      CALL AXIDRA(-1,-1,2)
      CALL MOVTO2(40.0,-20.0)
      CALL CHAHOL(38HWEIGHT OF CHARCOAL CLOTH IN KILOGRAM*.)
      CALL MOVTO2(-17.0,-50.0)
      CALL CHAHOL(40HFIGURE 4.21 TIME REQUIRED FOR OUTLET*.)
      CALL MOVTO2(62.0,-50.0)
      CALL CHAHOL(37HCONCENTRATION TO REACH 10% OF INLET*.)
      CALL MOVTO2(11.0,-60.0)
      CALL CHAHOL(43HCONCENTRATION VS WEIGHT OF CHARCOAL CLOTH*.)
      CALL MOVTO2(96.0,-60.0)
      CALL CHAHOL(11H(HEPTANE)*.)
      CALL MOVTO2(-17.0,90.0)
      CALL CHAANG(90.0)
      CALL CHAHOL(17HTIME IN SECONDS*.)
      DO 20 II=1,5
      READ *,N
      READ *,(X(I),Y(I),I=1,N)
      READ *,M,M1
      CALL E02ACF(X,Y,N,A,M1,REF)
      PRINT *,' CURVE FITTING RESULTS:- '
      PRINT *,' POLYNOMIAL COEFFICIENTS:- '
      DO 15 I=1,M1
      PRINT 16,A(I)
16     FORMAT (15X,F10.3)
15     CONTINUE

C
C
      PRINT 22
22     FORMAT(15X,' X Y FIT RESIDUAL ')
      PRINT 23
23     FORMAT(14X,46(' - '))
      DO 10 J=1, N
      Z(J)=X(J)
      S(J)=A(M+1)
      I=M
      S(J)=S(J)*Z(J)+A(I)
      IF (I-1) 30,30,40
40     I=I-1

```

```

GO TO 20
30  T(J)=Y(J)
    H=S(J)-T(J)
    PRINT 100,Z(J),T(J),S(J),H
100  FORMAT(14X,F7.1,3X,F10.3,2X,F10.3,2X,F10.3)
10  CONTINUE
    CALL PENSEL(1,1.0,1)
    CALL MOVTO2(0.0,0.0)
    CALL GRASYM(Z,T,N,II,0)
    CALL GRAPOL (Z,S,N)

C
20  CONTINUE
    P=110.0
    L=130.0
    DO 60 D=1,5,1
    READ (62,-) K(D)
    CALL MOVTO2(P,L)
    CALL CHAANG(0.0)
    CALL SYMBOL(D)
    CALL MOVTO2(P+2.0,L-2.0)
    CALL CHAHOL(5H = *.)
    CALL CHAFIX(K(D),4,2)
    CALL MOVTO2(P+20.0,L-2.0)
    CALL CHAHOL(8HML/MIN*.)
    L=L-7.0
60  CONTINUE
    CALL DEVEND
    STOP
    END

```